

---

**Development and characterization of new peptidomimetic  
inhibitors of the West Nile virus NS2B-NS3 protease**

**Dissertation**

zur

Erlangung des Doktorgrades

der Naturwissenschaften

(Dr. rer. nat.)

dem Fachbereich Pharmazie

der PHILIPPS-UNIVERSITÄT MARBURG

vorgelegt von

**M. Zouhir Hammamy**

aus Aleppo/Syrien

Marburg/Lahn 2014

---

Vom Fachbereich Pharmazie der Philipps-Universität Marburg  
als Dissertation angenommen am:

Erstgutachter: Prof. Dr. Torsten Steinmetzer

Zweitgutachterin: Prof. Dr. Wibke Diederich

Tag der mündlichen Prüfung: 26.03.2014

---

Die Untersuchungen zur vorliegenden Arbeit wurden auf Anregung von Herrn Prof. Dr. Torsten Steinmetzer am Institut für Pharmazeutische Chemie des Fachbereichs Pharmazie der Philipps-Universität Marburg in der Zeit von Mai 2009 bis März 2014 durchgeführt.



Dedicated to my family

For the sacrifices they made, their love and support

---

*All truths are easy to understand once they are discovered; the point is to discover them.*

Galileo Galilei

## Abbreviations

---

### Abbreviations

Å	Ångstrom ( $1\text{Å} = 10^{-10}\text{ m}$ )
A, Ala	alanine
Ac	acetyl
Aca	$\epsilon$ -aminocaproic acid
ACN	acetonitrile
AMC	7-amino-4-methylcoumarin
AMCA	<i>trans</i> -4-amidomethylcyclohexylamine
Amba	4-amidinobenzylamid
AMe	aminomethyl
Boc	<i>tert</i> -butoxycarbonyl
(Boc) <sub>2</sub> O	di- <i>tert</i> -butyl dicarbonate
BOP	(benzotriazol-1-yloxy)tris(dimethylamino)phosphonium hexafluorophosphate
Bz	benzoyl
C, Cys	cysteine
Cbz	carboxybenzyl
Cha	$\beta$ -cyclohexylalanine
D, Asp	aspartic acid
Da	Dalton
Dab	2,4-diaminobutyric acid
DCM	dichloromethane
DIPEA	<i>N,N</i> -diisopropylethylamine
DMF	dimethylformamide
DNV	dengue virus
E, Glu	glutamic acid
<i>EC</i> <sub>50</sub>	concentration of inhibitor required to reduce an effect to 50%.
<i>E. coli</i>	Escherichia coli
ER	endoplasmic reticulum
ESI	elektrospray ionisation
Equiv	equivalent
F, Phe	phenylalanine
Fmoc	fluorenylmethyloxycarbonyl
Gua	guanidino
Gaba	$\gamma$ -aminobutyric acid
GCMA	<i>trans</i> -(4-guanidino)cyclohexylmethanamide

---

GMe	guanidinomethyl
H, His	histidine
h	hour
<i>h</i> Ala(2-Pyr)	2-homopyridylalanine (2-amino-4-(pyridin-2-yl)butanoic acid)
HBTU	2-(1 <i>H</i> -benzotriazole-1-yl)-1,1,3,3-tetramethylammonium
HOBt	hydroxybenzotriazole
<i>h</i> Phe	homophenylalanine
HPLC	high-performance liquid chromatography
HSA	human serum albumin
<i>IC</i> <sub>50</sub>	inhibitor concentration required to reduce an enzyme activity to 50%.
I, Ile	isoleucine
JEV	Japanese encephalitis virus
<i>K</i> <sub>i</sub>	inhibition constant
K, Lys	lysine
L	liter
M	molarity (mol/L)
MHz	megahertz
min	minutes
MS	mass spectrometry
Naph	naphtyl
Nle	norleucine
NMM	N-methylmorpholine
NMR	nuclear magnetic resonance
n.d.	not determined
N, Asn	asparagine
Orn	ornithine, 2,5-diaminopentanoic acid
OSu	succinimide
P, Pro	proline
Pbf	2,2,4,6,7-pentamethyldihydrobenzofuran-5-sulfonyl
PDB	protein data bank
Phac	phenylacetyl
pNA	<i>para</i> -nitroaniline
ppm	parts per million
PyBOP	benzotriazol-1-yl-oxytripyrrolidinophosphonium hexafluorophosphate
Q, Gln	glutamine
R, Arg	arginine
R <sub>f</sub>	retention factor
RFU	relative fluorescence units

---

RT	room temperature
Sar	sarcosine, 2-(Methylamino)acetic acid
SPPS	solid-phase peptide synthesis
T, Thr	threonine
TFA	trifluoroacetic acid
TIS	triisopropylsilane
Tle	<i>tert</i> -leucine
Tris	tris(hydroxymethyl)aminomethane
V, Val	valine
W, Trp	tryptophane
WNV	West Nile virus
Y, Tyr	tyrosine



## Table of contents

<b>Abbreviations .....</b>	<b>7</b>
<b>Table of contents .....</b>	<b>11</b>
<b>1 Introduction.....</b>	<b>15</b>
1.1 Transmission .....	16
1.2 Pathogenesis .....	17
1.3 Pathological symptoms .....	17
1.4 West Nile virus classification.....	18
1.5 Morphology and structure of the WNV .....	19
1.6 Replication cycle .....	20
1.7 Genome structure and processing of the polyprotein.....	21
1.8 The biological roles of the nonstructural viral proteins .....	22
1.9 Substrate recognition site of the NS2B-NS3 protease .....	24
1.10 Antiviral strategies .....	25
1.11 Known WNV NS2B-NS3 protease inhibitors.....	26
1.12 Crystal structures of the WNV protease.....	29
<b>2 Aim of work.....</b>	<b>33</b>
<b>3 Results and discussion .....</b>	<b>34</b>
3.1 Inhibitors containing decarboxylated P1 arginine mimetics .....	34
3.2 Modification of P2 and P3 residues .....	39
3.3 Modification of P4 residue .....	44
3.4 Combination of the best P4 and P1 residues .....	46
3.5 Selectivity studies.....	46
3.6 Stability test with trypsin .....	47
3.7 Structure of the WNV NS2B-NS3 protease in complex with inhibitor 77 .....	48
3.8 Second modification of P2 and P3 residues .....	52
3.9 Incorporation of alkylated GCMA residues in P1 position.....	53
3.10 Design and synthesis of cyclic inhibitors .....	56

3.11 Determination of inhibitory constants .....	66
<b>4 Conclusion.....</b>	<b>69</b>
<b>4 Zusammenfassung.....</b>	<b>73</b>
<b>5 Experimental part .....</b>	<b>77</b>
5.1 Reagents and methods .....	77
5.1.1 Reagents and materials.....	77
5.1.2 Thin layer chromatography .....	77
5.1.3 High performance liquid chromatography (HPLC) .....	77
5.1.4 Lyophilization .....	78
5.1.5 NMR and mass spectrometry .....	78
5.2 Enzyme kinetic measurements .....	79
5.2.1 Kinetic measurement with the WNV NS2B-NS3 protease.....	79
5.2.2 Measurements with trypsin-like serine proteases.....	80
5.3 Synthesis.....	81
5.3.1 General synthetic procedures .....	81
5.3.2 Synthesis of the intermediates.....	87
5.3.3 Synthesis of inhibitors 23-39 containing different P1 residues.....	95
5.3.4 Synthesis of inhibitors 40-45 containing Phe(3/4-AMe) .....	98
5.3.5 Synthesis of inhibitors 46-51 containing Phe(3/4-GMe) .....	100
5.3.6 Synthesis of the inhibitors 52-53 containing Phe(4-Gua) .....	101
5.3.7 Synthesis of inhibitors 54-75 modified in P4 position.....	103
5.3.8 Synthesis of inhibitors 76-78 containing best P1 and P4 residues.....	105
5.3.9 Synthesis of P2 and P3 modified agmatine derivatives 79-88.....	106
5.3.10 Synthesis of inhibitors 89 and 90 with alkylated P1 guanidines.....	108
5.3.11 Synthesis of linearpeptides 91-105 .....	109
5.3.12 Synthesis of cyclic peptides 106-111 .....	111

## Table of contents

---

5.3.13 Synthesis of substrates 112-114 and related intermediates .....	119
5.4 Stability tests of peptides 91-105 .....	120
5.5 Crystal structure determination .....	121
<b>References.....</b>	<b>122</b>
<b>Publications .....</b>	<b>135</b>
<b>Acknowledgment.....</b>	<b>136</b>
<b>Erklärung .....</b>	<b>137</b>
<b>Curriculum Vitae .....</b>	<b>138</b>

---

## 1 Introduction

The mosquito-borne West Nile virus (WNV) was first isolated in 1937 in Uganda as Smithburn tried to isolate yellow fever virus (YFV) from an African woman<sup>1</sup> with suggestive YFV infection. The drawn serum from the infected woman was inoculated through the brains of ten mice, whereby only one mouse survived. Later studies demonstrated that the virus is pathogenic to mice by intracerebral, intranasal or intraperitoneal inoculation, while only a weak pathogenesis was found in mice by subcutaneous application. Rhesus monkeys were also intracerebrally and intranasally treated with the virus, upon which all infected monkeys developed fatal encephalitis. Virus neutralization studies showed immunological similarity between the new virus and the Japanese B encephalitis virus. A histological study demonstrated that the new virus is strictly neurotropic but produces lesions of the central nervous system, which differs from those produced by the other known neurotropic viruses. In 1940, Smithburn introduced the name West Nile virus for this new neurotropic virus, which was isolated from the West Nile district in Uganda.<sup>1</sup> WNV infections were not considered to be serious until the 1990s despite sporadic cases and outbreaks of the disease in humans and horses, which occurred in Europe and South Africa since the 1960s.<sup>2</sup> Individual cases have been also reported in the Middle East and Asia.<sup>3</sup> However, the WNV became a major risk after the first big pandemic in Romania 1996, which was followed by many outbreaks in various European countries (Italy 1998, France 2000–2003), in South Africa and the Middle East. The first WNV infection in the American continent was confirmed in New York in September 1999. The virus spread very rapidly in 46 states through the US and in Canada.<sup>4</sup> In 2012 in the US, 5674 cases of WNV infection in people, including 286 deaths, were reported to the CDC<sup>5</sup> (Centers for Disease, Control and Prevention, US). Therefore, there is a high need to develop drugs against WNV infection and it is important to understand all aspects of WNV life cycle in developing effective prevention and treatment strategies.

## 1.1 Transmission

The WNV proliferation takes place through circulation between two main vectors, birds and mosquitoes.<sup>6</sup> Mosquitoes, mainly *Culex* species act as bridge-vectors transmitting the WNV into dead-end vectors, like humans or horses (Figure 1.1). As the female mosquito draws blood from the infected birds, the WNV crosses the mosquito's midgut, and replicates in many tissues, mainly in the nervous system and salivary glands, developing nonpathogenic versions of the virus that persists for the normal life period of the mosquito.<sup>7</sup> Birds that are members of the *Corvidae* family (mainly crows) are highly susceptible to be infected by the mosquitoes, whereby they serve as amplifying hosts.<sup>8</sup> A study on the infected North American birds in 1999 demonstrated that the American crows have the highest viremia titers among the domestic birds ( $10^{10}$  plaque-forming units/ml serum at the fifth day of the infection).<sup>9</sup> Whereby, the WNV could be isolated from the brain, kidney, heart, spleen, liver, lung, intestine, esophagus, gonad, skin and eye of the dead crows.<sup>10</sup> In addition to the main vectors, WNV could be isolated from many other dead-end hosts like humans, equines, rodents, reptiles, amphibians, felines, canines, bats and sea mammals.<sup>11</sup> WNV could be also transmitted by non-mosquito ways like organ transplantation, blood transfusion, lactation, or by *in utero* infection.<sup>12</sup>

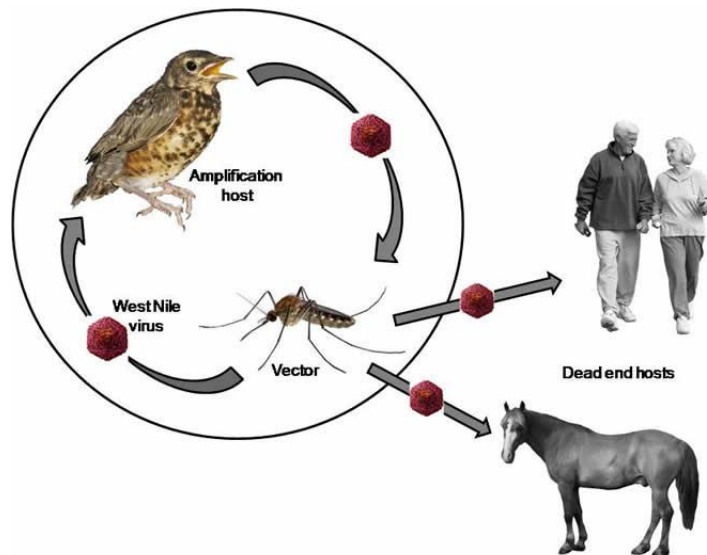


**Figure 1.1:** Transmission cycle of the WNV (<http://www.vetmed.wisc.edu/WNV/background.html>).

### 1.2 Pathogenesis

After an infected mosquito's sting, the WNV is transmitted into humans and mammals intradermally through mosquito's infectious saliva. The virus replicates in the Langerhans cells of the skin, where the virus has been first injected.<sup>13</sup> The infected Langerhans cells immigrate to the local lymph nodes, where the WNV cycle in the blood stream begins causing primary viremia,<sup>14</sup> which is followed by the secondary viremia after its distribution in peripheral tissues like spleen and kidney.<sup>15</sup> The WNV can be detected in the blood one or two days post-infection, while it could largely disappear by the seventh day after inoculation, accompanied with the appearance of IgM (Immunoglobulin M) neutralizing antibodies.<sup>15</sup> WNV can cross the blood brain barrier (BBB) to the central nervous system mainly in children, elderly and people with impaired immune system.<sup>16</sup> WNV is able to infect the spinal cord, brainstem, basal ganglia and neurons, causing meningitis or encephalitis.<sup>17</sup> The mechanism, by which the WNV crosses the BBB to the CNS is still unclear. However, two contradictory studies reported about the role of the Toll-like receptors 3 (TLR3). Wang reported that TLR3 knockdown mice are resistant to lethal WNV infections in comparison to normal mice, suggesting a positive role of TLR 3 in the pathogenesis.<sup>18</sup> Quite the opposite, Daffis demonstrated a protective role of the TLR3 against WNV.<sup>19</sup>

### 1.3 Pathological symptoms

Approximately, 80% of WNV infections are asymptomatic, whereas the symptoms in the other cases range between mild fever (95% of the symptomatic cases) to encephalitis or meningitis.<sup>6</sup> 20% of the cases develop WNV fever accompanied with headache, weakness, vomiting and nonspecific symptoms like muscle or neck pain, confusion and slurred speech. These symptoms could last one month after infection.<sup>20</sup> Less than 1% of the infected people exhibit neuroinvasive disease with neurological symptoms including confusion, delirium, trouble walking, tremors, blurry vision and numbness in limbs or body, which could last for two months to one year after onset.<sup>21</sup> The tendency to develop neuroinvasive diseases increases in people with impaired immune system and elderly.<sup>22</sup> Currently, there exists no specific antiviral treatments or vaccines against WNV infection.

#### 1.4 West Nile virus classification

WNV belongs to the family of *Flaviviridae*. The name is derived from the Latin *flavus* or yellow referring to Yellow fever prototype virus.<sup>23</sup> The *Flaviviridae* family contains four genera; *pestivirus*, *hepacivirus*, *pegivirus* and *flavivirus*.<sup>24</sup> The flavivirus genus is divided depending on the kind of transmission arthropod into tick-borne and mosquito-borne viruses. The mosquito-borne viruses are further subdivided into three serogroups; Dengue (DENV), Yellow Fever (YFV) and Japanese encephalitis (JEV) virus serotype. The JEV serogroup contains the WNV species, which is further subdivided into the WNV and Kunjin virus.<sup>25</sup> To sum up, WNV is classified in the *Flaviviridae* family, genus *flavivirus*, mosquito-borne, member of the JEV serogroup, grouped into the West Nile virus species, West Nile virus subtype.<sup>23,26</sup> (Figure 1.2)

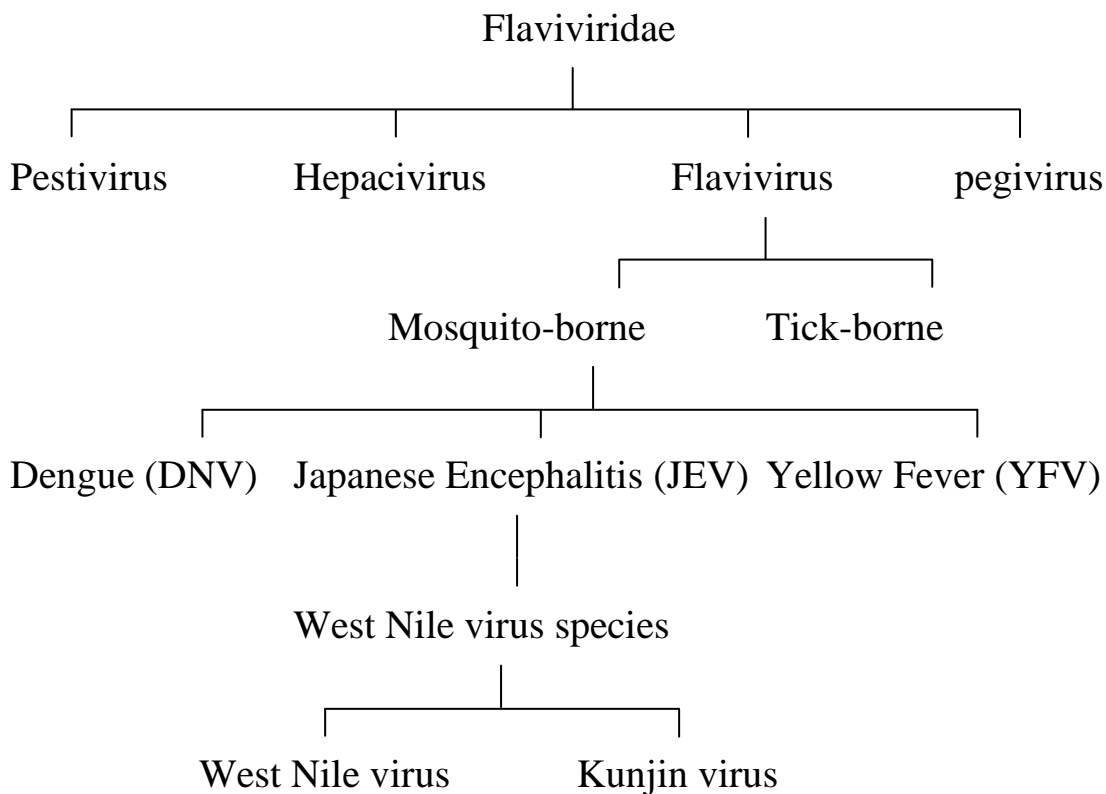


**Figure 1.2:** Pedigree of the WNV.

## 1.5 Morphology and structure of the WNV

The WNV is a relatively small virus, that contains a nucleocapsid with icosahedral shape surrounded by a lipid bilayer.<sup>27</sup> The nucleocapsid is composed of multiple copies of the C protein and the viral RNA. The surface of the virus is composed of two proteins, the envelope protein E and the membrane protein M. Envelope protein E mediates binding and fusion during virus entry into host cells.<sup>27</sup> The E proteins are arranged in head-to-tail homodimers that lie parallel to the lipid, on the viral surface in the mature version of the virus (Figure 1.3). The membrane protein M is produced by furin cleavage from the immature premembrane protein prM. The immature virus is larger than the mature virus due to its spiky shape (~ 60 nm in diameter), and the surface is slightly bigger than the mature virus (~ 50 nm in diameter).<sup>27, 28</sup> After cleavage of the prM-E by furin, the E protein changes the conformation forming a soft layer which lies in parallel to the lipid bilayer.<sup>29</sup> However, the cleaved pr peptide remains attached to the E protein, preventing membrane fusion during virion release at the host cell surface. After the virion entry into the extracellular environment, the pr liberates the E protein at low pH at the trans-Golgi network, allowing the membrane fusion to occur in the next replication cycle.<sup>30</sup>

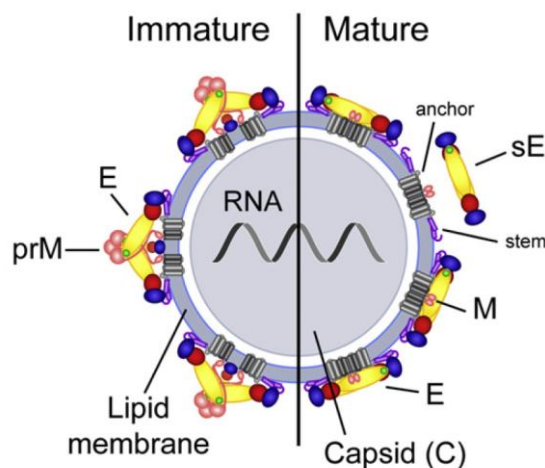


**Figure 1.3:** Schematic representation of a flavivirus particle. Left: immature virion; right: mature virion (figure taken from Heinz et al.).<sup>31</sup>

## 1.6 Replication cycle

The WNV replication cycle begins when the virus binds to the host cells via unknown receptors, possibly lectin DC-SIGNR (dendritic cell-specific intercellular adhesion molecule-3-grabbing nonintegrin)<sup>32</sup> or integrin  $\alpha_v\beta_3$ .<sup>33</sup> After binding to the host cells, the virus enters the cell via clathrin-mediated endocytosis.<sup>34</sup> At low pH, the nucleocapsid is released into the cytoplasm after fusion with the endoplasmic reticulum (ER) in lysosomal vesicles.<sup>32</sup> Afterwards, the viral RNA is translated into a single polyprotein.<sup>27</sup> Subsequently, the viral protease NS2B-NS3 and several host proteases cleave the polyprotein producing ten functional proteins.<sup>27</sup> The viral RNA-dependent RNA polymerase (RdRp) within NS5, in conjunction with other viral nonstructural proteins and possibly cell proteins produces complementary minus strands from the viral RNA template. The minus strand RNAs serve as template for the synthesis of new genomic RNAs, (Figure 1.4).<sup>35</sup> Assembly and arrangement of the new viral units take place in association with intracellular membranes and nascent virions transit through the secretory pathway, where furin mediates the final cleavage event of pr-M prior to virion release from the host cell surface.<sup>30</sup>

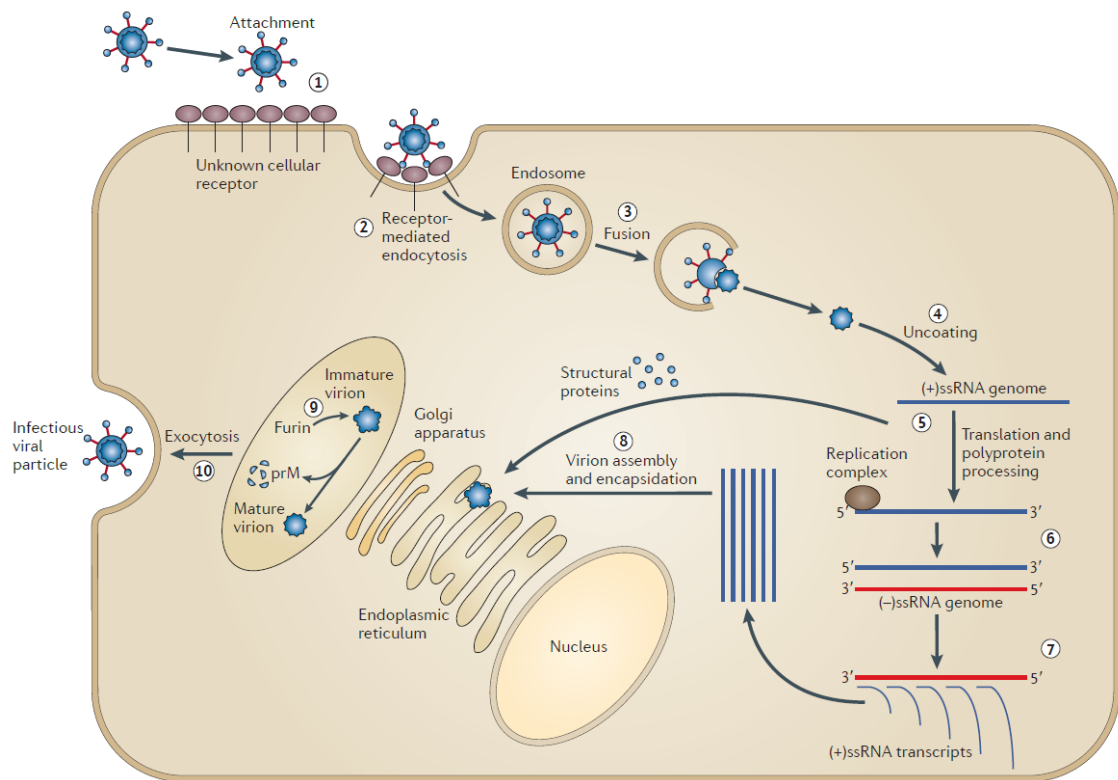


**Figure 1.4:** Life cycle of the West Nile virus; Step 1. Virion binding to the host cells. Step 2. Receptor-mediated endocytosis of the virus. Step 3. Viral fusion with the endosomal membrane due to the low pH environment within the endosomal vesicle. Step 4. Uncoating and release of the genome into the cytoplasm. Step 5. The translation of the viral RNA into a single polyprotein, which is processed by NS2B-NS3 protease to generate mature proteins. Step 6. The NS proteins, including the viral RNA-dependent RNA polymerase NS5, form the replication complex for the synthesis of full-length (+)ssRNAs. Step 7. The negative-stranded RNA serves as template for the synthesis of full length positive-strand RNA. Step 8. Encapsidation of the newly synthesized RNA with the viral capsid protein C, and virion assembly at the ER membranes. Step 9. Maturation of the virions through furin mediated-cleavage of the protein prM to the mature membrane protein. Step 10. Mature virions are transported to the plasma membrane and released by exocytosis (figure taken from Suthar et al.).<sup>36</sup>

### 1.7 Genome structure and processing of the polyprotein

The WNV genome is a single-stranded positive-sense RNA of 11,029 base pairs, which contains a single open reading frame (ORF) of 10,301 nt.<sup>26</sup> The open reading frame starts at the nucleotide 96 at the 5' terminus and stops 631 nucleotids before the 3' terminus.<sup>37, 38</sup> The viral genome serves as mRNA, due to the positive polarity, and is translated immediately by the host ribosomal machinery upon release from the nucleocapsid.<sup>27</sup> A single immature polyprotein precursor is produced by translation of the ORF, followed by co- and post-translationally procedures achieved by both host and viral proteases.

The polyprotein precursor is arranged in the following order from N- to C-terminus: C-prM-E-NS1-NS2A-NS2B-NS3-NS4A-NS4B-NS5 (Figure 1.5).<sup>23, 24, 26, 39, 40</sup> Host proteases cleave the polyprotein at the following junctions, C/prM, prM/E, E/NS1, whereas the viral protease (NS2B-NS3) is considered to cleave at the NS2A/NS2B, NS2B/NS3, NS3/NS4A, and NS4B/NS5 protein junctions.<sup>41</sup> However, the viral replication can not begin until all single proteins are cleaved and released from the polyprotein precursor. Therefore, inhibition of the viral protease (NS2B-NS3) or host proteases could be an attractive target for the design of effective WNV antiviral therapies.

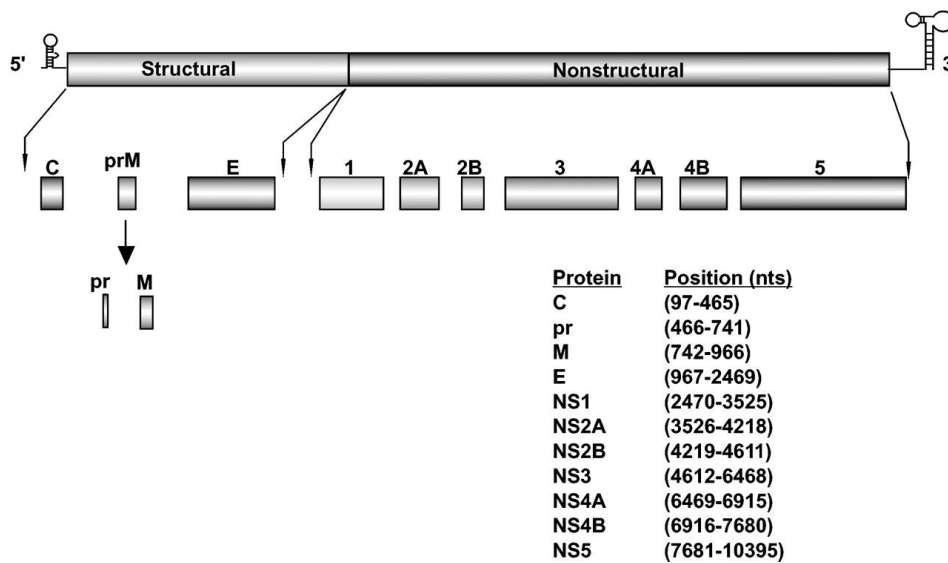


**Figure 1.5:** Viral RNA structure and the polyprotein precursor (figure taken from Brinton et al.).<sup>27</sup>

## 1.8 The biological roles of the nonstructural viral proteins

The viral proteins NS3 and the co-factor NS2B are attached together to form a heterocomplex. NS3 is a large ~70 kDa protein, that contains two distinct enzymatic domains, a protease domain within the N-terminus<sup>41-44</sup> and a helicase/ATPase domain within its C-terminus.<sup>41, 43</sup> The helicase/ATPase domain participates in viral RNA genome replication in association with RdRP in NS5 by unwinding the double-stranded RNA intermediates, facilitating NS5 polymerase activity.<sup>45</sup> The NS3 protease domain is a serine protease, containing the catalytic triad formed by residues Ser135, His51, and Asp75.<sup>46</sup> The main role of NS3 protease is the catalytic processing of the polyprotein to generate the single mature nonstructural proteins (Figure 1.6).<sup>41</sup> However, the viral

protease NS3 is inactive until it forms a complex with the cofactor NS2B. The NS2B is a small ~15 kDa protein, that contains a central hydrophilic domain (II) surrounded with two hydrophobic parts (I, III). It is proposed that the hydrophobic regions of NS2B associate the protein to the ER membrane.<sup>24, 47-49</sup>

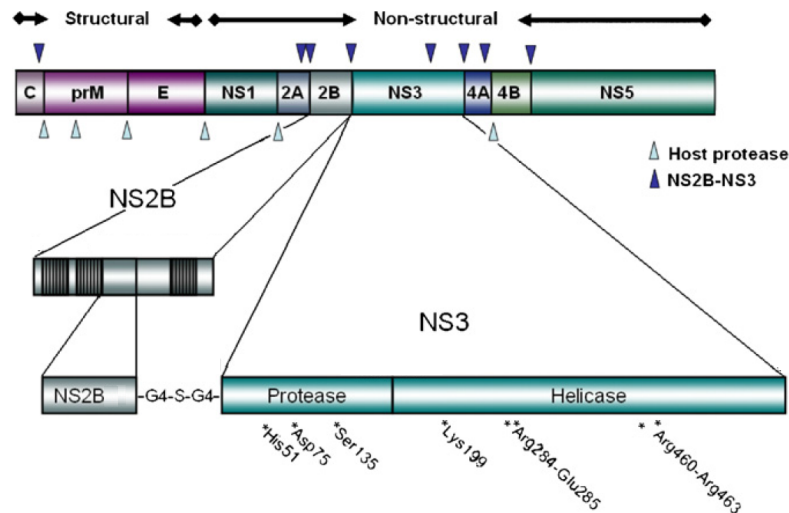


**Figure 1.6:** Schematic representation of the flaviviral polyprotein. Cleavage sites of the polyprotein by the viral NS2B-NS3 and by host proteases. To exhibit the artificial heterocomplex, the NS2B-NS3, is depicted in the enlarged section (figure was adopted from Lescar et al.).<sup>50</sup>

To generate a stable complex of NS2B and NS3 for enzymatic studies and crystallography, an artificial sequence consisting of a (Gly)<sub>4</sub>-Ser-(Gly)<sub>4</sub> sequence was introduced between both domains.<sup>51, 52</sup> A crystal structure of the recombinant NS2B40-G4SG4-NS3 protein domain has been resolved illustrating that NS2B40 wraps around NS3 protein in a belt-like manner.<sup>46, 53</sup> This suggests that NS2B may function as a cofactor to NS3, facilitating the arrangement of the catalytic triad into an active conformation.<sup>27</sup>

The other nonstructural viral proteins NS2A, NS4A, and NS4B are small, hydrophobic proteins and may facilitate the assembly of viral replication complexes and/or their localization on cytoplasmic membranes.<sup>27</sup> NS1 is a glycoprotein with two conserved N-linked glycosylation sites and 12 conserved cysteines that are necessary for the virus viability.<sup>27</sup> NS5 is the largest and most conserved viral protein which is located at the C-terminus of the viral polyprotein. The C-terminal portion of NS5 contains motifs characteristic of all RdRps.<sup>54</sup>

## 1.9 Substrate recognition site of the NS2B-NS3 protease

Studies with a 9-mer peptide library confirmed the strong preference of the WNV protease for substrate sequences with basic amino acids in P1 and P2 position.<sup>55</sup>

The used peptides were deduced from the cleavage sites in the immature WNV polyprotein and are summarized in Table 1.1. showing also the cleavage efficacies in percentage.

**Table 1.1:** Used peptides for the characterization of the substrate specificity of the WNV NS2B-NS3 protease. The sequences span the potential cleavage sites in the WNV polyprotein. The cleavage efficiency in percent is shown in parentheses.<sup>55</sup>

Proteins	WNV (cleavage efficiency, %)
Capsid C protein	Q <sup>0102</sup> KKR↓GGTA <sup>0109</sup> (62)
C/prM	C <sup>0120</sup> AGA↓VTLS <sup>0127</sup> (1)
prM	H <sup>0209</sup> SRR↓SRRS <sup>0216</sup> (6)
prM	R <sup>0212</sup> SRR↓SLTV <sup>0219</sup> (0)
prM/E	P <sup>0297</sup> AYS↓FNCL <sup>0304</sup> (0)
E/NS1	N <sup>0784</sup> VHA↓DTGC <sup>0791</sup> (0)
NS1/NS2A	R <sup>1140</sup> VNA↓YNAD <sup>1147</sup> (0)
NS2A	K <sup>1327</sup> EKR↓SSAA <sup>1334</sup> (0)
NS2A	A <sup>1334</sup> KKK↓GACL <sup>1341</sup> (31)
NS2A/NS2B	N <sup>1367</sup> RKR↓GWPA <sup>1374</sup> (64)
NS2B-NS3	Y <sup>1498</sup> TKR↓GGVL <sup>1505</sup> (73)
NS3Protein/helicase	R <sup>1686</sup> KKQ↓ITVL <sup>1693</sup> (4)
NS3Protein/helicase	K <sup>1700</sup> TRK↓ILPQ <sup>1707</sup> (3)
NS3Protein/helicase	K <sup>1716</sup> RLR↓TAVL <sup>1723</sup> (0)
NS3helicase	A <sup>1957</sup> QRR↓GRIG <sup>1964</sup> (2)
NS3/NS4A	S <sup>2117</sup> GKR↓SQIG <sup>2124</sup> (0)
NS4A	E <sup>2243</sup> KQR↓SQTD <sup>2250</sup> (0)
NS4A/NS4B	A <sup>2266</sup> VAA↓NEMG <sup>2273</sup> (0)
NS4B/NS5	G <sup>2522</sup> LKR↓GGAK <sup>2529</sup> (73)

These data showed the preference of the NS2B-NS3 protease for substrates containing arginine as P1 residue, whereby one sequence with lysine in the NS2A protein was also accepted. Furthermore, a strict requirement for the presence of a basic P2 residue was found, whereby a lysine seemed to be preferred over arginine. Many efficiently cleaved

sequences contained an additional basic amino acid in P3 position. However, some substrates possessed also a neutral amino acid as P3 residue.

Moreover, the protease showed a strong preference for glycine at P1' and P2' positions. However, the cleavage site between NS2A and NS2B containing a P2' tryptophan was also excellently cleaved.

In conclusion, substrates with the consensus sequence X-K/R-R↓GG were optimally recognized by the WNV protease.<sup>55</sup>

### **1.10 Antiviral strategies**

Presently, there is no specific antiviral treatment or vaccines against WNV infection. The most effective preventive measure is the avoidance of mosquitos' bites. The only treatment available is supportive management.<sup>6</sup> In severe cases, high dependency care, including ventilation, is required. Interferon alpha, ribavirin, and WNV-specific immunoglobulins from previously infected patients have also been proposed as antiviral treatments.<sup>56, 57</sup> Several human vaccines are available for infections by related viruses like YFV, JEV and tick-borne encephalitis virus, which employ the high antigenicity of their prM and E proteins.<sup>24</sup> Therefore, the prM and E proteins of the YFV vaccine strain were replaced with the WNV prM and E proteins in chimeric viruses, which have shown promise for vaccine development.<sup>58</sup>

The different stages of the WNV replication cycle could be used to develop new antiviral therapies. One strategy is the blocking of the virus entry utilizing antibodies directed against the E protein, subsequently inhibiting receptor binding and thus preventing the internalization of the virion into the host cell.<sup>59, 60</sup> Other treatments could be the inhibition of RdRp within NS5 and of the helicase activity of NS3, both approaches should prevent the synthesis of viral RNA.<sup>59</sup> As previously mentioned, the host protease furin plays a major role in virion maturation. Therefore, the inhibition of furin or other host proteases, which are involved in the processing of the WNV polyprotein, could be an alternative therapeutic strategy.<sup>59</sup> However, the blocking of host enzymes could result in nonspecific side effects due to the downregulation of normal physiological mechanisms. This problem could be overcome by the selective inhibition of viral targets. Therefore, the WNV NS2B-NS3 protease, which has a major

role in the processing of the polyprotein precursor, is an attractive target for new drugs against WNV.

### 1.11 Known WNV NS2B-NS3 protease inhibitors

Aprotinin is a nonspecific serine protease inhibitor and inhibits also the WNV protease with a  $K_i$  value of 26 nM. It is isolated from bovine lung and has a molecular weight of 6512 g/mol consisting of 58 amino acids.<sup>61</sup> Aprotinin was used in heart surgery with cardiopulmonary bypass to reduce bleeding by slowing down fibrinolysis through plasmin inhibition.<sup>62</sup> It was withdrawn from the market due to side effects in 2008.<sup>63</sup>

Various polypeptides composed of D-arginine residues have been reported as WNV protease inhibitors. Both, the undeca-D-Arg-NH<sub>2</sub> and dodeca-D-Arg-NH<sub>2</sub> possess  $K_i$  value of ~1 nM, whereas a relatively poor inhibition constant of ~ 500 nM was found for the hexa-D-Arg-NH<sub>2</sub> analogue (Table 1.2).<sup>64</sup>

**Table 1.2.** D-arginine-derived oligopeptide inhibitors of the WNV NS2B-NS3 protease

Comp.	$K_i$ (nM)
(D)RRRRRR-NH <sub>2</sub> ; hexa-D-Arg-NH <sub>2</sub>	478±20
(D)RRRRRRR-NH <sub>2</sub> ; hepta-D-Arg-NH <sub>2</sub>	41±18
(D)RRRRRRRR-NH <sub>2</sub> ; octa-D-Arg-NH <sub>2</sub>	17±11
(D)RRRRRRRRR-NH <sub>2</sub> ; nona-D-Arg-NH <sub>2</sub>	6±1
(D)RRRRRRRRRR-NH <sub>2</sub> ; deca-D-Arg-NH <sub>2</sub>	2±1
(D)RRRRRRRRRRR-NH <sub>2</sub> ; undeca-D-Arg-NH <sub>2</sub>	1±1
(D)RRRRRRRRRRRR-NH <sub>2</sub> ; dodeca-D-Arg-NH <sub>2</sub>	1±1

Well-known warheads of serine protease inhibitors are aldehydes, boronic acids, and various ketone derivatives.<sup>65</sup> Several tetrapeptides containing a C-terminal arginal or other aldehydes were reported by Knox with  $IC_{50}$  values range between 1 and 200  $\mu$ M.<sup>46</sup> The most potent inhibitors and their  $IC_{50}$  of this series are shown in Table 1.3.

**Table 1.3:** Arginal inhibitors of the WNV protease

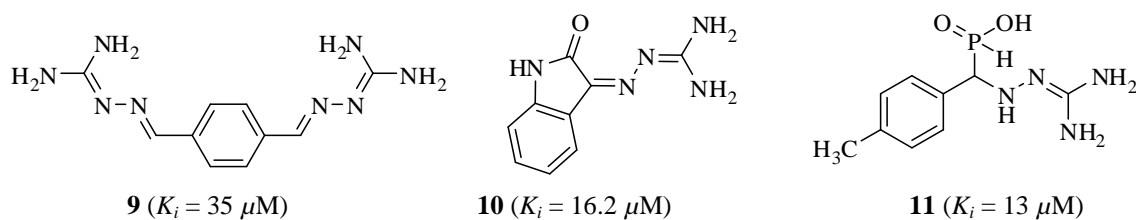
Comp.	aldehyde inhibitors	$IC_{50}$ ( $\mu$ M)
<b>1</b>	Bz-Nle-Lys-Arg-Arg-H	4.1
<b>2</b>	Bz-Ala-Lys-Arg-Arg-H	0.7
<b>3</b>	Bz-Phe-Lys-Arg-Arg-H	1.2
<b>4</b>	Bz-Nle-Lys-Lys-Arg-H	1.9

Later, additional arginal derivatives have been reported by Stoermer et al.<sup>66</sup> The use of the sequence P4-Lys-Lys-Arginal provided strongly improved inhibitors, selected analogues are shown in Table 1.4.

**Table 1.4:** P4-Lys-Lys-Arginal inhibitors of the WNV protease.

Comp.	P4	$K_i$ (nM)
<b>5</b>	2-naphthoyl-	41
<b>6</b>	phenylacetyl-	9
<b>7</b>	4-phenyl-phenylacetyl-	6
<b>8</b>	3-methoxy-phenylacetyl-	11

A HTS search for positively charged inhibitors that were able to mimic the bifurcated guanidine side chain of the P1 Arg residue led to the identification of the commercially available compounds **9-11**, which inhibit the WNV protease with  $K_i$  values in the micromolar range (Figure 1.7).<sup>67</sup>

**Figure 1.7:** Inhibition of the WNV NS2B-NS3 protease by guanylylhydrazones

A further screening of 32,000 small molecules provided two 8-hydroxyquinoline derivatives with  $K_i$  values of  $\sim 3 \mu$ M (**12** and **13**, Figure 1.8).<sup>68</sup> Furthermore, compound **13** was capable of inhibiting WNV RNA replication in cultured Vero cells with an  $EC_{50}$  of  $1.4 \mu$ M

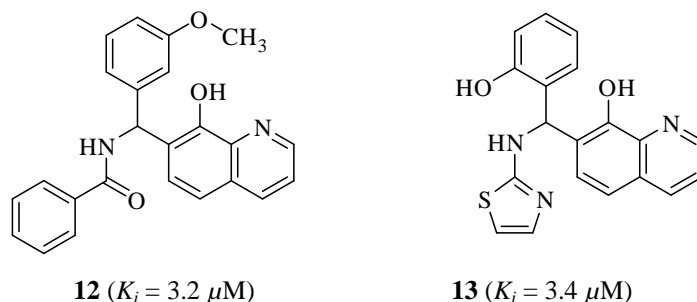


**Figure 1.8:** 8-hydroxyquinolin-derived WNV NS2B-NS3 inhibitors.

Various agmatine and agmatine-like peptidomimetic inhibitors of the WNV were first reported in 2011.<sup>69</sup> Such peptides with decarboxylated arginine mimetics in P1 position have been originally used for the inhibition of the trypsin-like serine protease thrombin,<sup>70</sup> urokinase<sup>71</sup>, factor Xa,<sup>72</sup> factor VIIa,<sup>73</sup> plasmin<sup>74</sup> and the proprotein convertase furin, which contains a  $\text{Ca}^{2+}$ -dependent subtilisin-like protease domain.<sup>75</sup> For the most potent analogue 2-(biphenyl)acetyl-Lys-Lys-agmatine a  $K_i$  value of  $2 \mu\text{M}$  was found (Figure 1.9).

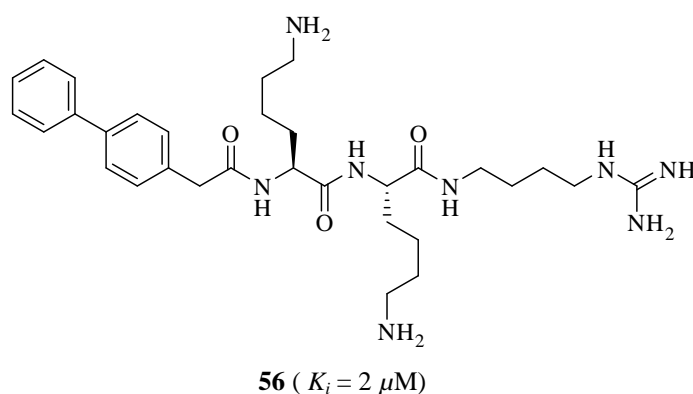


**Figure 1.9:** 2-(biphenyl)acetyl-Lys-Lys-agmatine

Moreover, some allosteric inhibitors of the WNV protease were identified by screening of a small molecule library. The found pyrazolyl benzoic acid ester derivatives inhibit the WNV protease with  $IC_{50}$  values of  $0.1 \mu\text{M}$  (Figure 1.10).<sup>76</sup>

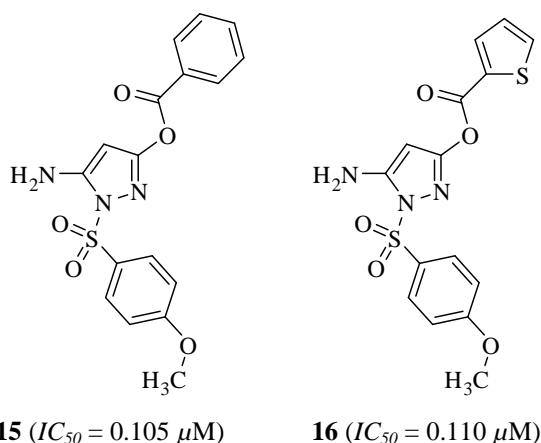


**Figure 1.10:** Pyrazolyl benzoic acid ester derived WNV protease inhibitors.

So far, only limited progress has been achieved in the field of synthetic WNV protease inhibitors. However, meanwhile several crystal structures of the WNV protease are available, which will enable a more rational, structure-based inhibitor design in the future.

### 1.12 Crystal structures of the WNV protease

In the native WNV protease the NS2B forms a non-covalent complex with NS3. However, all crystal structures have been solved with various artificial protease constructs expressed in *E. coli*, whereby the used proteins contain a flexible linker segment of 9 amino acids, which covalently connects the relevant parts of the NS2B and NS3 domains.<sup>51</sup>

In one of the known structures the WNV protease is inhibited by the natural inhibitor aprotinin. In contrast to small molecule inhibitors, aprotinin occupies with its P3-P4'-segment Pro-Cys-Lys(P1)-Ala-Arg-Ile-Ile all major binding pockets of the protease (2ijo.pdb)<sup>63</sup> (Figure. 1.11). The catalytic triad of the WNV protease is formed by residues His51, Asp75, and Ser135, which are arranged in a similar manner, as in several other serine proteases of the S1 and S8 subfamily. The distance of the side chain oxygen of the catalytic Ser135 and the carbon of the P1 Lys carbonyl group is approximately 2.8 Å, which indicates that, the P1-P1' peptide bond in this complex is not cleaved.<sup>63</sup>

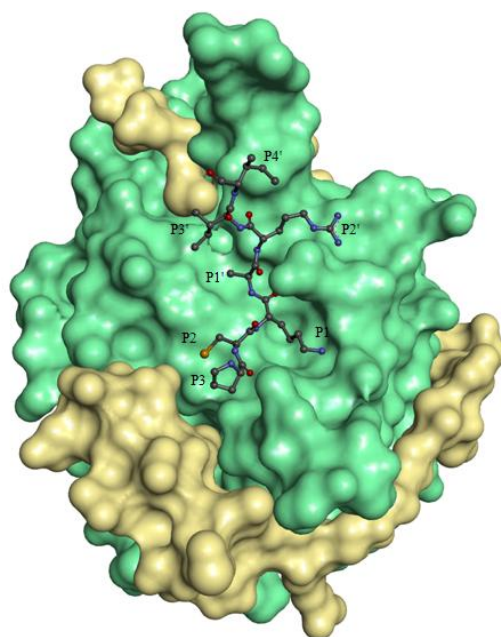


**Figure 1.11:** Crystal structure of the WNV protease in complex with aprotinin (2ijo.pdb). The surface of the NS2B and NS3 domains are colored in yellow and green, respectively. For better visualization only the P3-P4' segment (Pro-Cys-Lys-Ala-Arg-Ile-Ile) of aprotinin is shown.

The comparison of the aprotinin complex with the inhibitor-free structure (2ggv.pdb) revealed that the WNV NS2B-NS3 protease can exist in two distinct conformations; the inhibitor-bound close conformation and the inhibitor-free open conformation. The major difference between these two structures lies in the conformation of the NS2B cofactor. In both inhibitor-free and -bound structures, the  $\beta$ 1 strand of the NS2B have the same conformation, while the residues following Trp62 adopt a completely new conformation in the inhibitor-free protease.<sup>63</sup>

In complex with inhibitor, the NS2B cofactor forms a belt that wraps the NS3 protein (Figure 1.12). In contrast, a new turn-and-a-half helix ( $\alpha_1$ ) followed by an unexpected reversal of the protein chain is found for the NS2B in the inhibitor-free structure forming an enzymatically inactive open conformation<sup>63</sup> (Figure. 1.12).

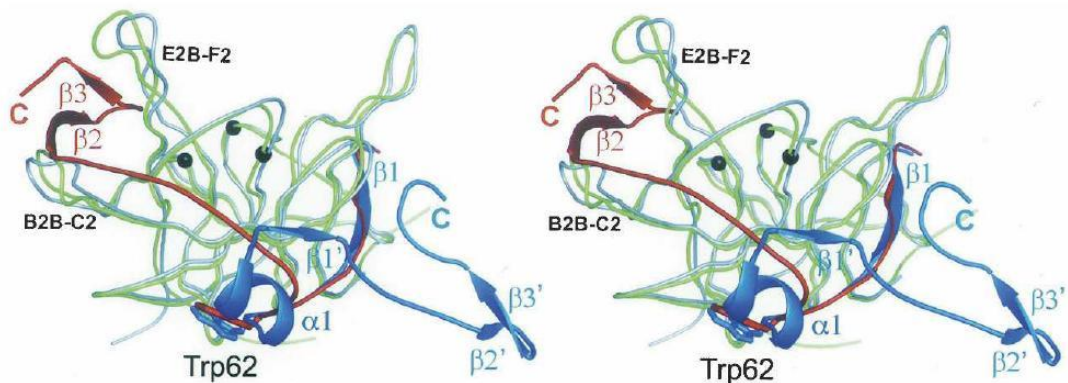


**Figure 1.12:** Stereo view of the two possible conformations of the NS2B cofactor. The NS3 of the closed conformation is shown in green and stabilized by the surrounding NS2B cofactor in red, forming the active protease. In contrast NS2B in the open conformation is shown in blue, where residues after Trp62 point in a completely different direction, which results in an inactive protease, (figure taken from Aleshin et al.).<sup>63</sup>

Furthermore, crystal structures of the WNV NS2B-NS3 protease in the closed conformation have been solved in complex with aldehyde-derived inhibitors. In the complex with Benzoyl-Nle-Lys-Arg-Arg-H (2fp7.pdb),<sup>46</sup> the crystal structure revealed that the S1 pocket is surrounded by Gly151, Tyr161, Tyr150, Asp129 and the backbone of residues of Tyr130–Thr132. Asp129 is located at the bottom of the S1 pocket and binds to the positively charged arginal side chain (Figure 1.13), whereby Tyr161 makes  $\pi$ -cation stacking interactions with the same residue. The S2 pocket is dominated by the negative electrostatic potential originating from the backbone carbonyl oxygen atoms of NS2B residues Asp82 and Gly83 and the O $\delta$ 1 atom of Asn84. These atoms are close to the positively charged guanidinium group of the P2 arginine, which was also within hydrogen bonding distance to Asn152 of NS3. The P3 lysine forms two H-Bonds, to the backbone carbonyl of Phe 85 and to the side chain carbonyl of Gln86, otherwise its side chain and the P4 norleucine are largely solvent exposed.<sup>46</sup>

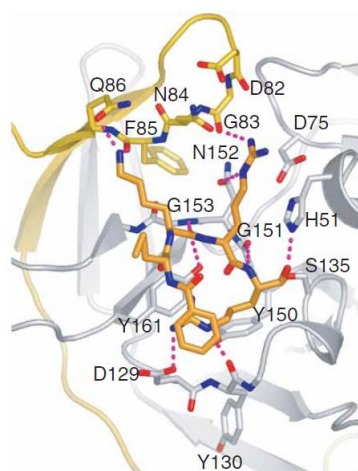


**Figure 1.13:** X-ray structure of the substrate-binding region of WNV NS2B–NS3pro, hydrogen bonds are indicated (dotted lines) (figure taken from Erbel et al.).<sup>46</sup>

An additional structure was solved in complex with the aldehyde 2-naphthoyl-Lys-Lys-Arg-H (3e90.pdb).<sup>77</sup> The structure revealed that the carbonyl oxygen of the P1 aldehyde is attacked by the serine hydroxyl and forms a tetrahedral hemiacetal. Interestingly, this oxygen is oriented in different ways in the asymmetric units, which contains two protein molecules. In one structure, it is rotated away from His51 and points into the oxyanion hole, forming H-bonds with the main chain nitrogens of Gly133 and Ser135 (Figure 1.14, a). In the second complex, the P1 carbonyl oxygen interacts via a H-bond with His51 (Figure 1.14, b).<sup>77</sup> Only this second interaction was observed in the complex with Benzoyl-Nle-Lys-Lys-Arg-H, described above.<sup>46</sup>

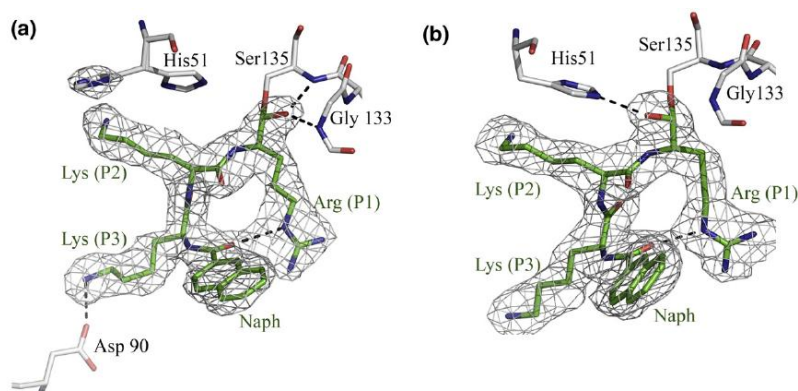


**Figure 1.14** Two different binding modes of 2-naphthoyl-Lys-Lys-Arg-H in complex with the WNV NS2B-NS3 protease. (a) The P1 carbonyl oxygen interacts with the backbone nitrogens of Gly133 and Ser135 in the oxyanion hole, and (b) is alternatively directed towards His51 in the second complex, (figure taken from Robin et al.).<sup>77</sup>

## 2 Aim of work

Currently, there are no vaccines or specific treatments for WNV infections available, despite an increased number of fatal cases worldwide. Since the West Nile virus NS2B-NS3 protease is essential for viral replication, it is a potential target for the development of new antiviral medicaments for the treatment of WNV infections. Therefore, the aim of this work was to design, synthesize and characterize new specific inhibitors against the WNV NS2B-NS3 protease. To achieve this objective, the following tasks should be performed:

- Incorporation of decarboxylated P1 arginine mimetics in substrate-analogue inhibitor structures, a strategy, which was known from the development of highly potent inhibitors against trypsin like serine proteases and proprotein convertases.
- Variation and optimization of the P2 and P3 residues by incorporation of various basic or hydrophobic amino acids.
- Optimization of the P4 residue using a constant P3-P1 Lys-Lys-arginine segment.
- Combination of the most suitable P4, P3, P2 and P1 residues.
- The inhibitory potency against the WNV NS2B-NS3-protease should be determined by an enzyme kinetic assay. For this purpose, a suitable fluorescence substrate should be developed. The specificity of selected derivatives should be tested with various trypsin like serine proteases.
- Appropriate inhibitors should be provided for crystal structure analysis in complex with the WNV protease.
- The information from crystal structure analysis should be used for further inhibitor optimization, e.g., for the development of cyclic inhibitors.
- All of these inhibitors should be prepared by a combination of solution and solid phase peptide synthesis (SPPS).

### 3 Results and discussion

#### 3.1 Inhibitors containing decarboxylated P1 arginine mimetics

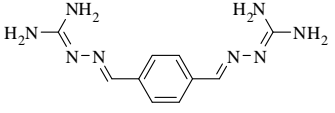
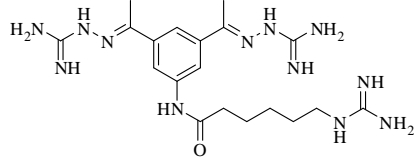
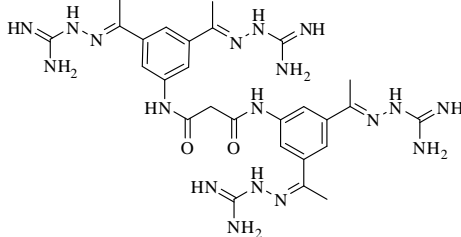
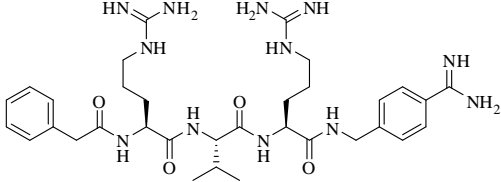
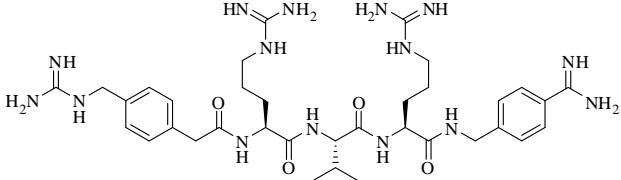
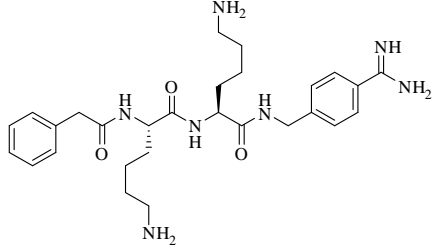
In previous HTS studies it was shown that multiple positively charged compounds like guanyldrazones inhibit the WNV protease with moderate  $K_i$  values.<sup>67</sup> Therefore, similar multibasic inhibitors, which were originally synthesized in our laboratories for inhibiting furin,<sup>75, 78</sup> were initially screened with the WNV protease.

In our assay, the guanyldrazones **9** and **115**<sup>78</sup> possess a moderate affinity against the WNV protease ( $K_i \sim 30 \mu\text{M}$ , Table 3.1), whereby a further increase in potency was determined for compound **116** ( $K_i = 1.7 \mu\text{M}$ ) containing four guanyldrazone groups, which confirms the known preference of the WNV protease for multibasic substrates and inhibitors.<sup>64</sup>

Substrate-analogue inhibitors containing the decarboxylated P1 arginine mimetic 4-amidinobenzylamid or related analogues have been used for a long time to inhibit the trypsin-like serine protease thrombin,<sup>70</sup> urokinase,<sup>71</sup> factor Xa,<sup>72</sup> factor VIIa,<sup>73</sup> plasmin,<sup>74</sup> and the proprotein convertase furin.<sup>75, 79</sup> Some of the multibasic 4-amidinobenzylamide-derived furin inhibitors such as compounds **117** and **118**, also reveal a moderate inhibition of the WNV protease with  $K_i$  values of 35 and 5.7  $\mu\text{M}$ , respectively. Deletion of the P3 valine and replacement of both arginines with lysine residues of compound **117** led to a slightly improved potency against the WNV protease (**37**,  $K_i = 11.5 \mu\text{M}$ ) and a reduced furin affinity.

## Results and discussion

**Table 3.1:** Screening of previously synthesized multibasic furin inhibitors<sup>75, 78, 79</sup> with WNV protease.

No.	Structure	$K_i$ ( $\mu\text{M}$ )	
		WNV	Furin
9 (MI-0307)		29 <sup>a</sup>	1.5
115 (MI-0037)		27	1.42
116 (MI-0035)		1.7	1.13
117 (MI-0227)		35	$8 \times 10^{-4}$
118 (MI0701)		5.7	$1.6 \times 10^{-5}$
37 (MI-0324)		11.5	14.5

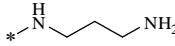
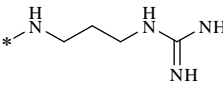
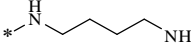
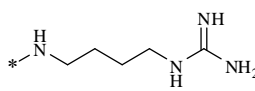
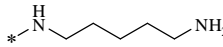
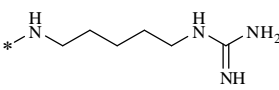
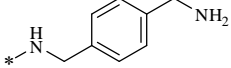
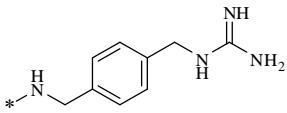
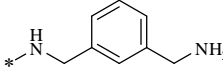
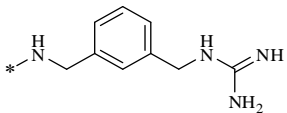
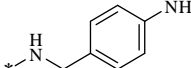
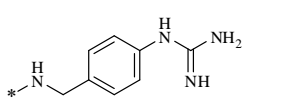
<sup>a</sup> a  $K_i$  of 35  $\mu\text{M}$  was previously described in literature for this compound.<sup>67</sup>

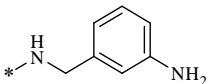
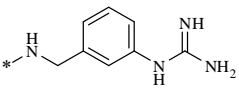
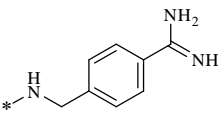
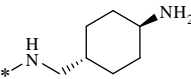
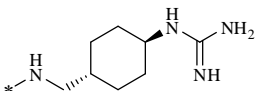
The determined  $K_i$  values shown in Table 3.1 revealed that the 4-amidinobenzylamide is less suitable as P1 residue in WNV protease inhibitors. To enhance the potency of these substrate-analogue inhibitors, the 4-amidinobenzylamide was replaced by other decarboxylated arginine mimetics (Table 3.2). However, during the course of our work,

## Results and discussion

substrate analogue agmatine derivatives were already published as WNV protease inhibitors by Lim and coworkers.<sup>69</sup> The most potent analogue of Lim's first inhibitor series, 2-(biphenyl)acetyl-Lys-Lys-agmatine, inhibits the WNV protease with a  $K_i$  value of 2  $\mu\text{M}$ . This compound was resynthesized in our laboratory as reference, whereby a similar inhibition constant of 1.8  $\mu\text{M}$  against the WNV protease was determined under our assay conditions.

**Table 3.2:** Inhibition of WNV protease by substrate analogue inhibitors with the general formula Phac-Lys-Lys-P1.

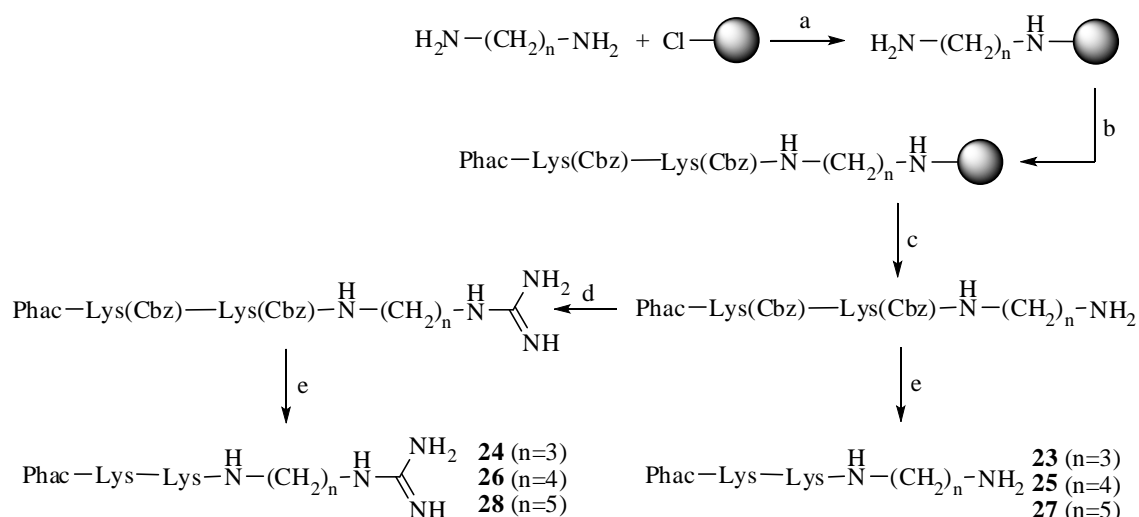
No.	P1	$K_i$ ( $\mu\text{M}$ )
23 (MI-0631)		134
24 (MI-0638)		16
25 (MI-0629)		31
26 (MI-0637)		3.9
27 (MI-0632)		34
28 (MI-0635)		7.2
29 (MI-0639)		52
30 (MI-0642)		19
31 (MI-0633)		46
32 (MI-0636)		25
33 (MI-0640)		54
34 (MI-0643)		16

<b>35</b> (MI-0641)		52
<b>36</b> (MI-0644)		23
<b>37</b> (MI-0324)		11.5
<b>38</b> (MI-0645)		84
<b>39</b> (MI-0646)		1.2

In this series, the P1 residue was modified keeping Phac-Lys-Lys as a constant P4–P2 segment derived from inhibitor **37**, which was also previously used in tripeptidic arginal inhibitors.<sup>66</sup> Among derivatives **23–28** possessing a linear P1 residue, the highest potency with  $K_i = 3.9 \mu\text{M}$  was found for the agmatine analogue **26** (Table 3.2). This confirms previous results from a related series containing a slightly different P4 residue.<sup>69</sup> However, we found only a twofold decrease in potency for the homoagmatine derivative **28**, which was  $> 20$ -fold less active in the previous work.<sup>69</sup> In general, all compounds containing a primary amino group at the P1 position are less active than their guanidino analogues. No improvement was observed for derivatives **29–37** containing more rigid aromatic P1 residues. As already described above, the 4-amidinobenzylamide inhibitor **37** has relatively a poor affinity against the WNV protease, although it is an excellent P1 residue in inhibitors targeting serine proteases of families S1 and S8.<sup>75</sup> This might be explained by the significant structural differences between their S1 pockets. The S1 pocket of the WNV protease, which belongs to the serine protease family S7, is shallower and partially solvent exposed relative to that of the trypsin- and furin-like serine proteases, both of which possess a deeply buried S1 site perfectly suited for efficient binding of a benzamidine group. Negligible activity was determined for inhibitor **38** containing *trans*-4-amidomethylcyclohexylamine, although this P1 group is well suited for the design of thrombin inhibitors.<sup>80, 81</sup> However, its conversion into a guanidine residue in analogue **39** provided the most potent inhibitor of this series, possessing a  $K_i$  value of  $1.2 \mu\text{M}$ .

### Synthesis of inhibitors listed in Table 3.2

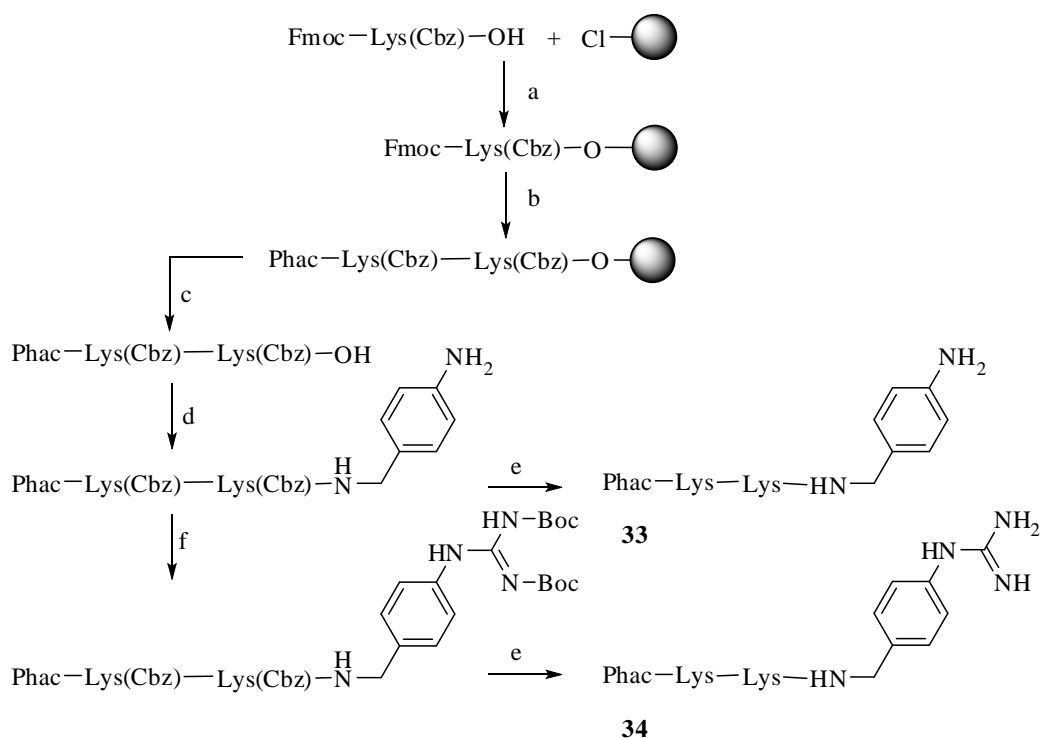
For the preparation of these analogues, a solid-phase approach on acid-sensitive trityl chloride resin was used, as previously described for the synthesis of furin inhibitors.<sup>75</sup> Scheme 3.1 shows the synthetic strategy for all inhibitors containing a symmetric diamine moiety at the P1 position. Conversion of the C-terminal free amino group of the side-chain-protected intermediates with 1*H*-pyrazole-1-carboxamide × HCl provided the corresponding guanidines after final deprotection. The same strategy was used for the synthesis of inhibitors **29–32**; however, in that case, the synthesis was started by loading the trityl chloride resin with para- and meta-aminomethylbenzylamine.



**Scheme 3.1.** Synthesis of inhibitors **23–28**. Reagents and conditions: a) Loading of the trityl chloride resin, 4 equiv diamine in dry DCM, 2 h, RT; b) standard Fmoc-SPPS, single couplings with 4 equiv amino acid (or phenylacetic acid), HOBT and HBTU, respectively, and 8 equiv DIPEA, 2 h, RT; c) TFA/TIS/H<sub>2</sub>O (95:2.5:2.5, v/v/v), 2 × 20 min; d) 3 equiv 1*H*-pyrazole-1-carboxamide × HCl, 4 equiv DIPEA in DMF, 16 h; e) 32% HBr/AcOH, 1 h, RT, preparative HPLC.

Inhibitors **33** and **34** were prepared according to Scheme 3.2, starting with loading of the protected P2 residue onto the 2-chlorotrityl chloride resin. The analogous compounds **35** and **36** and the benzamidine derivative **37** were synthesized by an identical strategy, using 3-(aminomethyl)aniline or 4-(aminomethyl)benzamide<sup>75</sup> instead of 4-(aminomethyl)aniline for coupling to the intermediate Phac-Lys(Cbz)-Lys(Cbz)-OH. For the synthesis of inhibitors **38** and **39**, the intermediate trans-(4-Fmoc-aminomethyl)cyclohexylamine (**17**) was prepared by starting from trans-N-(4-tert-butoxycarbonylamino)cyclohexylmethylamine.<sup>80</sup> Intermediate **17** was used for loading of the trityl chloride resin. The inhibitors **38** and **39** were further synthesized

according to Scheme 3.1, whereby *N,N'*-di-Boc-1*H*-pyrazole-1-carboxamide was used for the conversion of the C-terminal amino group into a Boc-protected guanidine.



**Scheme 3.2:** Synthesis of inhibitors **33-34**. (a) Loading of 2-chlorotrityl chloride resin, Fmoc-Lys(Cbz)-OH, 4 equiv DIPEA, dry DCM, 2h; (b) Fmoc SPPS (see Scheme 3.1); (c) TFA/TIS/H<sub>2</sub>O (95/2.5/2.5, v/v/v), 2×20 min; (d) 1 equiv 4-(aminomethyl)aniline, 1 equiv PyBOP, 1 equiv DIPEA, DMF; (f) 2 equiv *N,N'*-di-Boc-1*H*-pyrazole-1-carboxamide, 4 equiv DIPEA in DMF, 16 h; (e) HBr/ acetic acid, 1h, preparative HPLC.

### 3.2 Modification of P2 and P3 residues

The results of the first inhibitor series revealed a preference of the WNV protease for the GCMA residue in P1 position (Table 3.2). Therefore, an attempt to replace lysine at P2, P3 or both of them with bigger and more rigid basic residues was performed, whereby the P1 GCMA- and P4 phenylacetyl-residue were maintained (Table 3.3).

**Table 3.3:** Inhibition of WNV protease by inhibitors with the general formula Phac-P3-P2-GCMA.

No.	P3	P2	$K_i$ ( $\mu\text{M}$ )
<b>40</b> (MI-0648)	Phe(4-AMe)	Lys	4.7
<b>41</b> (MI-0649)	Lys	Phe(4-AMe)	29
<b>42</b> (MI-0647)	Phe(4-AMe)	Phe(4-AMe)	13.6
<b>43</b> (MI-0656)	Phe(3-AMe)	Lys	22.2
<b>44</b> (MI-0653)	Lys	Phe(3-AMe)	134
<b>45</b> (MI-0655)	Phe(3-AMe)	Phe(3-AMe)	44
<b>46</b> (MI-0651)	Phe(4-GMe)	Lys	43
<b>47</b> (MI-0650)	Lys	Phe(4-GMe)	76
<b>48</b> (MI-0652)	Phe(4-GMe)	Phe(4-GMe)	85
<b>49</b> (MI-0657)	Phe(3-GMe)	Lys	30
<b>50</b> (MI-0654)	Lys	Phe(3-GMe)	99
<b>51</b> (MI-0658)	Phe(3-GMe)	Phe(3-GMe)	21.5
<b>52</b> (MI-0659)	Lys	Phe(4-Gua)	18.2
<b>53</b> (MI-0660)	Phe(4-Gua)	Lys	29.8

All inhibitors listed in Table 3.3 have reduced potency compared with the reference compound **39**. Among them, the best  $K_i$  value was found for Phac-Phe(4-AMe)-Lys-GCMA **40** with a 4 fold reduced potency of 4.7  $\mu\text{M}$ . Furthermore, the conversion of the free amino group at the P3 side chain of inhibitor **40** into guanidine (compound **46**) is not accepted and results in a 10-fold weaker WNV protease inhibition ( $K_i > 40 \mu\text{M}$ ).

The P2 and P3 residues in the derivatives **40** and **46** were reversed to obtain analogues **41** and **47**, however, this modification led to a dramatic loss of potency. These results raise the assumption that the S2 pocket of the WNV protease is too small to accommodate the more bulky substituted phenylalanines, and is only accepting the flexible lysine in P2 position. Additional replacement of the P2 and P3 lysine residues by Phe(4-AMe) led also to a nearly 13-fold reduced inhibitory potency (inhibitor **42**). Further deterioration was found after the guanylation of the Phe(4-AMe) side chain at P2 and P3 in compound **48**.

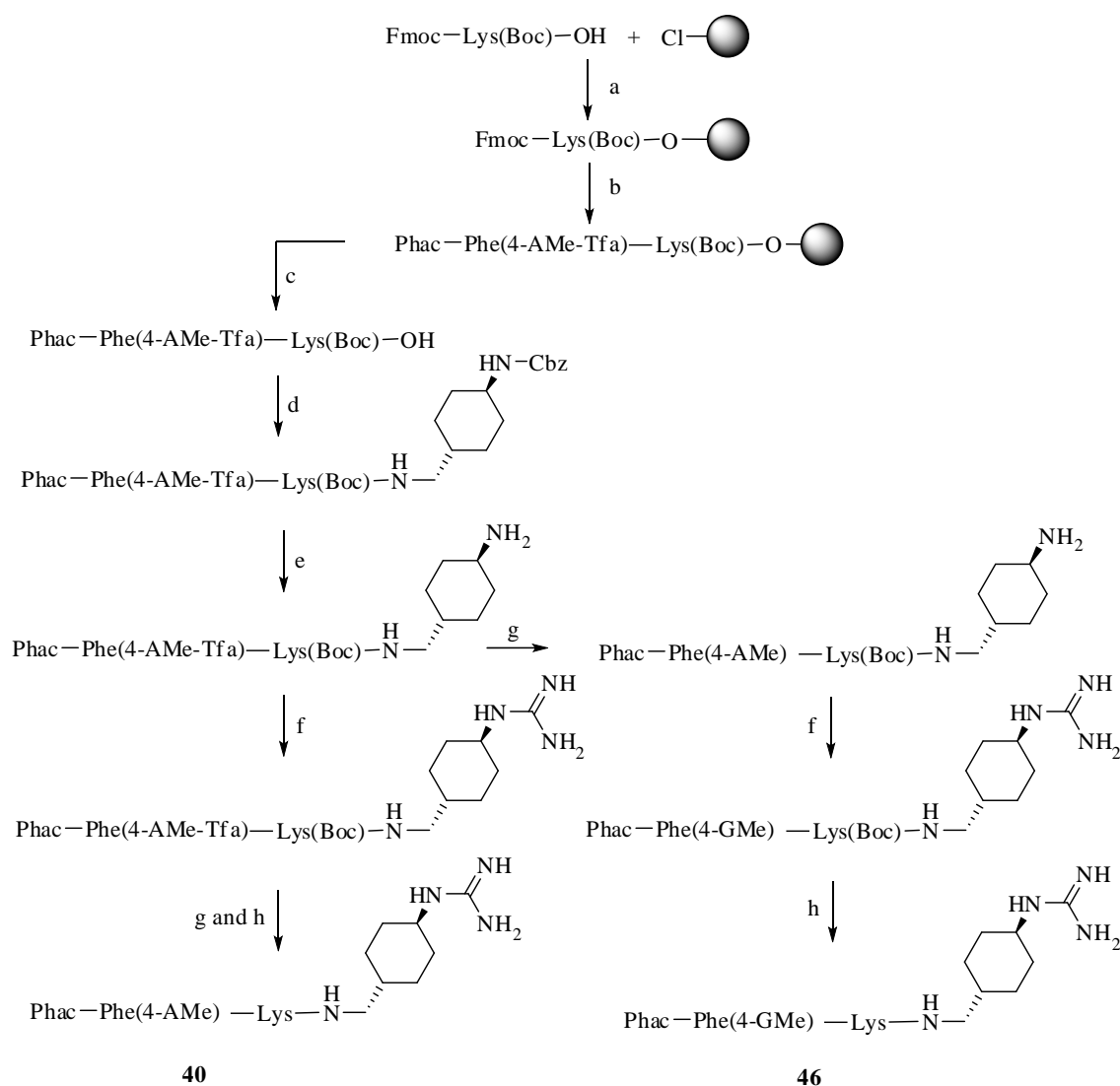
Additional analogues **43-45** and **49-51** were prepared using the meta-substituted phenylalanine derivatives Phe(3-AMe) and Phe(3-GMe). The  $K_i$  values of these inhibitors are summarized in Table 3.3, however, all of them have a poor affinity

against the WNV protease ( $K_i > 20 \mu\text{M}$ ). Two additional inhibitors **52** and **53** were prepared using para- guanylated phenylalanine in P2 or P3 positions, whereby they also possess poor potency ( $K_i$  values 18 and 30  $\mu\text{M}$ , respectively). All of these data reveal that lysine is the most suitable P2 and P3 residues in substrate-analogue WNV protease inhibitors known so far.

### Synthesis of inhibitors listed in Table 3.3

Inhibitors **40** and **46** were prepared according to Scheme 3.3, starting with the loading of the protected P2 residue onto the 2-chlorotrityl chloride resin. After mild acidic cleavage the side chain protected intermediate Phac-P3-P2-OH was coupled to the commercially available benzyl (1*r*,4*r*)-4-(aminomethyl)cyclohexylcarbamate (AMCA-Cbz) in solution, followed by Cbz-deprotection by hydrogenation. The half amount of the obtained intermediate was guanylated using 1*H*-pyrazole-1-carboxamidine  $\times$  HCl. Afterwards, this intermediate was completely deprotected to reveal inhibitor **40**. The rest amount of the intermediate after the hydrogenation step was Tfa-deprotected, further guanylated and finally Boc-deprotected to obtain the inhibitor **46** (Scheme 3.3).

The compounds **41-45** and **47-51** were synthesized in analogy to inhibitors **40** and **46**, whereby the protected *N,N'*-di-Boc-1*H*-pyrazole-1-carboxamidine was used in the guanylation step (f) for the synthesis of inhibitors **45**, **49** and **50** (not shown in Scheme 3.3).

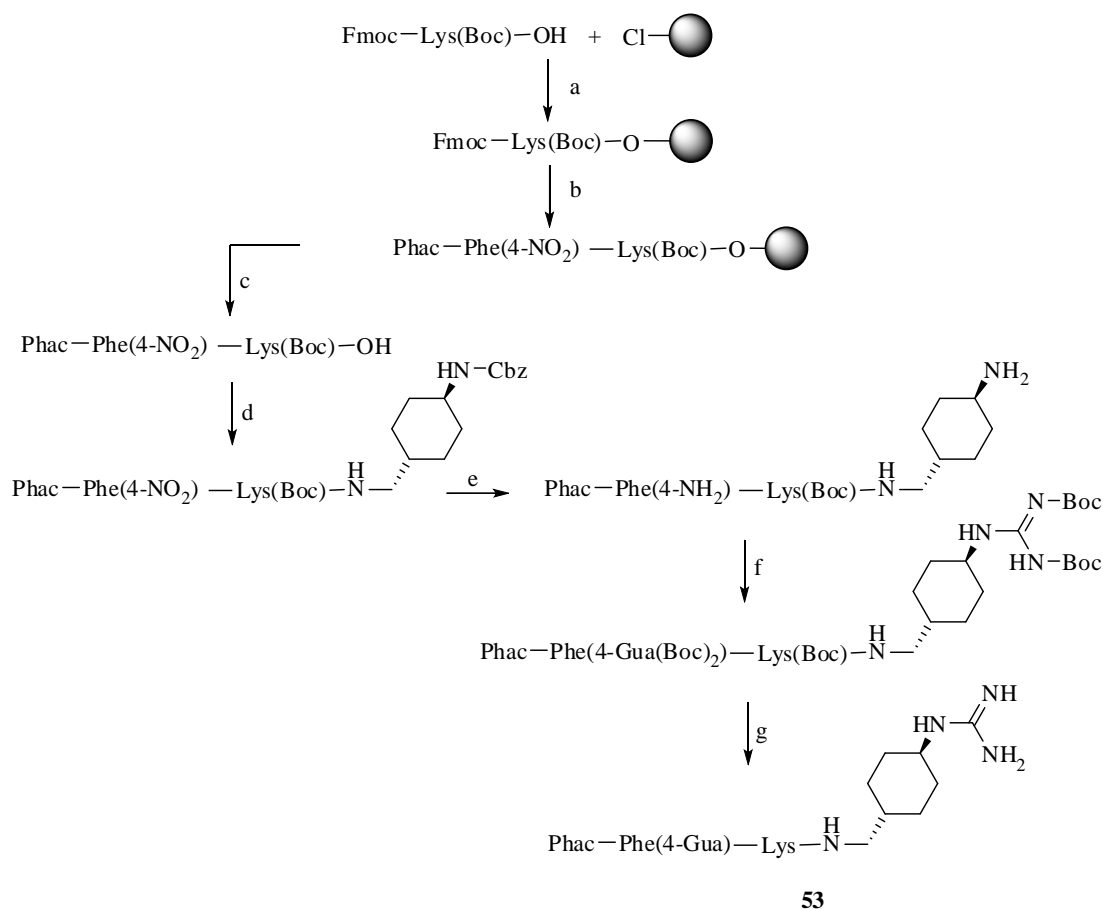


**Scheme 3.3:** Synthesis of inhibitors **40** and **46**. (a) Loading of 2-chlorotrityl chloride resin, Fmoc-Lys(Boc)-OH, 4 equiv DIPEA, dry DCM, 2h; (b) Fmoc SPPS (see Scheme 3.1); (c) 1% TFA in DCM, 3×30 min; (d) 1 equiv benzyl (1*r*,4*r*)-4-(aminomethyl)cyclohexylcarbamate, 1 equiv PyBOP, 1 equiv DIPEA, DMF; (e) H<sub>2</sub> and Pd/C as catalyst in 90% HAc, stirring overnight at RT (f) 3-6 equiv 1*H*-pyrazole-1-carboxamide × HCl, 4 equiv DIPEA in DMF, 16 h; (g) 1 N NaOH in dioxane/water, pH 12 at RT 3 h, neutralization by 10% TFA; (h) 90% TFA, at RT 1 h, preparative HPLC.

Inhibitor **53** was synthesized according to Scheme 3.4, starting with the loading of the protected P2 residue onto the 2-chlorotrityl chloride resin. The intermediate Phac-P3-P2-OH was coupled to the commercially available AMCA-Cbz in solution, followed by hydrogenation (step e) to remove the Cbz-protection and to reduce the nitro into amino group.

The free amino groups at the P1 residue and P3 side chain were converted into guanidine using *N,N'*-di-Boc-1*H*-pyrazole-1-carboxamide (step f), followed by Boc-

deprotection to obtain inhibitor **53**. Compound **52** was prepared using the same strategy, whereby the P2 and P3 residues were reversed.



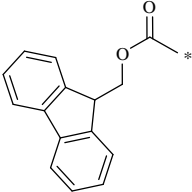
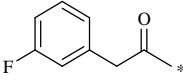
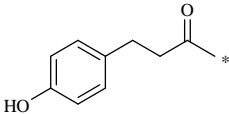
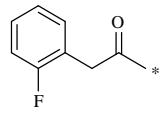
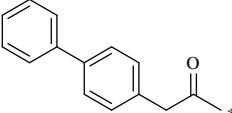
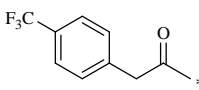
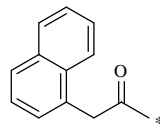
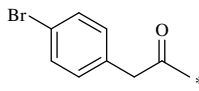
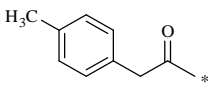
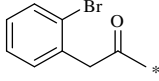
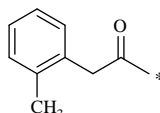
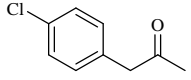
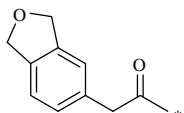
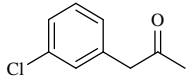
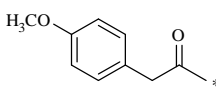
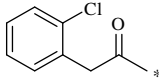
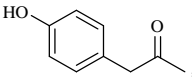
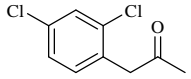
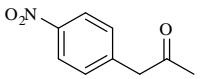
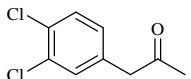
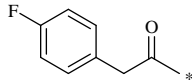
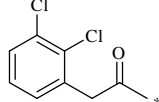
**Scheme 3.4:** Synthesis of inhibitor **53**. (a) Loading of 2-chlorotrityl chloride resin, Fmoc-Lys(Boc)-OH, 4 equiv DIPEA, dry DCM, 2h; (b) Fmoc SPPS (see Scheme 3.1); (c) 1% TFA in DCM, 3×30 min; (d) 1 equiv benzyl (1*r*,4*r*)-4-(aminomethyl)cyclohexylcarbamate, 1 equiv PyBOP, 1 equiv DIPEA, DMF; (e) H<sub>2</sub> and Pd/C as catalyst in 90% HAC, stirring overnight at RT (f) 2 equiv *N,N'*-di-Boc-1*H*-pyrazole-1-carboxamidine, 4 equiv DIPEA in DMF, 16 h; (g) TFA, at RT 1 h, preparative HPLC.

### 3.3 Modification of P4 residue

In an additional series, a search for more suitable P4 residues was performed, whereas Lys-Lys-*agmatine* was maintained as a constant P3–P1 segment, based on previous studies.<sup>66</sup> In most cases ring-substituted phenylacetyl moieties were incorporated, and in two inhibitors an N-terminal Fmoc- or *p*-hydroxyphenyl-propionyl group was used (Table 3.4). Compared with the reference inhibitor **26** (phenylacetyl-Lys-Lys-*agmatine*,  $K_i = 3.9 \mu\text{M}$ ), a twofold improvement in affinity was observed for the 4-phenyl-phenylacetyl analogue **56**. This tendency was also observed in the previously described arginal series.<sup>66</sup> A similar activity was also found for most other analogues, whereby the lowest  $K_i$  values were determined for the dichloro-substituted inhibitors **73–75**.

## Results and discussion

**Table 3.4:** Inhibition constants of the WNV protease by inhibitors with the general formula P4-Lys-Lys-*agmatine*.

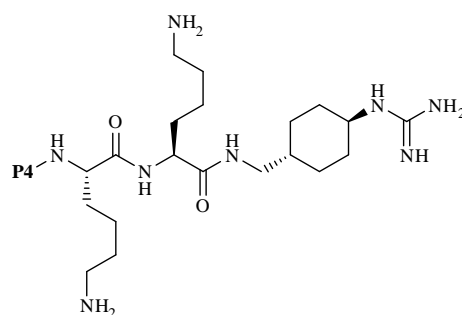
No.	P4	$K_i$ ( $\mu\text{M}$ )	No.	P4	$K_i$ ( $\mu\text{M}$ )
<b>54</b> (MI-0662)		11.2	<b>65</b> (MI-0677)		1.1
<b>55</b> (MI-0666)		17.8	<b>66</b> (MI-0681)		1.35
<b>56</b> (MI-0661)		1.7	<b>67</b> (MI-0675)		1.0
<b>57</b> (MI-0668)		0.82	<b>68</b> (MI-0670)		1.15
<b>58</b> (MI-0665)		1.5	<b>69</b> (MI-0671)		0.9
<b>59</b> (MI-0664)		1.5	<b>70</b> (MI-0672)		2.0
<b>60</b> (MI-0676)		0.83	<b>71</b> (MI-0682)		0.76
<b>61</b> (MI-0674)		1.5	<b>72</b> (MI-0678)		0.7
<b>62</b> (MI-0667)		0.93	<b>73</b> (MI-0680)		0.6
<b>63</b> (MI-0669)		1.15	<b>74</b> (MI-0663)		0.4
<b>64</b> (MI-0673)		2.5	<b>75</b> (MI-0679)		0.45

Derivatives **54–75** were prepared as described for inhibitor **26** in Scheme 3.1 using commercially available P4 acyl residues.

### 3.4 Combination of the best P4 and P1 residues

In the previous series, the strongest WNV protease inhibition was found for the P4 dichloro-substituted inhibitors **73–75** and compound **39** containing the GCMA residue in P1 position. Therefore, both moieties were combined providing analogues **76–78**, which are the most potent inhibitors of the WNV protease with  $K_i$  values  $< 0.15 \mu\text{M}$  (Table 3.5). These inhibitors were synthesized in analogy to the synthesis of **39**.

**Table 3.5:** Inhibition constants of the WNV protease with by inhibitors with the general formula P4-Lys-Lys-GCMA



No.	P4	$K_i$ ( $\mu\text{M}$ )
<b>76</b> (MI-0685)		0.14
<b>77</b> (MI-0683)		0.13
<b>78</b> (MI-0684)		0.12

### 3.5 Selectivity studies

Some inhibitors were exemplarily tested against three trypsin-like serine proteases. Thrombin and factor Xa (fXa) are important enzymes in the blood coagulation cascade, and their inhibition could lead to bleeding complications. Matriptase belongs to the type II transmembrane serine proteases (TTSPs).<sup>82</sup> It is involved in the terminal differentiation of the oral epithelium and the epidermis, and is critical for hair follicle

growth, but also emerged as a potential target for anticancer drugs.<sup>83</sup> The results of these selectivity studies are summarized in Table 3.6. Both agmatine derivatives **56** and **73** inhibit also matriptase in the low micromolar range, whereas the selected GCMA analogues **76-78** possess an improved selectivity with negligible affinity against the tested trypsin-like serine proteases.

**Table 3.6:** Inhibition of the WNV and trypsin-like serine proteases by selected inhibitors.

No.	$K_i$ $\mu\text{M}$			
	matriptase	fXa <sup>(a)</sup>	thrombin <sup>(a)</sup>	WNV
<b>56</b> (MI-0661)	1.8	>200	>500	1.7
<b>73</b> (MI-0680)	5.2	>200	>500	0.6
<b>76</b> (MI-0680)	93	>200	>500	0.14
<b>77</b> (MI-0663)	84	>200	>500	0.13
<b>78</b> (MI-0679)	102	>200	>500	0.12

<sup>(a)</sup>Due to poor inhibitory potency, the provided data were calculated only from pre-assays using a single substrate concentration of 180  $\mu\text{M}$ ; these assays were performed with the substrates  $\text{CH}_3\text{OCO-dCha-Gly-Arg-pNA}$  ( $K_m=105$   $\mu\text{M}$ ) and  $\text{CH}_3\text{SO}_2\text{-dCha-Gly-Arg-pNA}$  ( $K_m=40$   $\mu\text{M}$ ) for fXa and thrombin, respectively.

### 3.6 Stability test with trypsin

Since these inhibitors contain additional basic residues in P2 and P3 position, they could be potential substrates of trypsin-like serine proteases. Therefore, inhibitor **76** (2,4-dichloro-Phac-Lys-Lys-GCMA) was incubated with the nonspecific protease trypsin in tris buffer at pH 8.0 over a period of one hour, followed by HPLC analysis of the remaining inhibitor (detection at 220 nm, data not shown). Under the used condition approximately 8 % of inhibitor **76** was cleaved. The newly formed product elutes at 30.8 min on HPLC (start at 1% solvent B), suggesting a cleavage after the P3 lysine, because its retention time is identical with that of 2,4-dichloro-Phac-Lys-OH, which was synthesized as reference. In contrast, no cleavage could be observed after the P2 lysine, because the reference 2,4-dichlorophenylacetyl-Lys-Lys-OH is more hydrophilic and elutes at 25.95 min. Moreover, under identical conditions approximately 42% of the known chromogenic trypsin substrate methylsulfonyl-D-cyclohexylalanine-Gly-Arg-p-nitroanilide<sup>84</sup> was hydrolyzed after the P1-Arg residue.

### 3.7 Structure of the WNV NS2B-NS3 protease in complex with inhibitor **77**<sup>[1]</sup>

A crystal structure of the WNV NS2B-NS3 protease was solved in complex with one of the most potent inhibitors (3,4-dichlorophenylacetyl-Lys-Lys-GCMA) **77** (resolution 3.2 Å, refined to a crystallographic R factor of 18.8%,  $R_{\text{free}}=20.7\%$ ). Despite the limited resolution, the electron density maps were clear and easily interpretable in most regions. At the N terminus of the NS2B chain (molecule A), electron density was visible for residues Ser47, His48, and Met49, which remained from the N-terminal His tag after cleavage by thrombin. The first authentic residue of NS2B is Thr50. At the C terminus of NS2B, the last residue defined by electron density was Pro91, leaving the five C-terminal residues of NS2B and all nine residues of the artificial Gly4-Ser-Gly4 linker between the NS2B and NS3 (molecule B) chains without interpretable density. Beyond this linker, the first amino acid residue of NS3 also lacked meaningful electron density. At the C terminus of the NS3 chain, all residues were well defined by electron density except the very C-terminal Arg170. Although all other residues of the enzyme were included in the structural model, a number of individual side chains (Met49 of molecule A (Met49/A), Asp65/A, Glu67/A, Arg78/A, and Asp6 of molecule B (Asp6/B), Lys11/B, Glu12/B, Lys88/B, Lys117/B, Glu120/B, Lys142/B) lacked well-defined electron density. The corresponding atoms were refined with occupancy of less than one or even assigned zero occupancy. For the side chains of Met88/A and Gln86/B, alternative conformations were modeled, each refined with an occupancy of 50 %.

Owing to limitations in the resolution of the diffraction data, only seven water molecules and one chloride ion could be located in the electron density maps. Only one of these water molecules is located in the active site region, forming 2.5 Å hydrogen bonds to the carbonyl oxygen atom of Gly153 and to O $\delta$ 1 of Asn152. However, it does not interact with the inhibitor. In the crystals, the protease is in the closed conformation, with the NS2B chain wrapping around NS3, with two strands (residues 53–58 and 73–

---

<sup>[1]</sup> The crystal structure of inhibitor **77** in complex with the WNV NS2B-NS3 protease has been solved by Caroline Haase in the group of Prof. Dr. Rolf Hilgenfeld (Institute of Biochemistry, University Lübeck). The text and figures of this chapter were provided by C. Haase and R. Hilgenfeld and are nearly identical as already published.<sup>[90]</sup>

76) of NS2B contributing to two  $\beta$ -sheets formed by NS3. The C-terminal portion (residues 78–86) of NS2B forms a  $\beta$ -hairpin, which is involved in inhibitor binding.

**Catalytic site:** With the protease being in the closed conformation, the catalytic triad consisting of Ser 135, His51 and Asp75 is in active state. There is a 3.0 Å interaction between the hydroxyl group of the serine and N $\epsilon$ 2 of the histidine. The N $\delta$ 1 atom of the latter is involved in a 2.8Å hydrogen bond to O $\delta$ 2 of Asp75. The oxyanion hole, formed by the amides of Gly133, Thr134, and Ser135, is in a non-catalytic conformation and would require a flip of the Thr132–Gly133 peptide bond to adopt the catalytically competent conformation.

**Inhibitor binding:** Figure 3.1a shows a stereo view of inhibitor **77** within the active site of the WNV protease, displayed with its solvent-accessible surface. Key interactions between the protease and the inhibitor are indicated in Figure 3.1b.

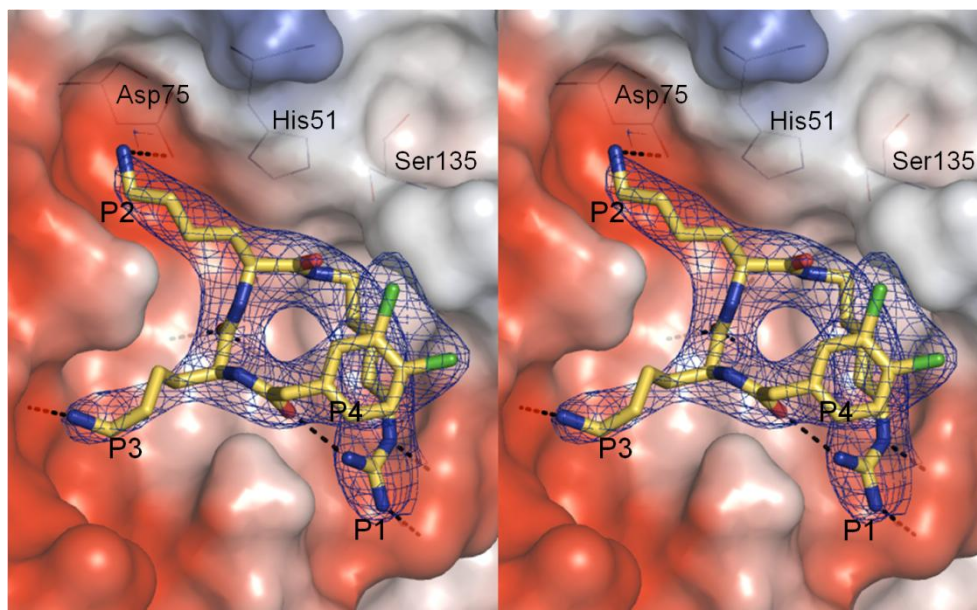
**P1 residue:** The GCMA moiety of the inhibitor is inserted into the relatively shallow S1 pocket of the protease. As the compound lacks a covalent interaction with the catalytic nucleophile of the protease, the carbon atom adjacent to the amide NH of the P1 residue is at a distance of 3.3 Å from Ser135 O $\gamma$ . The P1 amide NH is involved in a 2.9 Å hydrogen bond to the carbonyl oxygen atom of Gly151. The P1 cyclohexyl ring is in a chair conformation and makes van der Waals interactions with tyrosine residues 150 and 161. The latter interaction possibly involves a C-H $\cdots$   $\pi$  hydrogen bond<sup>85, 86</sup> of ~3.3 Å length between a methylene carbon atom of the cyclohexyl ring and the aromatic plane. Interestingly, the other side of the cyclohexyl ring is shielded from bulk solvent by the aromatic P4 residue of the inhibitor at a distance of ~3.8 Å (see below). The terminal P1 guanidinium group interacts with the carboxylate of Asp129 through two hydrogen bonds (2.7 and 2.9 Å), whereas the third guanidinium nitrogen atom is involved in a 2.7 Å hydrogen bond to the P4 carbonyl oxygen. There is also a 3.1 Å salt bridge between the guanidinium moiety and the carboxylate of Glu55 of the NS2B chain of a neighboring protease molecule in the crystal lattice.

**P2 residue:** The lysine P2 side chain is well embedded in the S2 pocket, which is lined by His51 of the catalytic site, Asn152 of molecule B, and Gly83 and Asn84 of NS2B. The terminal amino group of the lysine makes a 3.2 Å interaction with the carboxylate of Asp75 of the catalytic site.

**P3 residue:** The main-chain carbonyl oxygen atom of the P3 residue accepts a 2.8 Å hydrogen bond from the hydroxyl group of Tyr161 and a 2.9 Å hydrogen bond from the NH of Gly153. The terminal amino group of the lysine side chain donates a 2.8 Å hydrogen bond to the carbonyl oxygen of Phe85 of NS2B. Thus, the NS2B polypeptide contributes to the formation of the S3 pocket in the closed conformation of the enzyme.

**P4 residue:** As mentioned above, the carbonyl oxygen of the 3,4-dichlorophenylacetyl moiety accepts a 2.7 Å hydrogen bond from one terminal N $\omega$  of the P1 guanidinium group. A similar interaction between the P4 carbonyl and the P1 guanidine was also found in the crystal structure of the WNV protease in complex with the arginal-derived inhibitor Naph-KKRH (3e90.pdb).<sup>77</sup> This intramolecular interaction constrains the inhibitor into a closed, horseshoe-like conformation, thereby positioning the aromatic plane above the P1 cyclohexyl ring and shielding it from bulk solvent. The distances between the aromatic plane and the two adjacent methylene units of the cyclohexyl ring are 3.8 Å, indicative of possible CH $\cdots\pi$  interactions.<sup>85, 86</sup>

a)



b)

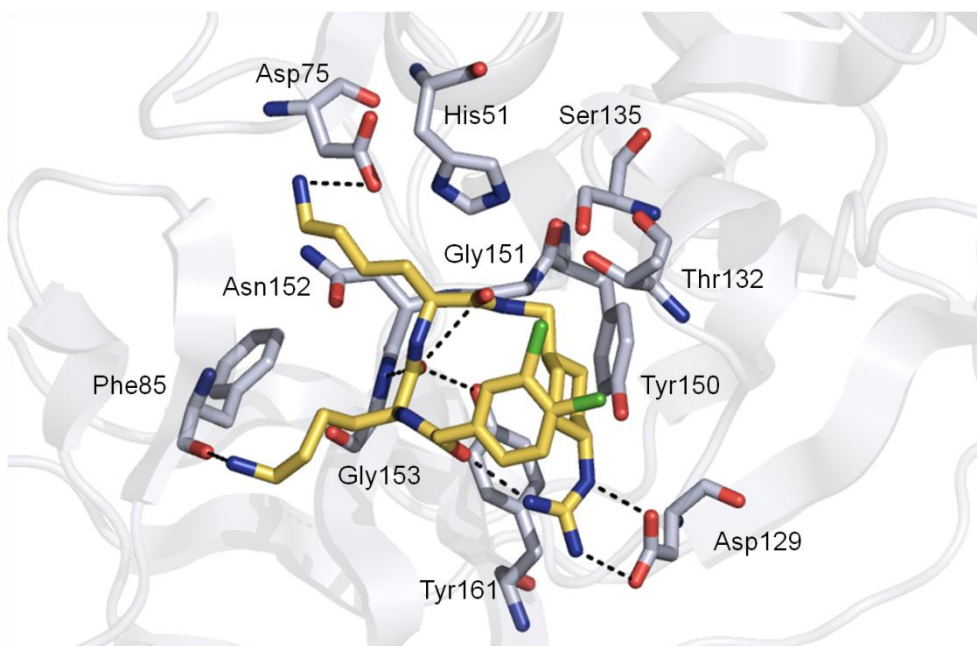


**Figure 3.1:** Complex of inhibitor **77** in the active site of the WNV protease (2yol.pdb). Hydrogen bonds are indicated as black dashed lines. a) Stereo view of the complex, whereby the protease is shown with its solvent-accessible surface colored by electrostatic potential: negative and positive potentials are shown in red and blue, respectively. The residues of the catalytic triad are labeled. The 2 Fo-Fc electron density maps, contoured at a level of  $1.1\sigma$ , are only shown for the inhibitor; its carbon atoms are shown in yellow, oxygen in red, nitrogen in blue, and chlorine in green. b) Key interactions observed in the complex, as discussed in the text. The carbon atoms of the protease and inhibitor are shown in grey and yellow, respectively.

The obtained crystal structure of inhibitor **77** in complex with the WNV NS2B-NS3 protease encouraged us to perform further modifications within this substrate-analogue inhibitor type. These modifications are described in the following chapters.

### 3.8 Second modification of P2 and P3 residues

The initial modification of the P2 and P3 Lys residues with basic substituted phenylalanine analogues has only provided inhibitors with reduced potency (see Table 3.3 in chapter 3.2). On the other side, the crystal structure of inhibitor **77** in complex with the viral NS2B-NS3 protease suggested that there is some empty space left in the S2 and S3 pockets and it might be possible to replace both lysines by other bulky basic or hydrophobic residues.

Therefore, additional amino acids like norarginine (norArg), arginine, homo-2-pyridylalanine (*hAla*(2-Pyr)) or bulky uncharged residues like phenylalanine and serine-benzylether (Ser(Bzl)) were incorporated in a new inhibitor series with C-terminal agmatine (Table 3.7).

**Table 3.7:** Inhibition of the WNV-NS2B-NS3 protease by inhibitors of the formula 3,4-dichlorophenylacetyl-P3-P2-agmatine.

No.	P3	P2	$K_i$ ( $\mu$ M)
<b>74</b> (MI-0663)	Lys	Lys	0.40
<b>79</b> (MI-0686)	Lys	norArg	0.85
<b>80</b> (MI-0687)	norArg	Lys	6.5
<b>81</b> (MI-0693)	Lys	Arg	9
<b>82</b> (MI-0694)	Arg	Arg	15.8
<b>83</b> (MI-0691)	Lys	hPhe	29.5
<b>84</b> (MI-0692)	hPhe	Lys	8.5
<b>85</b> (MI-0697)	Lys	Ser(Bzl)	97.6
<b>86</b> (MI-0698)	Ser(Bzl)	Lys	10.2
<b>87</b> (MI-0699)	Lys	D/L- <i>hAla</i> (2-Pyr)	>500
<b>88</b> (MI-0731)	D/L- <i>hAla</i> (2-Pyr)	Lys	28.3

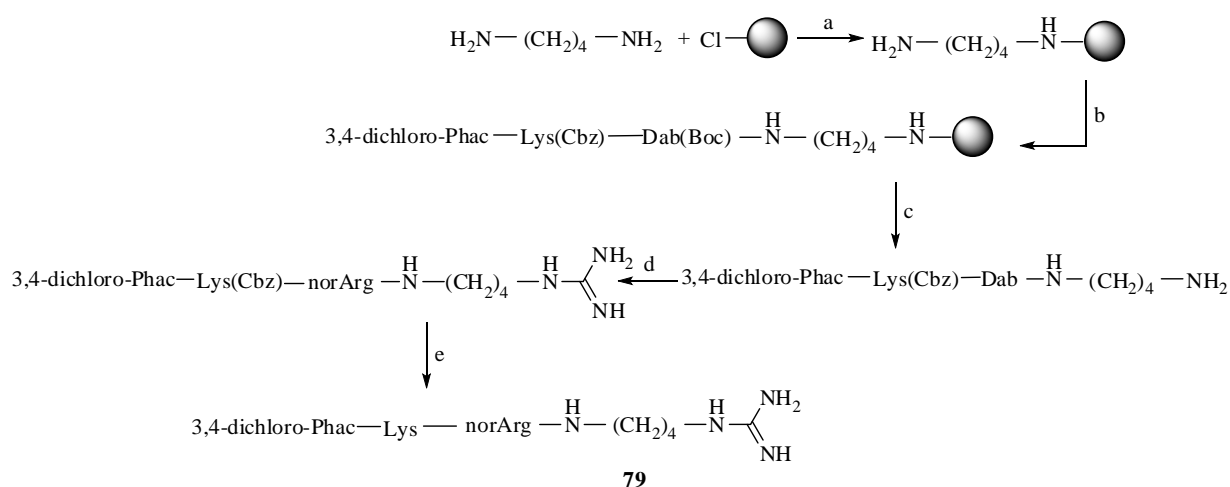
Compared to inhibitor **74** the replacement of the lysine residues at P2 or P3 positions by norarginine in inhibitors **79** and **80** led to about 2- or more than 10 fold reduced inhibitory potency, respectively. A strong drop in affinity was also observed after incorporation of arginine in P2 position (derivative **81**,  $K_i$  value of 9  $\mu$ M), whereby the replacement of

both lysines at P2 and P3 further reduced the potency (compound **82**,  $K_i$  value of  $16 \mu\text{M}$ ). A significantly weaker potency was also observed after replacement of the P2 and P3 lysine residues with more bulky amino acids such as *h*Phe, Ser(Bzl) or D/L-*h*Als(2-Pyr).

So far, the results from Tables 3.3 and 3.7 clearly reveal that all attempts to replace the lysine in P2 or P3 position were not successful and provided only compounds with relatively poor inhibitory potency against the WNV protease. Similar results have been published by other groups<sup>66, 87</sup>

### Synthesis of inhibitors 79-88

Inhibitors **81-88** were prepared as described for inhibitor **26** in Scheme 3.1. A slightly modified strategy was used for the synthesis of compound **79**. This inhibitor was prepared using Fmoc-Dab(Boc)-OH to generate the norArg at P2 after guanylation as shown in Scheme 3.5. Inhibitor **80** was also synthesized according to the same strategy, whereby the P2 and P3 residues were reversed.

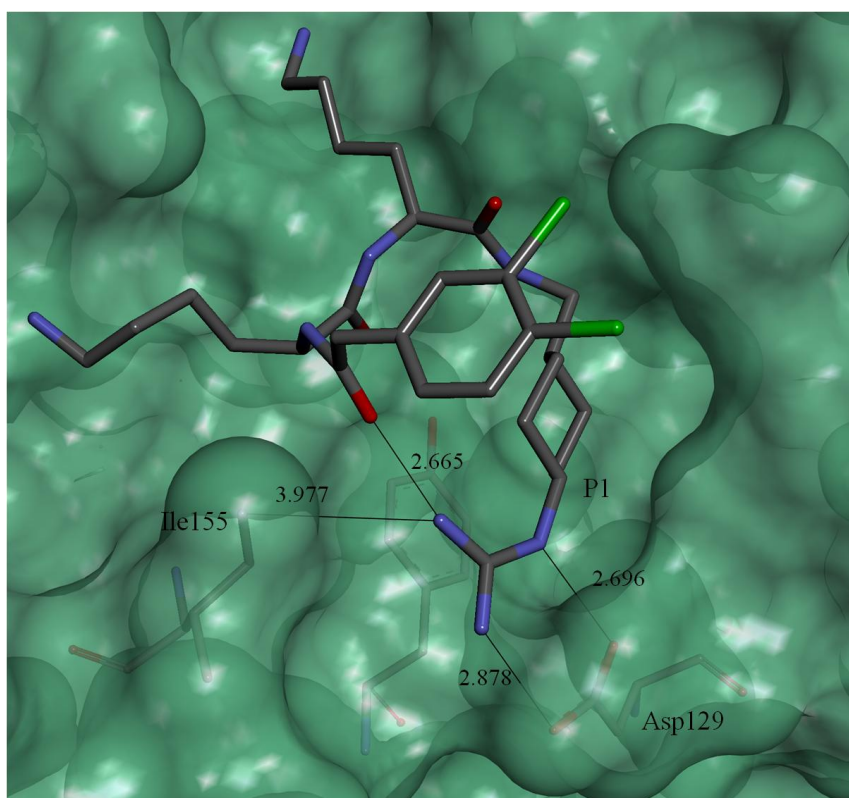


**Scheme 3.5:** Synthesis of inhibitors **79**: Reagents and conditions: a) Loading of the trityl chloride resin, 4 equiv diamine in dry DCM, 2 h, RT; b) standard Fmoc-SPPS, single couplings with 4 equiv amino acid (or phenylacetic acid), HOBT and HBTU, respectively, and 8 equiv DIPEA, 2 h, RT; c) TFA/TIS/H<sub>2</sub>O (95:2.5:2.5, v/v/v), 2×20 min; d) 6 equiv 1*H*-pyrazole-1-carboxamide × HCl, 4 equiv DIPEA in DMF, 16 h; e) 32% HBr/AcOH, 1 h, RT, preparative HPLC.

### 3.9 Incorporation of alkylated GCMA residues in P1 position

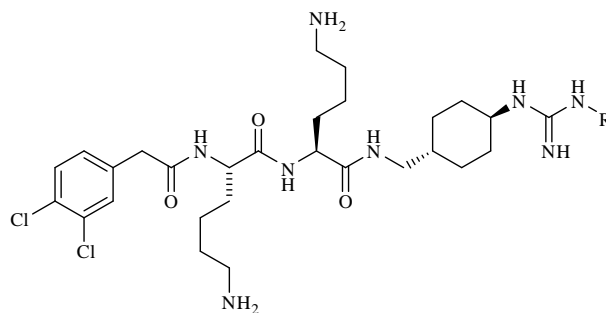
The crystal structure of inhibitor **77** in complex with WNV NS2B-NS3 protease revealed two intermolecular hydrogen bonds (2.7 and 2.9 Å) between the guanidinium group of the P1 GCMA residue and Asp129 in the S1 pocket. The third nitrogen atom

of the guanidinium group makes a close intramolecular contact to the carbonyl oxygen of the P4 acyl group (2.7 Å). Moreover, this guanidinium nitrogen is approximately 4 Å away from the terminal C $\delta$  carbon of the Ile155 side chain (Figure 3.2.). This suggested that an alkylation of the P1 guanidino group by a short methyl or ethyl group, which maintains its basic character, could make a beneficial hydrophobic interaction to Ile155 without disturbing the intramolecular H-bond to the P4 carbonyl oxygen or influencing the intermolecular salt bridge to Asp129.



**Figure 3.2:** Interaction of the P1 guanidino group of inhibitor 77 with the S1 pocket of the WNV protease.

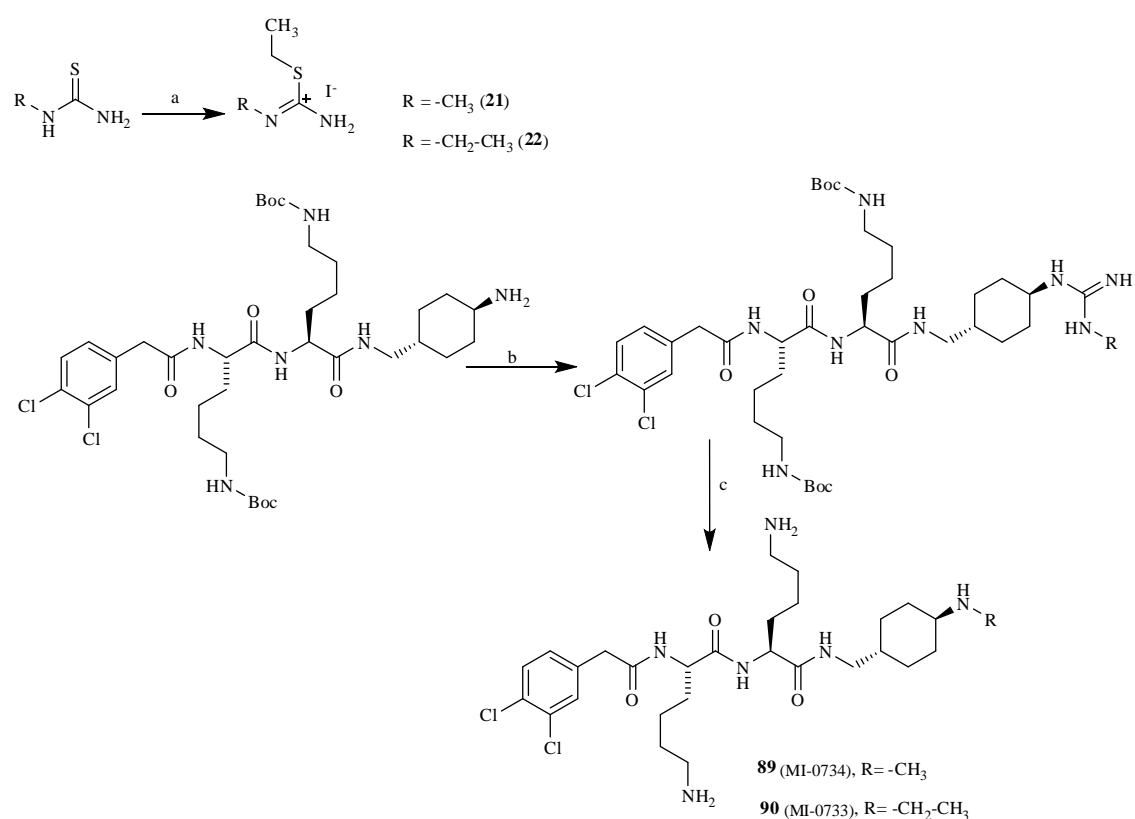
Therefore, two inhibitors of the general formula 3,4-dichloro-Phac-Lys-Lys-P1 containing such alkylated guanidinium groups were synthesized to proof this assumption. However, the determined  $K_i$  values revealed a strongly reduced inhibitory potency for both compounds (Table 3.8).

**Table 3.8:** Inhibition of the WNV NS2B-NS3 protease by inhibitors with the general formula

No.	R	$K_i$ ( $\mu\text{M}$ )
<b>77</b> (MI-0683)	H	0.13
<b>89</b> (MI-0734)	methyl	7
<b>90</b> (MI-0733)	ethyl	11

### Synthesis of alkylated P1-GCMA derivatives

The synthesis of the inhibitors **89** and **90** was performed according to Scheme 3.6. The used guanylation reagents ethyl methylcarbamimidothioate hydroiodide **21** or ethyl ethylcarbamimidothioate hydroiodide **22**<sup>88</sup> were prepared from the appropriate alkylated thioureas by treatment with iodoethane and were used without further purification. The intermediate 3,4-dichloro-Phac-Lys(Boc)-Lys(Boc)-AMCA was prepared by standard Fmoc-SPPS using Fmoc-AMCA (**17**) for the initial loading of the 2-chloro-tritylchlorid resin. After mild acidic cleavage the subsequent guanylation using reagents **21** or **22** was performed in solution. The final removal of the Boc groups provided inhibitors **89** and **90**, respectively.



**Scheme 3.6:** Synthesis of inhibitors **89** and **90**. Reagents and conditions: a) abs. EtOH, 3.5 h, 60°C.; b) 2 equiv **21** or **22**, 4 equiv DIPEA in DMF, 24 h at RT; c) 90% TFA, at RT 1 h, preparative HPLC.

### 3.10 Design and synthesis of cyclic inhibitors

Many cyclic peptides with a wide spectrum of biological activities have been isolated from natural sources, like the antibiotics cyclosporine or gramicidin S. Therefore, the cyclization of peptides has also become a promising strategy for drug design. A key benefit of this modification is the reduction in conformational freedom, which can result in higher receptor binding affinities. Frequently, extra conformational constraints are incorporated, such as D- and N-alkylated-amino acids,  $\alpha,\beta$ -dehydro amino acids or  $\alpha,\alpha$ -disubstituted amino acid residues.<sup>89</sup> These modifications also enhance the stability of the peptides against proteolytic degradation.

Based on the crystal structure of the WNV protease with inhibitor **77** various cyclic inhibitors have been designed. The structure showed the inhibitor **77** in a horseshoe-like conformation, thereby positioning the aromatic P4 plane above the P1 cyclohexyl ring and covering it from bulk solvent. The distances between the phenyl ring and the two adjacent methylene units of the cyclohexyl group are 3.8 Å, indicative of possible

CH $\cdots\pi$  interactions.<sup>90</sup> It was also found that the distance between the *meta* chloro atom on the P4 phenyl ring and the carbon adjacent to the P1 amide NH is about 5.3 Å. This carbon should be located at a similar position as the putative C $\alpha$ -atom of a P1 arginine in substrate-analogue structures.

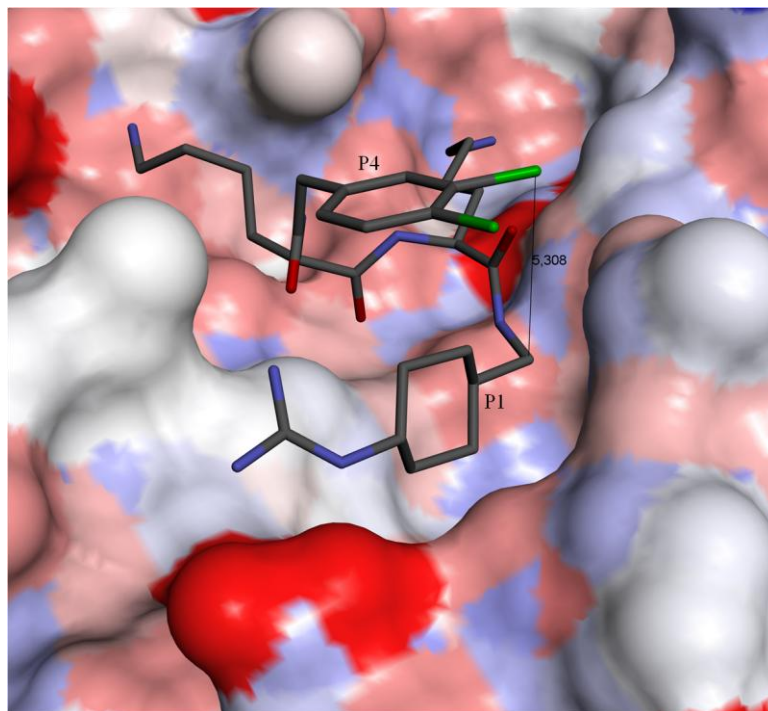


**Figure 3.3:** Inhibitor **77** in complex with the WNV NS2B-NS3 protease. The distance between the C $\alpha$  atom of the P1 residue and the meta chloro atom at the P4 phenyl ring is approximately 5.3 Å.

Therefore, we assumed that it should be possible to connect the P4 and P1 residues via a suitable P1' linker residue. However, with this strategy it could come to a simple proteolytic cleavage after the P1 residue, providing a product with a C-terminal carboxylate structure, which should be repelled by the nucleophilic side chain of the active site Ser135. There exist several strategies to enhance the stability of a peptide bond via modification of the P1' residue. One approach is the incorporation of N $\alpha$ -alkylated P1' residues, like sarcosine or proline. A P1' proline was successfully incorporated into the clinically used thrombin inhibitor hirulog-1 (bivalirudin, Angiomax<sup>®</sup>), compared to its glycine analogue it was approximately 1000-fold more stable against thrombin.<sup>91</sup> An alternative strategy is the incorporation of P1' residues in D-configuration or of very bulky residues.

Therefore, before synthesizing the first cyclic inhibitors, several linear peptides have been prepared and their inhibition constants and proteolytic stability were analyzed (Table 3.9).

**Table 3.9:** Inhibition of the WNV protease by linear peptides of the general formula P4-Lys-Lys-P1-R

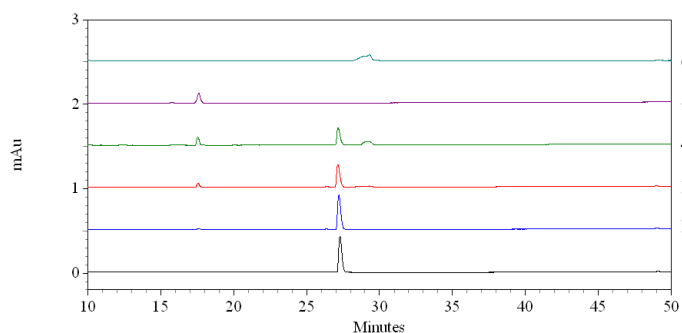
No.	P4	P1	R	$K_i$ ( $\mu\text{M}$ )
<b>91</b> (MI-0751)	Phac	Arg	Gly-Gly-NH <sub>2</sub>	0.8
<b>92</b> (MI-0737)	Phac	Arg	Gly-NH <sub>2</sub>	2
<b>93</b> (MI-0740)	Phac	Arg	Ala-NH <sub>2</sub>	25
<b>94</b> (MI-0741)	Phac	Arg	Val-NH <sub>2</sub>	105
<b>95</b> (MI-0739)	Phac	Arg	Tle-NH <sub>2</sub>	140
<b>96</b> (MI-0738)	Phac	Arg	Pro-NH <sub>2</sub>	200
<b>97</b> (MI-0752)	Phac	Arg	D-Ala-NH <sub>2</sub>	75
<b>98</b> (MI-0753)	Phac	Arg	Sar-NH <sub>2</sub>	50
<b>99</b> (MI-0754)	Phac	Arg	Gaba-NH <sub>2</sub>	15
<b>100</b> (MI-0755)	Phac	Arg	Aca-NH <sub>2</sub>	17
<b>101</b> (MI-0756)	Phac	Arg	NH <sub>2</sub>	0.4
<b>102</b> (MI-0742)	3,4-dichloro-phac	Arg	Gly-NH <sub>2</sub>	1.3
<b>103</b> (MI-0757)	3,4-dichloro-phac	Arg	NH <sub>2</sub>	0.39
<b>104</b> (MI-0763)	Phac	hArg	NH <sub>2</sub>	1.9
<b>105</b> (MI-0762)	3,4-dichloro-phac	hArg	NH <sub>2</sub>	1.7

The first peptide **91** contains a Gly-Gly-NH<sub>2</sub> as P1'-P2' segment and inhibits the WNV protease with a  $K_i$  value of 0.8  $\mu\text{M}$ . Elimination of the P2' residue resulted in slightly reduced potency, in contrast additional deletion of P1' Gly enhanced the affinity, a  $K_i$  value of 0.4  $\mu\text{M}$  was determined for compound **101**.

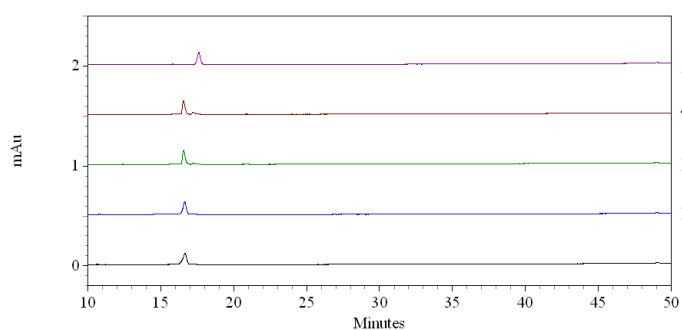
Additional modifications of the P1' residue, like incorporation of N $\alpha$ -alkylated amino acids (proline and sarcosin), of amino acids in D-configuration or several nonproteinogenic amino acids, dramatically reduced the potency of peptides **93–100**. Moreover, peptides containing a P1 Arg-NH<sub>2</sub> moiety could be also potential substrates of trypsin-like serine proteases, therefore additional inhibitors **104** and **105** containing a homoarginine amide were prepared, which should have an improved proteolytic stability (not tested so far). As expected, a relatively weak inhibition constant of 27.1  $\mu\text{M}$  was determined for the cleavage product Phac-Lys-Lys-Arg-OH with a free carboxylate structure in P1 position (MI-0764).

From the kinetic measurements, there was no hint that compound **91** was substantially cleaved as a substrate of the WNV protease during the 10 min assay time. The enzyme kinetic analysis revealed linear progress curves and normal Dixon plots typical for a reversible competitive inhibition mechanism. To further prove this result, this compound was also incubated with the WNV protease and at various time points samples were analyzed by HPLC (Figure 3.4). As reference, an identical concentration of the chromogenic substrate Phac-Lys-Lys-Arg-pNA **112** (MI-0744) containing the same P4-P1 segment was used, which provides a yellow color after cleavage. The HPLC analysis after 4 and 8 h incubation with peptide **91** (traces 3 and 4 in Figure 3.4b) revealed a minor formation of the cleavage product Phac-Lys-Lys-Arg-OH (elution at 17.6 min, trace 5), whereas a significantly larger amount was detected after incubation with the pNA substrate **112** at the same time points (Figure 3.4a). The decrease of the peak areas for compound Phac-Lys-Lys-Arg-pNA (**112**) revealed that approximately 33 % and 51 % were cleaved after 4 and 8 hours, respectively. In analogy, only 19 % of peptide **91** was cleaved after 8 h. It is well known that strong binding substrates with low  $K_m$  values often suffer from poor  $k_{cat}$  values and therefore, are considered as inhibitors. A similar situation was described for the thrombin inhibitor hirulog-1<sup>91</sup> and the dipeptidyl peptidase IV inhibitors Diprotin A (H-Ile-Pro-Ile-OH) and B (H-Val-Pro-Leu-OH)<sup>92</sup>, although all of them are simply poor substrates with low conversion rates.

a)



b)



c)

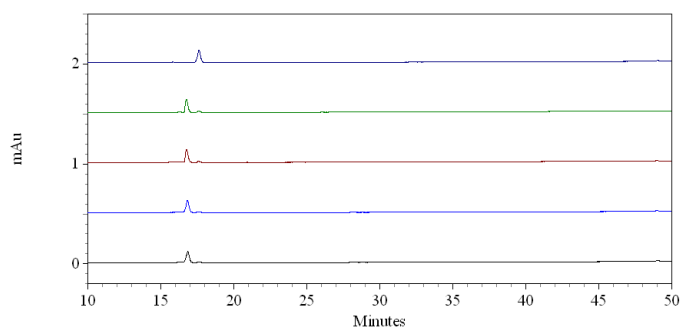


**Figure 3.4:** HPLC analysis of peptides **91**, **101** and **112** incubated with the WNV-protease. (a). Phac-Lys-Lys-Arg-pNA (**112**, elution at 27,1 min) was incubated with the WNV protease and analysed by HPLC at 0 (trace 1), 1 (trace 2), 4 (trace 3) and 8 hours (trace 4). The reference compound Phac-Lys-Lys-Arg-OH elutes at 17.6 min (trace 5) and *p*-nitroaniline at 29.3 min (broad peak in trace 6). (b). The peptide Phac-Lys-Lys-Arg-Gly-Gly-NH<sub>2</sub> (**91**, elution at 16.4 min) was incubated with the WNV protease at 0 (trace 1), 1 (trace 2), 4 (trace 3) and 8 (trace 4) hours. The reference compound Phac-Lys-Lys-Arg-OH is shown in trace 5, whereas the second cleavage product H-Gly-Gly-NH<sub>2</sub> is not detectable to poor absorbance under this condition. (c) The peptide Phac-Lys-Lys-Arg-NH<sub>2</sub> (**101**, elution at 16.7 min) was incubated with the WNV protease at 0 (trace 1), 1 (trace 2), 4 (trace 3) and 8 (trace 4) hours. The reference compound Phac-Lys-Lys-Arg-OH is shown in trace 5.

Several other peptides (**92**, **99** and **100**) were incubated with the WNV-protease under identical conditions. For all of these peptides no or negligible cleavage was observed

(data not shown). As an additional example the incubation of the best inhibitory peptide Phac-Lys-Lys-Arg-NH<sub>2</sub> (**101**) with the WNV protease is shown in Figure 3.4c. Under the used conditions only a minor cleavage was observed.

These results encouraged us to synthesize the cyclic inhibitors **106** and **107** (Figure 3.5) containing a P1' 4-aminobutanoic acid interconnected to the P4 2-(3-aminophenyl)acetyl or 2-(3-(aminomethyl)phenyl)acetyl residues. However, only weak inhibition was observed for both compounds. Most likely, this P1' linker was too short to maintain the optimal backbone conformation of the inhibitor.

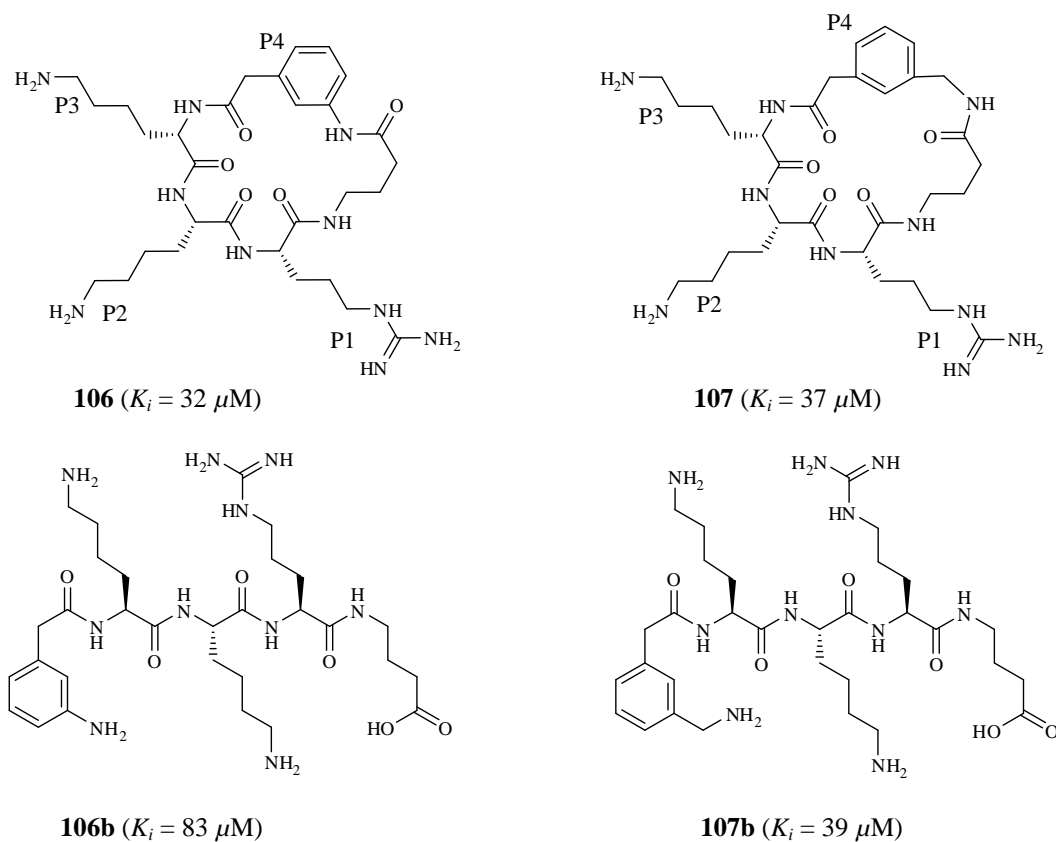


**Figure 3.5:** Structures and  $K_i$  values of cyclic inhibitors **106** and **107**, including their linear analogues.

An alternative cyclization without a P1' linker was performed by direct interconnection of the P1 side chain to the P4 group. To enable such a coupling a suitable functional group is needed in the P1 side chain. Therefore, lysine or ornithine residues in both configurations were coupled via their side chain amino function to the P2 residue and their  $\alpha$ -amino group was finally converted into guanidine, whereby the  $\alpha$ -carboxyl function can be used for cyclization (Figure 3.6).

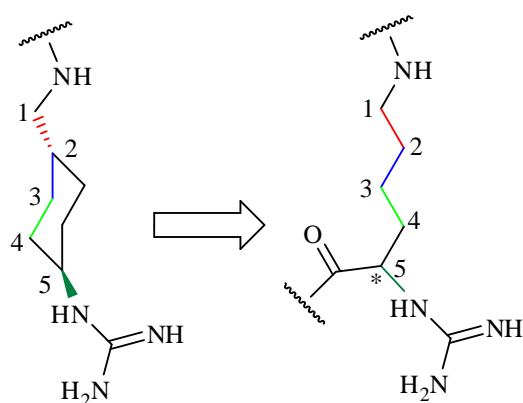
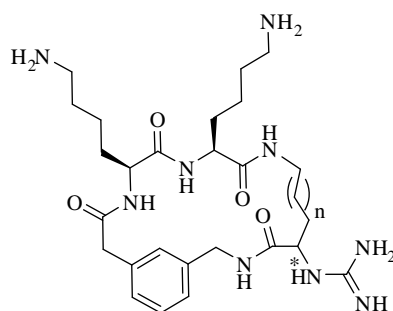


**Figure 3.6:** The GCMA residue of inhibitor **77** as template for the design of a new P1 residue suitable for cyclization.

According to this strategy, four inhibitors were synthesized using lysine or ornithine in D and L configuration (Table 3.10).

**Table 3.10:** Inhibition of the WNV protease by cyclic peptides **108-111** of the general formula



No.	n	*	$K_i$ ( $\mu\text{M}$ )
<b>108</b> (MI-0758)	2	L	14.5
<b>109</b> (MI-0759)	2	D	26.4
<b>110</b> (MI-0760)	1	L	44.7
<b>111</b> (MI-0761)	1	D	49

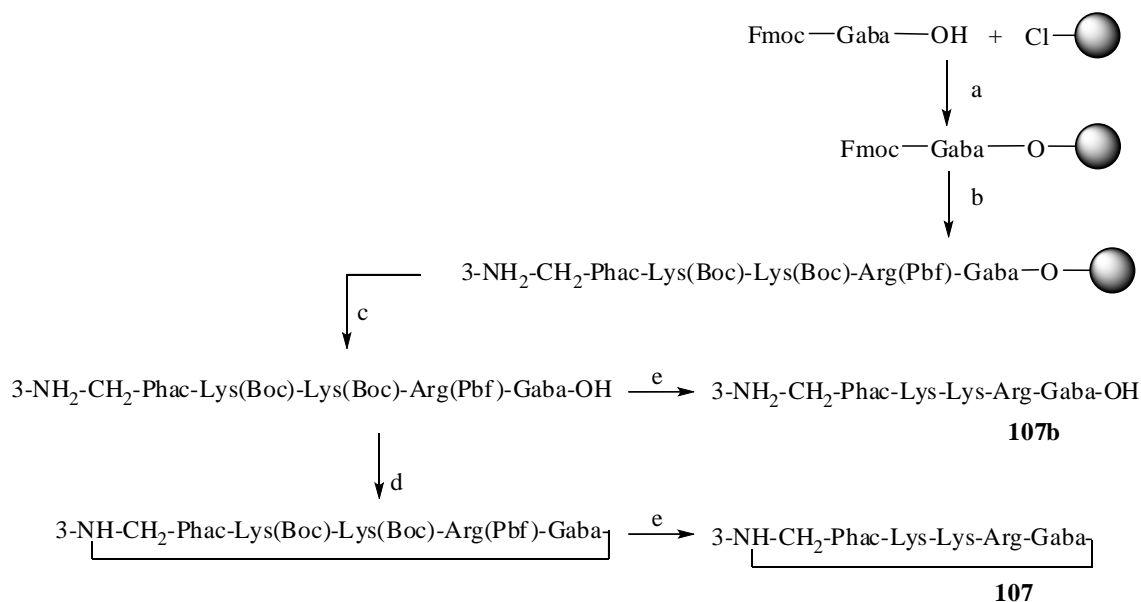
However, for all of these peptides only poor  $K_i$  values  $> 10 \mu\text{M}$  were determined. Therefore, these cyclic peptides are more than 25-fold weaker inhibitors than the linear peptide Phac-Lys-Lys-Arg-NH<sub>2</sub> (**101**). The lysine-derived peptides are slightly better than the shorter ornithine-based compounds, however, their  $K_i$  values are very similar. Although these first results of the cyclic peptides are discouraging, it might be possible to modify the interconnection between the P1 and P4 residues by insertion of suitable

linkers, which could provide more flexibility. Such compounds should be chemically well accessible, as seen from the used synthesis protocol described in the next paragraph.

### Synthesis of the linear peptides and cyclic inhibitors

All peptides with a C-terminal amide function were synthesized by SPPS on Fmoc-Rink-Amide resin using a standard Fmoc protocol. The peptides were cleaved from the resin using strong acidic conditions.

The synthesis of the cyclic inhibitor **107** was performed according to Scheme 3.7. A solid-phase approach on acid-sensitive 2-chlorotrityl chloride resin was used for the preparation of the protected linear intermediate (steps a, b and c). A small amount of this intermediate was completely deprotected to reveal the linear peptide as reference (step e), where the residual amount was cyclized in solution to give the protected cyclic intermediate (step d). The final deprotection was performed using strong acidic conditions (step e) to reveal inhibitor **107** (Scheme 3.7). Peptide **106** was prepared by the same strategy, whereby a 3-NH<sub>2</sub>-Phac-residue was incorporated as P4 group.



**Scheme 3.7:** Synthesis of inhibitor **107**. (a) Loading of 2-chlorotrityl chloride resin, Fmoc-Gaba-OH, 4 equiv DIPEA, dry DCM, 2 h; (b) Standard Fmoc SPPS (see Scheme 3.1); (c) 1% TFA in DCM, 3×30 min; (d) 3 equiv Bop; 3-5 equiv DIPEA pH ~ 8-9, DMF, ~ 72 h (e) TFA, at RT 1 h, preparative HPLC.

The critical step during the preparation of cyclic peptides is normally the ring closure reaction, which is exemplarily shown for step d in Scheme 3.7. The HPLC chromatograms reveal a relatively clean cyclization reaction (Figure 3.7).

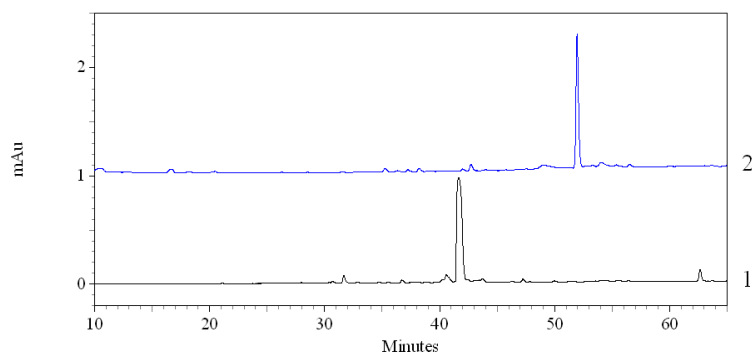
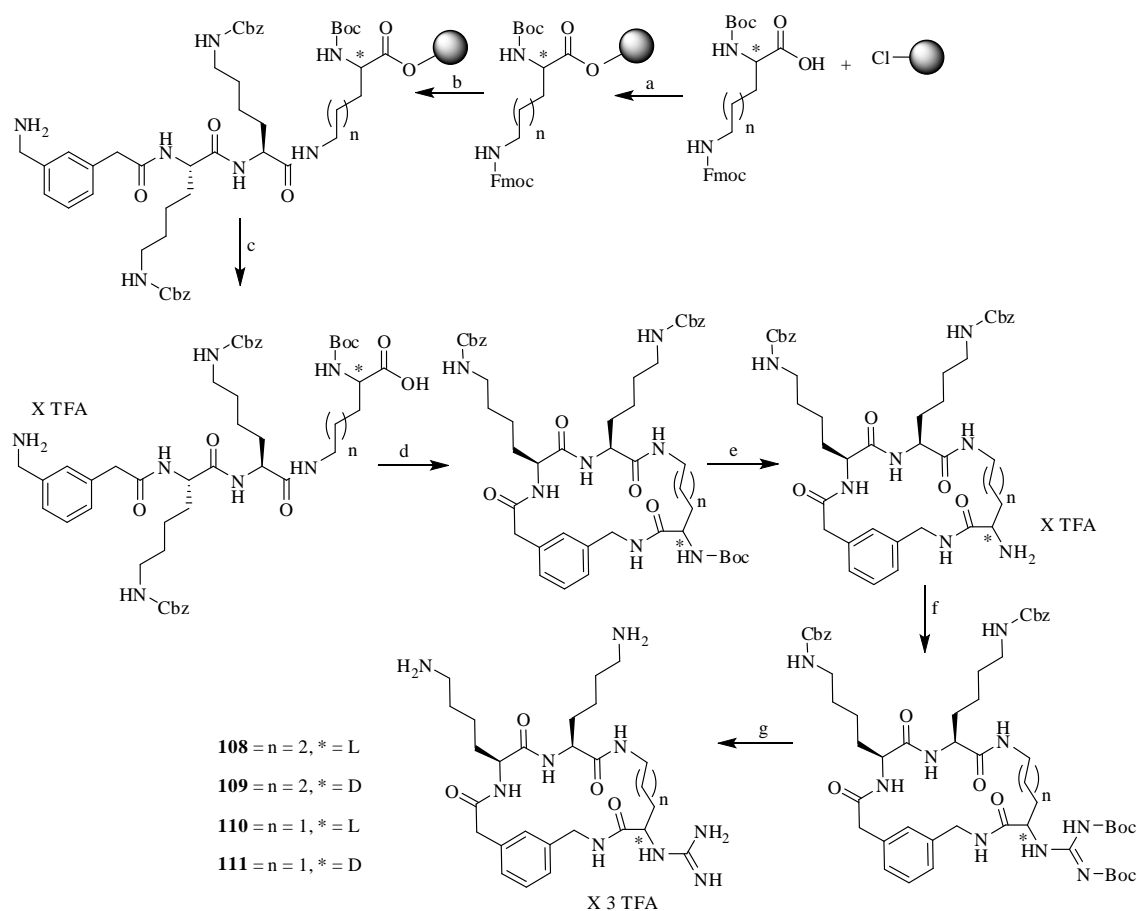


**Figure 3.7:** HPLC analysis of the intermediates after step c and step d in Scheme 3.7 (start at 10% solvent B).  $3\text{-NH}_2\text{-CH}_2\text{-Phac-Lys(Boc)-Lys(Boc)-Arg(Pbf)-Gaba-OH}$  is shown in black and elutes at 41.6 min (trace 1), whereas  $c[3\text{-NH}_2\text{-CH}_2\text{-Phac-Lys(Boc)-Lys(Boc)-Arg(Pbf)-Gaba}]$  is shown in blue and elutes at 51.9 min (trace 2).

The four cyclic inhibitors **108-111** were prepared as described in Scheme 3.8. The 2-chlorotriylchlorid resin was loaded with the L- or D-derivatives of Boc-Lys(Fmoc)-OH or Boc-Orn(Fmoc)-OH. After removal of the Fmoc group in the side chain, the following residues were coupled by standard Fmoc SPPS (step b). After mild acidic cleavage of the peptide from resin (step c), the linear intermediates were cyclized in solution to give the Cbz- and Boc-protected cyclic peptides (step d). The Boc-protection was removed by TFA (step e), and the obtained free amine was converted into the bis-Boc-protected guanidine (step f). Final deprotection by HBr in acetic acid provided the cyclic peptides **108-109** (step g).



**Scheme 3.8:** Synthesis of inhibitors **108-111**. (a) Loading of 2-chlorotrityl chloride resin with 1 equiv of the indicated amino acid derivative, 4 equiv DIPEA, dry DCM, 2 h; (b) Standard Fmoc SPPS (see Scheme 3.1); (c) 1% TFA in DCM, 3×30 min; (d) 3 equiv Bop; 3 equiv DIPEA, DMF, ~ 72 h; (e) 90% TFA, at RT 1 h; (f) 2 equiv *N,N'*-di-Boc-1*H*-pyrazole-1-carboxamide, 4 equiv DIPEA in DMF, 16 h (g) 32% HBr in acetic acid, 1h, preparative HPLC.

The exemplarily shown HPLC chromatograms for the cyclization step d during the synthesis of compound **108** revealed also a relatively clean cyclization, which was similar for the other three intermediates (Figure 3.8).

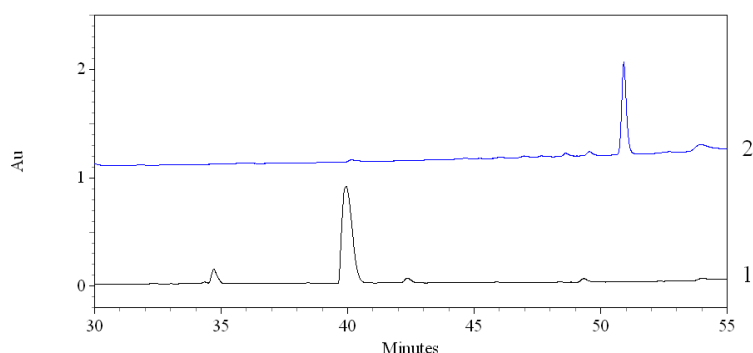


**Figure 3.8:** HPLC analysis of the intermediates after step c (linear peptide in trace 1 shown in black, elution at 39.6 min) and step d (cyclic peptide in trace 2 shown in blue, elution at 50.9 min) during the synthesis of inhibitor **108** (Scheme 3.8). The HPLC runs started at 10% solvent B.

### 3.11 Determination of inhibitory constants

The  $K_i$  values of all inhibitors were determined using the fluorogenic substrate Phac-Leu-Lys-Lys-Arg-AMC (**114**). This compound was derived from the widely used chromogenic substrate Ac-Leu-Lys-Lys-Arg-pNA<sup>66</sup> with two modifications. The incorporation of a fluorogenic AMC group improves its sensitivity and enables the use of lower enzyme concentrations in the assay, while the N-terminal phenylacetyl residue is known to be a suitable P4 moiety based on various inhibitor studies.<sup>66</sup> For the  $K_i$  determinations according to the method of Dixon three different substrate concentrations (200, 100 and 50  $\mu\text{M}$  in the assay) were used. The  $K_m$  and  $V_{max}$  of substrate **114** were determined at pH 8.5 ( $K_m = 47.5 \pm 1.7 \mu\text{M}$ ,  $k_{cat} = 0.26 \pm 0.003 \text{ s}^{-1}$ , and  $k_{cat}/K_m = 5460 \text{ s}^{-1}\text{M}^{-1}$ ). The steady-state rates  $v$  were calculated from the linear progress curves. The  $K_i$  values were obtained from Dixon plots, as shown in Figure 3.9 for inhibitor **78**, which has a  $K_i$  value of 0.12  $\mu\text{M}$ .

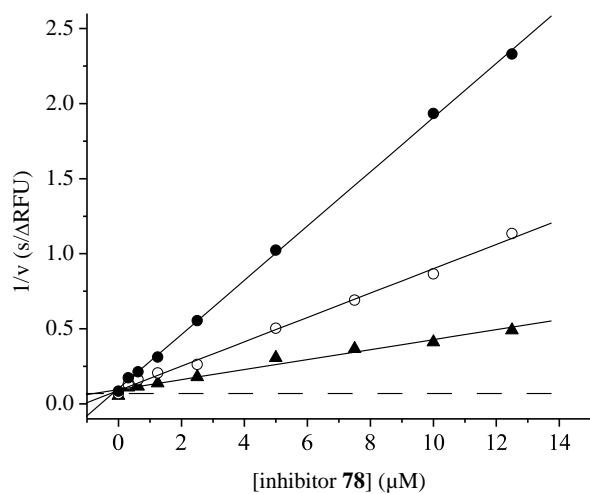


**Figure 3.9.** Dixon plot of inhibitor **78**. Kinetic measurements were performed with three different substrate concentrations (Phac-Leu-Lys-Lys-Arg-AMC: ● 50, ○ 100, and ▲ 200  $\mu$ M) in the presence of 2 nM WNV NS2B-NS3 protease using various inhibitor concentrations. The dashed line represents  $1/V_{max}$ , which was obtained from a Michaelis-Menten curve measured in parallel on the same 96-well plate.

During the course of work and based on the preferred P4-P2 segment in substrate-analogue inhibitors a second fluorogenic substrate Phac-Lys-Lys-Arg-AMC (**113**, MI-0743) was prepared. For this substrate a  $K_m$  of 12.16  $\mu$ M and a  $k_{cat}$  of 0.58  $s^{-1}$  were determined, resulting in a  $k_{cat}/K_m$  value of 48,100  $s^{-1}M^{-1}$ , which is nearly 9 times higher than for substrate **114**.



## 4 Conclusion

Potent inhibitors of the West Nile virus NS2B-NS3 protease could be useful drugs for the treatment of WNV infections. Therefore, in the present work, new substrate analogue inhibitors against the WNV protease have been developed.

### **Inhibitors with decarboxylated P1 arginine mimetics**

In the first series, new inhibitors containing various decarboxylated arginine mimetics in P1 position have been synthesized and characterized. Most of these arginine mimetics were incorporated in form of their amine precursors, which were finally converted into the corresponding guanidine analogues. In all cases the P1 guanidine inhibitors were more potent than their amine analogues. Moreover, most of the inhibitors with aliphatic P1 moieties showed higher potency than analogues containing aromatic P1 groups. In this series the cyclic *trans*-(4-guanidino)cyclohexylmethylamide (GCMA) was identified as the most suitable P1 residue. The strongest inhibitory potency was determined for compound Phac-Lys-Lys-GCMA (**39**) possessing an inhibition constant of 1.2  $\mu\text{M}$ . The best analogue containing a linear P1 residue Phac-Lys-Lys-*agmatine* (**26**) was identified, which inhibits the WNV protease with a  $K_i$  value of 3.9  $\mu\text{M}$ .

### **Modification of P2 and P3 residues**

It was known from literature that lysine is the most suitable P2 and P3 residue among the proteinogenic amino acids, when incorporated in substrate analogue inhibitors against the WNV protease. However, the lysine sidechain in P2 and P3 position is very flexible, therefore it should be replaced by more rigid basic amino acids. Various amino or guanidino substituted phenylalanines were incorporated in a second inhibitor series, whereby the P1 GCMA and P4 phenylacetyl residues were maintained. However, all of these inhibitors have reduced inhibitory potency (Table 3.3).

### **Modification of P4 residues**

In this series, a P3-P1 Lys-Lys-*agmatine* segment was maintained, whereby only the P4 residue was modified. Based on the known preference of the WNV protease for

inhibitors with a P4 phenylacetyl group in most cases substituted phenylacetyl residues were incorporated. Surprisingly, all of the substituted phenylacetyl residues led to an improved potency, whereby the incorporation of a Fmoc- or *p*-hydroxyphenylpropionyl group led to dramatic loss in potency. The dichloro-substituted phenylacetyl moieties were found to be the most suitable P4 residues providing agmatine-derived inhibitors with  $K_i$  values of approximately 0.5  $\mu\text{M}$  (Table 3.4).

### Combination of the best P4 and P1 residues

From the previous series, the guanidine-substituted cyclohexylmethyl amide (GCMA) and the dichloro-substituted phenylacetyl moieties were found to be the most appropriate P1 and P4 residues. In contrast, no improvement was achieved by replacement of lysine in P2 or P3 position with other basic amino acids. Therefore, a combination of the different dichloro-substituted phenylacetyl residues in P4 position with the P1 GCMA residue provided further improved inhibitors with  $K_i$  values < 0.15  $\mu\text{M}$  (Table 3.5).

### Selectivity studies of selected inhibitors

Selected inhibitors, including the three most potent inhibitors containing a P1 GCMA group and two additional agmatine derivatives, were tested against the three trypsin-like serine proteases thrombin, factor Xa and matriptase (Table 3.6). The agmatine derivatives **56** and **73** have shown a low micromolar inhibitory range against matriptase, whereas the selected GCMA analogues **76-78** possess an improved selectivity with negligible affinity against the tested trypsin-like serine proteases.

### X-ray structure of the WNV NS2B-NS3 protease in complex with inhibitor **77**

In the group of Prof. Hilgenfeld (University Lübeck) a crystal structure of the WNV NS2B-NS3 protease in complex with compound 3,4-dichlorophenylacetyl-Lys-Lys-GCMA (**77**) was solved, which is one of the most potent inhibitors. The inhibitor adopts a compact horseshoe-like conformation, whereby the P4 phenyl group comes in close contact to the P1 cyclohexyl ring. This conformation is stabilized by intramolecular hydrogen bond between the P4 carbonyl oxygen and the P1 guanidino group. Additionally, double salt bridges were observed between P1 guanidino group and the

Asp129 sidechain. These interactions explain the high potency of the inhibitors with P1 *trans*-(4-guanidino)cyclohexylmethanamide residue.

### Modifications deduced from the crystal structure

The obtained crystal structure revealed the binding of inhibitor **77** in the active site of the WNV NS2B-NS3 protease. The observed binding mode motivated us to perform further modifications within this substrate-analogue inhibitor type, the results are summarized in the following points:

- The observed empty space left in the S2 and S3 pockets of the crystal structure suggested that it might be possible to replace both lysines by additional basic or more bulky hydrophobic residues. However, a relatively poor inhibitory potency was determined for all of these inhibitors (Table 3.7). Therefore, lysine is still the most suitable P2 and P3 residue in substrate-analogue inhibitors, so far.
- The distance between the nitrogen atom of the GCMA guanidinium group and the side chain of Ile155 is about 4 Å. This suggested that an alkylation of the P1 guanidine by a small alkyl group could provide an additional hydrophobic interaction in the extended S1 pocket. However, a reduced potency was found for these alkylated inhibitors (Table 3.8).
- Inhibitor **77** adopts a horseshoe-like conformation, whereby the P4 phenyl ring comes in close contact to the P1 residue. This conformation encouraged us to prepare various cyclic analogues, which should possess a reduced flexibility compared to their linear analogues. In a first attempt, a head-to-tail cyclization using a P1' linker to interconnect the P1 with the P4 residue was performed. Due to a potential proteolytic cleavage after the P1 residue, a series of peptides containing various P1'-moieties were synthesized and tested for stability. Incubation of most of these peptides with the WNV protease revealed a relatively high stability against proteolytic degradation. For some of these analogues a relatively strong inhibitory potency was determined, e.g., Phac-Lys-Lys-Arg-NH<sub>2</sub> (**101**) inhibits the WNV protease with a  $K_i$  value of 0.4  $\mu$ M according to a reversible competitive inhibition mechanism. In a second cyclization attempt a direct coupling between the P1 and P4 residues was performed. Therefore, the P4-P2 segment was bound to a side chain instead

amino group of a lysine or ornithine residue in P1 position. Their  $\alpha$ -amino groups were converted into a guanidine, whereas their  $\alpha$ -carboxyl moieties were coupled to the P4 residue. However, only a weak inhibition was determined for all of these cyclic compounds.

In this present work, new decarboxylated arginine memtics inhibitors against the WNV NS2B-NS3 protease were developed. In comparison to the known agmatine derivatives, the P1 *trans*-4-Guanidinocyclohexylmethyamid containing inhibitors have higher potency and selectivity against the WNV. Moreover, the first crystal structure of the WNV protease in complex with small noncovalently-binding inhibitor was solved.

## 4 Zusammenfassung

Wirksame Hemmstoffe der WNV NS2B-NS3-Protease könnten nützliche Wirkstoffe für die Behandlung von Erkrankungen nach WNV-Infektionen sein. Daher wurden in der vorliegenden Arbeit neue, substratanaloge Inhibitoren gegen die WNV-Protease entwickelt und charakterisiert.

### **Inhibitoren mit decarboxylierten P1 Argininmimetika**

In einer ersten Serie wurden neue Inhibitoren mit verschiedenen decarboxylierten Argininmimetika in P1-Position synthetisiert und charakterisiert. Der Einbau dieser Argininmimetika erfolgte in der Regel in Form ihrer Aminvorstufen, welche anschließend in die entsprechenden Guanidinanaloga umgewandelt wurden. In allen Fällen waren die Hemmstoffe mit den Guanidinoesten in P1-Position wirksamer als ihre Aminanaloga. In der Regel waren die Verbindungen mit aliphatischen P1-Resten stärkere Inhibitoren als die Analoga mit aromatischen P1-Gruppen. Als besonders wirksames P1-Derivat innerhalb dieser Serie wurde der *trans*-4-Guanidinocyclohexylmethylamid-Rest (GCMA) identifiziert. Die stärkste Hemmwirkung mit einem  $K_i$ -Wert von 1,2  $\mu\text{M}$  wurde für die Verbindung Phac-Lys-Lys-GCMA (**39**) bestimmt. Als wirksamstes Derivat mit einem linearen P1-Rest wurde der Inhibitor Phac-Lys-Lys-Agmatin (**26**) erhalten, das die WNV-Protease mit einer Hemmkonstanten von 3,9  $\mu\text{M}$  inhibiert.

### **Modifizierung der P2- und P3-Reste**

Aus der Literatur ist bekannt, dass Lysin die günstigste proteinogene Aminosäure für die P2- und P3-Position in substratanalogen Inhibitoren der WNV-Protease ist. Jedoch ist die Seitenkette des Lysins sehr flexibel. Deshalb wurde in einer weiteren Serie das Lysin in diesen beiden Positionen durch rigidere, basische Aminosäurereste ersetzt. Dabei wurden mit Amino- oder Guanidinogruppen substituierte Phenylalanine eingebaut, wobei der *trans*-4-Guanidinocyclohexylmethylamid-Rest in P1-Position und die P4-Phenylacetylgruppe beibehalten wurden. Jedoch wurde für alle Inhibitoren dieser Serie eine verringerte Hemmwirkung festgestellt (Tabelle 3.3).

### Modifizierung des P4-Restes

In diesem Falle wurde der Baustein Lys-Lys-Agmatin als P3-P1-Segment beibehalten und nur der P4-Rest modifiziert. Da aus der Literatur bereits bekannt war, dass die WNV-Protease eine Phenylacetylgruppe in P4-Position bevorzugt, wurden vor allem substituierte Phenylacetylreste verwendet. Überraschenderweise bewirkte der Einbau sämtlicher substituierten Phenylacetyl-Derivate eine Verstärkung der Hemmwirkung, im Gegensatz dazu kam es nach Ankopplung einer N-terminalen Fmoc – oder *p*-Hydroxyphenylpropionylgruppe zu einem drastischen Aktivitätsverlust. Als besonders geeignet haben sich Phenylacetylreste in P4-Position erwiesen, die mit zwei Chloratomen substituiert sind. Jedoch wurde die Hemmwirkung durch das Substituierungsmuster am Phenylring kaum beeinflusst, für die drei wirksamsten Inhibitoren wurden  $K_i$ -Werte um  $0,5 \mu\text{M}$  bestimmt (Tabelle 3.4).

### Kombination der wirksamsten P4- und P1-Reste

Aus den zuvor untersuchten Inhibitorserien war bekannt, dass das *trans*-4-Guanidinocyclohexylmethylamid und die dichlorsubstituierten Phenylacetylgruppen besonders geeignete P1- und P4-Reste sind. Im Gegensatz dazu führte der Austausch des Lysins in P2- und/oder P3-Position durch andere basische Aminosäuren zu einem deutlichen Aktivitätsverlust. Deshalb wurden neue Inhibitoren durch Kombination der besten P1- und P4-Reste synthetisiert, wobei die beiden Lysinreste in P2- und P3-Position beibehalten wurden. Dadurch konnte die Hemmwirkung weiter verbessert werden und es wurden drei Inhibitoren mit  $K_i$ -Werten  $< 0,15 \mu\text{M}$  erhalten (Tabelle 3.5).

### Selektivitätsstudien ausgewählter Inhibitoren

Für einige Inhibitoren, darunter die drei wirksamsten Verbindungen mit einem *trans*-4-Guanidinocyclohexylmethylamid in P1-Position und zwei zusätzliche Agmatinderivate, wurde die Hemmwirkung auf die drei trypsinartigen Serinproteasen, Thrombin, Faktor Xa und Matriptase untersucht (Tabelle 3.6). Die Agmatinderivate **56** und **73** inhibieren neben der WNV-Protease auch Matriptase im niedrig-mikromolaren Bereich. Dagegen besitzen die ausgewählten Inhibitoren **76-78** mit einem *trans*-4-Guanidinocyclohexylmethylamid eine höhere Selektivität und haben nur eine vernachlässigbare Hemmwirkung auf die untersuchten trypsinartigen Serinproteasen.

### **Struktur der WNV NS2B-NS3-Protease im Komplex mit Inhibitor 77**

Im Arbeitskreis Hilgenfeld (Universität Lübeck) wurde eine Kristallstruktur der WNV NS2B-NS3-Protease im Komplex mit der Verbindung 3,4-dichlorphenylacetyl-Lys-Lys-*trans*-4-Guanidinocyclohexylmethylamid (**77**) gelöst. Der gebundene Inhibitor nimmt eine kompakte hufeisenförmige Konformation an, in der der P4 Phenylring in engen Kontakt mit dem Cyclohexylring des P1-Restes kommt. Diese Konformation wird durch eine intramolekulare Wasserstoffbrückenbindung zwischen dem P4 Carbonylsauerstoff und der P1-Guanidinogruppe stabilisiert. Daneben wurde eine doppelte Salzbrücke der P1-Guanidinogruppe zur Seitenkette des Asp129 gefunden. Diese Wechselwirkungen erklären die starke Hemmwirkung der Inhibitoren mit einem *trans*-4-Guanidinocyclohexylmethylamid in P1-Position.

### **Aus der Kristallstruktur abgeleitete Modifizierungen**

Aufgrund des beobachteten Bindungsmodus des Inhibitors **77** im aktiven Zentrum der WNV NS2B-NS3-Protease wurden die substratanalogen Inhibitoren weiter modifiziert, die Ergebnisse sind in den folgenden Punkten zusammengefasst.

- Da in der Kristallstruktur beobachtet wurde, dass die S2- und S3-Taschen durch die Lysinseitenketten nicht vollständig ausgefüllt sind, wurden die Lysine durch andere basische oder sterisch anspruchsvollere und hydrophobe Aminosäurereste ersetzt. Es wurde jedoch für all diese Inhibitoren nur eine schwache Hemmwirkung bestimmt. (Tabelle 3.7). Nach derzeitigem Erkenntnisstand ist Lysin der bevorzugte P2- und P3-Rest in substratanalogen Inhibitoren der WNV-Protease.
- Die Distanz zwischen dem Stickstoffatom der Guanidinogruppen des *trans*-4-Guanidinocyclohexylmethylamid und der Seitenkette des Ile155 beträgt etwa 4 Å. Deshalb wurde das P1-Guanidin mit einer Methyl- oder Ethylgruppe alkyliert, um eine zusätzliche hydrophobe Wechselwirkungen zum Ile155 am Rande der S1-Tasche zu generieren, wobei der basische Charakter der Guanidinogruppe erhalten bleiben sollte. Es wurde jedoch eine deutlich verringerte Wirksamkeit für diese beiden alkylierten Inhibitoren bestimmt (Tabelle 3.8).

- Inhibitor **77** nimmt eine hufeisenförmige Konformation an, bei der der P4 Phenylring nah an den P1-Rest kommt. Deshalb wurden erste cyclische Derivate synthetisiert, um diese gebundene Konformation bereits in Lösung zu stabilisieren und dadurch die Flexibilität der Inhibitoren einzuschränken. In einem ersten Ansatz wurde eine *head to tail* Zyklisierung über einen P1'-Linker vorgenommen, der an den P4-Rest gekoppelt wurde. Für die beiden zyklischen Derivate (Figure 3.5) wurden jedoch nur Hemmkonstanten um  $35 \mu\text{M}$  bestimmt. Um eine mögliche Spaltung dieser substratanalogen Strukturen nach dem P1-Rest zu vermeiden, wurde parallel eine Serie mit unterschiedlichen P'-Resten synthetisiert und die Stabilität dieser Inhibitoren nach Inkubation mit der WNV-Protease mittels HPLC geprüft. Für alle untersuchten Derivate wurde eine relativ hohe Stabilität gefunden, die deutlich über der des chromogenen Substrates Phac-Lys-Lys-Arg-pNA liegt. Für einige lineare Verbindungen wurde eine starke inhibitorische Wirksamkeit bestimmt, z.B. hemmt Phac-Lys-Lys-Arg-NH<sub>2</sub> (**101**) die WNV-Protease mit einem  $K_i$ -Wert von  $0,4 \mu\text{M}$  nach einem reversibel-kompetitiven Hemmmechanismus. In einem zweiten Ansatz wurde eine Zyklisierung durch direkte Kopplung der P1- und P4-Reste vorgenommen. Dafür wurde das P4-P2 Segment an die Seitenkette eines Lysin- oder Ornithinrestes gekoppelt. Am Ende wurde die  $\alpha$ -Aminogruppe der P1-Reste in ein Guanidin überführt und deren freie Carboxylfunktion an den P4-Rest gekoppelt. Für alle zyklischen Verbindungen wurde jedoch nur eine schwache Hemmwirkung bestimmt.

Im Rahmen dieser Arbeit ist es durch Einbau besonders geeigneter, decarboxylierter Argininmimetika gelungen, Hemmstoffe der WNV NS2B-NS3-Protease mit Hemmkonstanten um  $0,15 \mu\text{M}$  zu erhalten. Im Vergleich zu den bereits bekannten Verbindungen mit Agmatin in P1-Position besitzen die Derivate mit einem *trans*-4-Guanidinocyclohexylmethylamid eine erhöhte Selektivität gegenüber einigen trypsinartigen Serinproteasen, wie Matriptase. Mit einem der neu entwickelten Inhibitoren konnte erstmals eine Kristallstruktur der WNV-Protease mit einem nichtkovalent-bindenden niedermolekularen Inhibitor gelöst werden.

## 5 Experimental part

### 5.1 Reagents and methods

#### 5.1.1 Reagents and materials

Standard chemicals and solvents were obtained from Acros, VWR, Fisher Scientific, Fluka, Sigma-Aldrich, Merck, or Roth. The used solvents had p.a or HPLC-grade quality. Dry solvents were stored over molecular sieves. The acetonitrile for analytical and preparative HPLC was purchased from VWR (HiPerSolv CHROMANORM). Ultra pure water was prepared using a NOWA pure select system (KSN Water Technology, Nistertal). Aqueous solutions of acids, bases or salts were prepared using demineralized water. Trifluoroacetic acid was a gift from Solvay. Amino acids and their derivatives were purchased from Bachem, Novabiochem, Orpegen Pharma, PolyPeptide, or IRIS Biotech.

#### 5.1.2 Thin layer chromatography

Thin layer chromatography (TLC) was performed on precoated "silica gel 60 F254" plates from Merck. A mixture of n-butanol/acetic acid/water (4:1:1, v/v/v) was used as a mobile phase. The compounds were visualized either by fluorescence detection ( $\lambda_{\text{ex}}$  254 nm), or by spraying with a ninhydrin solution and heating (300 mg ninhydrin dissolved in 100 mL n-butanol and 3 mL glacial AcOH) followed by incubation in a chlorine gas atmosphere and spraying with an o-toluidine solution (filtered solution of 150 mg o-toluidine and 2.1 g KI dissolved in 2 mL AcOH and 148 mL water) to reveal the spots.

#### 5.1.3 High performance liquid chromatography (HPLC)

For all HPLC experiments the following solvents were used:

- solvent A: 0.1% TFA in ultrapure water
- solvent B: 0.1% TFA in ACN

### *Analytical HPLC*

Unless otherwise mentioned, all analytical reversed-phase HPLC chromatograms were performed using a Shimadzu LC-10A gradient HPLC system consisting of the subsystems CTO-10A column oven, LC-10ATvp pumps (2 x), DGU-14A degasser, SIL-10Axl autoinjector, SCL-10Avp system controller, SPD-M 10Avp photodiode array detector, Shimadzu Class-VP software and a reversed phase column (Nucleodur 100-5 C<sub>18</sub> ec, 250 mm x 4.6 mm, Macherey-Nagel, Düren, Germany). The detection was performed at 220 nm. Solvents A and B served as eluents at a flow rate of 1 mL/min and a linear gradient of 1 % increase in solvent B/min. Different starting conditions (1, 10, 20 and 30% B) were used for analytical HPLC depending on the properties of the compounds, which are indicated for each derivative. The given purity for all intermediates is based on HPLC detection at 220 nm.

### *Preparative HPLC*

The final inhibitors were purified using a preparative HPLC system (pumps: Varian PrepStar Model 218 gradient system, detector: ProStar Model 320, fraction collector: Varian Model 701). The following columns (dimensions 250 mm × 32 mm) were used:

1. Nucleosil, 300-5 C<sub>18</sub>, 300 Å, Macherey-Nagel, Düren
2. Prontosil 120-5-C<sub>18</sub>-SH, 120 Å, Bischoff Chromatography

All purifications were performed using a linear gradient of acetonitrile/water containing 0.1 % TFA at a flow rate of 20 mL/min, using different starting conditions.

### **5.1.4 Lyophilization**

All final inhibitors and some intermediates were obtained as TFA salts after preparative HPLC followed by lyophilization from water or 80% *tert*-butanol using a *vacuum* freeze-drying system Alpha 2-4 LD plus (Christ, Osterode am Harz, Germany).

### **5.1.5 NMR and mass spectrometry**

<sup>1</sup>H and <sup>13</sup>C spectra were recorded by using ECX-400 (Jeol., USA) at 400 and 100 MHz or Jeol Eclipse Plus (Jeol Inc., USA) at 500 and 126 MHz and are referenced to internal solvent signals; the chemical shifts are given in ppm. The molecular mass of the

synthesized compounds was determined by a QTrap 2000 ESI mass spectrometry (Applied Biosystems, USA) or a VG Autospec (Micromass, USA).

## 5.2 Enzyme kinetic measurements

### 5.2.1 Kinetic measurement with the WNV NS2B-NS3 protease

All enzyme kinetic measurements with the WNV NS2B-NS3 protease were performed using the fluorogenic substrate Phac-Leu-Lys-Lys-Arg-AMC at  $\lambda_{\text{ex}} = 380$  nm and  $\lambda_{\text{em}} = 460$  nm using a microplate fluorescence plates reader Tecan Safire II (Männedorf, Switzerland). The substrate was dissolved and further diluted in ultrapure water, 1 mM stock solutions of the inhibitors were prepared and diluted in WNV protease assay buffer (100 mM Tris·HCl pH 8.5 containing 20% glycerol and 0.01% Triton X-100). The concentrations of the inhibitors in the assay were at least 200-fold higher than the used enzyme concentration. For the calculation of the molecular weight of the inhibitors, one TFA molecule was added for each basic group. The measurements were performed for 10 min at RT with the following volumina:

- 125  $\mu\text{L}$  buffer pH 8.5 containing the inhibitor
- 50  $\mu\text{L}$  aqueous substrate solution
- start of reaction with 25  $\mu\text{L}$  enzyme solution

$K_i$  values  $< 100$   $\mu\text{M}$  were calculated according to the method of Dixon<sup>93</sup> at three different substrate concentrations and six to eight different inhibitor concentrations. The inhibition constants for the weaker inhibitors were determined at a substrate concentration of 50  $\mu\text{M}$  using equation (1) for competitive reversible inhibition, where  $V_{\text{max}}$  is the maximum reaction rate could be achieved by the enzyme,  $K_m$  is the Michaelis-Menten constant and S is the substrate concentration

Equation

$$v = \frac{V_{\text{max}} \cdot S}{K_m \left(1 + \frac{I}{K_i}\right) + S} \quad (1)$$

### 5.2.2 Measurements with trypsin-like serine proteases

Chromogenic p-nitroanilide substrates were used for the determination of the inhibition constants ( $K_i$ ) for the trypsin-like serine proteases matriptase, factor Xa, and thrombin.<sup>94</sup> Measurements were performed at 405 nm using a microplate IEMS Reader MF 1401 (Labsystems, Helsinki, Finland). The substrates were dissolved in ultrapure water, 1 mM stock solutions of the synthesized inhibitors were prepared in Tris-HCl buffer pH 8.0 containing 0.154 M NaCl, and 2 % ethanol. The measurements were performed at RT with the following volumina:

- 200  $\mu$ L buffer pH 8.0 containing the inhibitor
- 25  $\mu$ L aqueous substrate solution
- start of reaction with 50  $\mu$ L enzyme solution

The measurements were stopped by the addition of 25  $\mu$ L 50% AcOH after an appropriate reaction time, when the absorbance at the highest substrate concentration in the absence of an inhibitor had reached a value between 0.15 and 0.18.<sup>94</sup> The  $K_i$  values were calculated from Dixon plots<sup>93</sup> at two substrate concentrations and five inhibitor concentrations using an EXCEL template developed by Stürzebecher. The  $K_i$  values are the mean of at least two independent measurements.

The used enzyme and substrate concentrations are summarized in Table 5.1.

## Experimental part

---

**Table 5.1:** Used enzymes and substrates.

<b>Enzyme stock and assay concentrations*</b>	<b>Substrate stock and assay concentrations</b>
WNV NS2B-NS3 protease <sup>90</sup> 16 nM (2 nM)	Phac-Leu-Lys-Lys-Arg-AMC; 0.8 mM (200 $\mu$ M in assay) 0.4 mM (100 $\mu$ M in assay) 0.2 mM (50 $\mu$ M in assay)
matriptase <sup>a</sup> (catalytic domain) <sup>95</sup> 1.44 nM (0.262 nM)	MeSO <sub>2</sub> -D-Cha-Gly-Arg-pNA; 2 mM (182 $\mu$ M in assay) 1 mM (91 $\mu$ M in assay) 0.5 mM (45.5 $\mu$ M in assay)
human factor Xa (fXa) <sup>a</sup> 200.35 IE/mg, Enzyme Research South Bend 2.72 nM (0.494 nM)	CH <sub>3</sub> OCO-D-Cha-Gly-Arg-pNA, 2 mM (182 $\mu$ M in assay) 1 mM (91 $\mu$ M in assay) 0.5 mM (45.5 $\mu$ M in assay)
bovine thrombin <sup>a96</sup> 1425 IE/mg 3.725 nM (0.677 nM)	MeSO <sub>2</sub> -D-Cha-Gly-Arg-pNA; 2 mM (182 $\mu$ M in assay) 1 mM (91 $\mu$ M in assay) 0.5 mM (45.5 $\mu$ M in assay)

<sup>a</sup>Matriptase, fXa and thrombin stock solutions were prepared in 0.9% NaCl solution containing 0.1% HSA or BSA. \* The concentrations in the assay are given in brackets.

## 5.3 Synthesis

### 5.3.1 General synthetic procedures

The following standard procedures A-Q for the synthesis of precursors, intermediates, and inhibitors were performed as described previously in several textbooks.<sup>97, 98</sup>

#### *Method A*

#### **Loading of Fmoc amino acids on 2-Cl-tritylchlorid (2Cl-Trt-Cl) resin**

The Fmoc amino acid (1 equiv) was suspended in dry DCM and treated with 4 equiv DIPEA to reveal a clear solution, which was added to 1 equiv resin in a polypropylene-syringe for manual SPPS equipped with a PTFE filter (Intavis Bioanalytical Instruments, Köln). After 2 h shaking at RT, the reaction solution was removed, and the resin was washed 3  $\times$  1 min with DCM/MeOH/DIPEA (17:2:1, v/v/v), followed by

multiple washing with DCM, DMF and again with DCM. The loaded resin was dried *in vacuum*.

### **Method B**

#### **Loading of diamines on tritylchlorid resin**

The amino component (4 equiv) was dissolved in dry DCM and loaded to the tritylchloride resin as described on method A, followed by an identical washing procedure. If the amines were used as salts additional 4 equiv DIEPA was added.

### **Method C**

#### **Fmoc solid phase peptide synthesis**

The manual Fmoc SPPS was performed in 2 or 5 mL polypropylene-syringes (Multisynthech GmbH, Witten, Germany) equipped with PTFE (polytetrafluoroethylene) filters using a standard Fmoc protocol. A solution of 20% piperidine in DMF was used for Fmoc cleavage and, after washing with DMF, the coupling of the following residue was achieved using 4 equiv of acid, HBTU, and HOBT in presence of 8 equiv of DIPEA. The used synthesis cycle is shown in Table 5.2

**Table 5.2:** Steps of the used standard SPPS cycle.

Step	Procedure and reagent	Time (min)
1	resin swelling (only for first cycle)	1 × 10
2	Fmoc cleavage	1 × 5 and 1 × 20
3	washing with DMF 1	3 × 1
4	washing with DMF 2	3 × 1
5	washing with DMF 3	2 × 1
6	Fmoc amino acid coupling	1 × 120
7	washing with DMF 4	3 × 1
8	washing with DMF 1	1 × 1

### **Method D**

#### **Weak acidic cleavage from resin keeping side chain protections**

After completing the SPPS, the peptide was cleaved from the resin using 1% TFA in DCM (3 × 30 min). The solution containing the cleaved peptide was immediately neutralized with DIPEA after each cleavage step. Finally, the solvents were removed *in vacuum*.

### **Method E**

#### **Strong acidic cleavage from resin**

After completing the SPPS, the peptide was cleaved (approximately 1 h) from resin using a mixture of TFA/TIS/H<sub>2</sub>O (95/2.5/2.5, v/v/v). For intermediates the solvent was removed *in vacuum* and used for the next step.

If the desired inhibitor/peptide was obtained at this cleavage, the TFA was partially removed and the remaining solution was added dropwise to cold diethyl ether. The precipitate was obtained by centrifugation, washed with diethyl ether, and dried *in vacuum*. The product was purified by preparative HPLC, and lyophilized from water or 80% *tert*-butanol.

### **Method F**

#### **PyBOP coupling<sup>99</sup>**

1 equiv of an amino component and 1 equiv of the carboxyl derivative were dissolved in DMF (5 mL/mmol) and treated with 1 equiv PyBOP and 2-3 equiv DIPEA to reach a pH value between 8.5 and 9.5. The mixture was stirred at 0 °C for 30 minutes and at RT for 2 h. The solvent was removed *in vacuum*. The residue was dissolved in EtOAc and washed trice with 5% KHSO<sub>4</sub>-solution, once with brine, trice with saturated NaHCO<sub>3</sub>-solution, and trice with brine. The EtOAc phase was dried over Na<sub>2</sub>SO<sub>4</sub>, filtered, and the solvent was removed *in vacuum*.

### **Method G**

#### **Cleavage of Cbz-protecting group by HBr/acetic acid<sup>98</sup>**

1 equiv of Cbz-protected compound was dissolved in 32% HBr in glacial AcOH (10 mL/mmol). The mixture was shaken several times within 1 h at RT. The solvent was partially removed *in vacuum* and the product was precipitated by diethyl ether, filtered,

washed with diethyl ether, and dried *in vacuo*. Alternatively, the product was purified by preparative HPLC, and lyophilized from water or 80% *tert*-butanol.

### ***Method H***

#### **Introduction of Boc protecting group<sup>98</sup>**

1 equiv of the amino acid was dissolved in a mixture of organic solvent (dioxane or acetonitrile) and water (2:1, v/v, 5 mL/mmol) at 0 °C. This mixture was treated with 1.1 equiv 1 N NaOH and 1.1 equiv di-*tert*-butyl dicarbonate. The pH was adjusted to 8.5-9.5 with 1 N NaOH. The mixture was stirred for 3 h at RT, whereby the reaction was controlled by HPLC. If necessary, an additional amount of (Boc)<sub>2</sub>O and 1 N NaOH were added and the mixture was further stirred at RT overnight. The solvent was removed *in vacuo*. The residue was dissolved in EtOAc, washed trice with 5% KHSO<sub>4</sub>-solution, and trice with brine. The EtOAc phase was dried over Na<sub>2</sub>SO<sub>4</sub>, filtered and removed *in vacuo*.

### ***Method I***

#### **Cleavage of Boc-protecting group by 90% TFA<sup>100</sup>**

1 equiv of Boc-protected compound was dissolved in 90% TFA (5 mL/mmol) and the mixture was stirred for 1 to 2 h at RT. The solvent was removed *in vacuo*. If the desired inhibitor/peptide was obtained at this step, the TFA was partially removed and the product was precipitated by diethyl ether, filtered, washed with diethyl ether, and dried *in vacuo*. The product was purified by preparative HPLC, and lyophilized from water or 80% *tert*-butanol.

### ***Method J***

#### **Hydrogenation<sup>101</sup>**

The compound was dissolved in 90% AcOH and treated with approximately 10 mass percent of catalyst (10% Pd/C). The mixture was stirred at least overnight under a hydrogen atmosphere. If necessary (HPLC control), the hydrogenation was continued at RT for additional 24 h. The catalyst was removed by filtration and the solvent was evaporated. Alternatively, the product was purified by preparative HPLC and lyophilized from water or 80% *tert*-butanol.

**Method K**

**Introduction of the Tfa-group**<sup>97</sup>

1 equiv of the amino component was dissolved in methanol and treated with 1 equiv of trifluoroacetic anhydride and 1 equiv of DIPEA. The mixture was stirred at 0 °C for 1 h and at RT for 2 h. The reaction progress was monitored by HPLC, and if necessary, an additional amount of trifluoroacetic anhydride was added and stirring was continued at RT overnight. The solvent was removed *in vacuum*. The remaining residue was dissolved in EtOAc and washed trice with 5% KHSO<sub>4</sub>-solution and trice with brine. The EtOAc phase was dried over Na<sub>2</sub>SO<sub>4</sub>, filtered and the solvent was removed *in vacuum*.

**Method L**

**Cleavage of the Tfa-protecting group with 1 N NaOH**<sup>100</sup>

The corresponding Tfa-protected amino derivative was dissolved in a mixture of dioxane and water (1:1, 10 mL/mmol) and the pH was adjusted to 12 using 1 N NaOH. The mixture was stirred for 3 h (HPLC control), and if necessary, stirring was continued for some hours until the end of the reaction. The solution was neutralized by the addition of 10% TFA and the solvent was removed *in vacuum*. The product was purified by preparative HPLC and lyophilized from 80% *tert*-butanol.

**Method M**

**Conversion of amino into guanidino group**<sup>102</sup>

1 equiv of the free amino intermediate was dissolved in DMF (10 mL/mmol), treated with 2 equiv 1*H*-pyrazole-1-carboxamidine × HCl, and 3 equiv DIPEA. The mixture was stirred at RT for 24 h (HPLC control) and if necessary, an additional amount of 1*H*-pyrazole-1-carboxamidine × HCl and DIPEA were added, and stirring was continued until completion of the reaction. The solvent was removed *in vacuum*.

**Method N**

**Conversion of amino into di-Boc-protected guanidino group**<sup>103</sup>

1 equiv of the free amino intermediate was dissolved in DMF (10 mL/mmol), treated with 2 equiv *N,N'*-di-Boc-1*H*-pyrazole-1-carboxamidine, and 3 equiv DIPEA. The mixture was stirred at RT for 24 h (HPLC control) and if necessary, an additional

amount of *N,N'*-di-Boc-1*H*pyrazole-1-carboxamidine and DIPEA were added, and stirring was continued until completion of the reaction. The solvent was removed *in vacuum*.

### **Method O**

#### **Conversion of amino into methyl/ethyl-guanidine group<sup>88</sup>**

1 equiv of the free amino intermediate was dissolved in DMF (10 mL/mmol), treated with 2 equiv 2-Ethyl-1-methyl-isothiourea hydroiodide or 2-Ethyl-1-ethyl-isothiourea hydroiodide, and 2 equiv DIPEA. The mixture was stirred at RT for 24 h (HPLC control) and if necessary, an additional amount of the guanylation reagent and DIPEA were added, and stirring was continued until completion of the reaction. The solvent was removed *in vacuum*.

### **Method P**

#### **Introduction of Fmoc protecting group<sup>98</sup>**

1 equiv of the amino derivative was dissolved in ACN (10 mL/mmol) and treated with 2 equiv NMM or DIPEA. 1 equiv Fmoc-OSu dissolved in ACN<sup>80</sup> (5 mL/mmol) was added in two portions and the mixture was stirred at 0°C for 1h. The pH value was set to 8.5-9.5 by the addition of NMM or DIPEA. The mixture was stirred at RT for 3 h (HPLC control). If necessary, additional amounts of Fmoc-OSu and NMM or DIPEA were added and the mixture was further stirred at RT overnight. The solvent was removed *in vacuum*.

### **Method Q**

#### **Intramolecular cyclization in solution<sup>89</sup>**

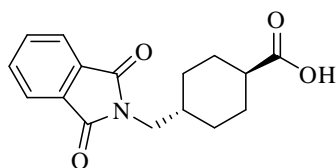
The peptide containing one free amino and one carboxyl group was dissolved in DMF (100 mL/0.1mmol). The mixture was treated with 3 equiv BOP and initially with 3 equiv DIPEA, followed by stirring at 0°C for 1h. During the reaction the pH was controlled several times and adjusted to 8.5-9.5 by adding small portions of DIPEA. The mixture was stirred at RT for 48-72 h and the reaction progress was controlled by HPLC. Finally, the solvent was removed *in vacuum*, the remaining residue was

dissolved in EtOAc and washed with 5% KHSO<sub>4</sub>-solution and trice with brine. The EtOAc phase was dried over Na<sub>2</sub>SO<sub>4</sub>, filtered, and the solvent was removed *in vacuo*.

### 5.3.2 Synthesis of the intermediates

#### **N-(trans-4-carboxycyclohexylmethyl)phtalimide**<sup>80</sup> **17a**<sup>[2]</sup>

(1r,4r)-4-((1,3-dioxoisindolin-2-yl)methyl)cyclohexanecarboxylic acid



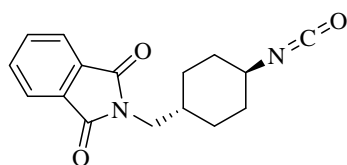
7.85 g trans-4-(aminomethyl)cyclohexane (50 mmol) suspended in 50 mL THF were treated with 10.95 g ethyl 1,3-dioxoisindoline-2-carboxylate (carboethoxyphthalimide) (50 mmol) and 7 mL triethylamine and refluxed for 18 h. The reaction mixture was concentrated *in vacuo*. The remaining oil was treated with 200 mL water containing 5 mL acetic acid, which resulted in the precipitation of the product. The white solid was filtered and dried.

Yield: 11.7 g (40.7 mmol), white powder.

HPLC: 46% B (purity: 89.5%).

#### **N-(trans-4-isocyanatocyclohexylmethyl)phtalimide**<sup>80</sup> **17b**

2-(((1r,4r)-4-isocyanatocyclohexyl)methyl)isoindoline-1,3-dione



11.7 g N-(trans-4-carboxycyclohexylmethyl)phtalimide **17a** (40.7 mmol) suspended in 100 mL carbon tetrachloride was treated with 5 mL thionyl chloride and refluxed for 4 h. The mixture was cooled and concentrated to approximately 50 % under reduced pressure. 7 mL trimethylsilyl azide were added and the mixture was further refluxed for

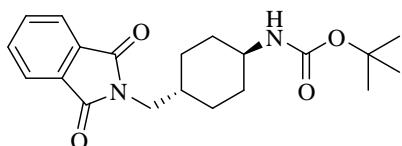
---

[2] The compound names provided in bold are trivial names and have been used in previous publications, in contrast the additional names below were generated according to the IUPAC nomenclature using the software ChemOffice Ultra 12.0 (Cambridge Soft).

18 h. Finally, the solvent was removed *in vacuum* providing a brown oil. The crude isocyanate was directly used for the next step.

**Boc-N-(trans-cyclohexylmethyl)phtalimide<sup>80</sup> 17c**

tert-butyl (1r,4r)-4-((1,3-dioxoisindolin-2-yl)methyl)cyclohexylcarbamate



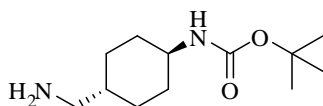
The crude intermediate **17b** was dissolved in 50 mL THF and treated with 3.2 g lithium *tert.*butoxide (40 mmol). The mixture was stirred at RT for 2 h forming a dark solution. The mixture was diluted with aqueous acetic acid. The crude product immediately precipitated and was recrystallized from 1-chlorobutane.

Yield: 2.2 g, gray crystals.

HPLC: 63.8% B (purity: 75%).

**trans-N-(4-tertbutoxycarbonylamino)cyclohexylmethyl amine<sup>80</sup> 17d**

tert-butyl (1r,4r)-4-(aminomethyl)cyclohexylcarbamate

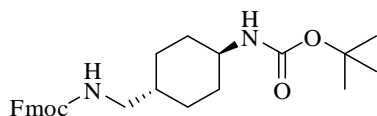


1.5 g Boc-N-(trans-cyclohexylmethyl)phtalimide **17c** (6.57 mmol) was treated with 1.6 mL hydrazine hydrate (50 mmol) in 200 mL isopropanol and stirred for 18 h followed by 4 h reflux. The mixture was concentrated, treated with cold aqueous acetic acid and filtered to remove the phthalazinedione. The aqueous layer was basified with NaOH, followed by extraction with ethyl acetate. The organic layer was dried with MgSO<sub>4</sub>, filtered and evaporated to give the product.

Yield: 0.9 g, white powder.

HPLC: 25.7% B (purity: 85.6%).

**Fmoc-AMCA-Boc 17e**



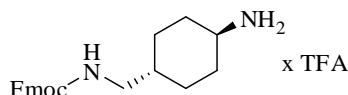
0.85 g trans-N-(4-tert-butoxycarbonylamino)cyclohexylmethyl amine **17d** (3.7 mmol) was treated with 1.25 g Fmoc-OSu (3.7 mmol) according to method P.

Yield: 1.3 g (2.88 mmol), yellow oil.

HPLC: 41.2% B (purity: 51.5%).

**trans-(4-Fmoc-aminomethyl)cyclohexylamine × TFA (Fmoc-AMCA × TFA) 17**

(9H-fluoren-9-yl)methyl ((1r,4r)-4-aminocyclohexyl)methylcarbamate



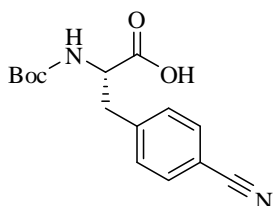
1.3 g of the intermediate **17e** (2.88 mmol) was treated with 12 mL TFA according to method I.

Yield: 1.1 g (2.37 mmol), white powder.

HPLC: 39.9% B (purity: 97.8%); MS calcd: 350.2, found: 351.3 [M+H]<sup>+</sup>; <sup>13</sup>C NMR ([D<sub>6</sub>]DMSO, 126 MHz): δ = 156.0, 143.8, 140.7, 127.5, 126.9, 125.0, 120.0, 65.0, 49.4, 46.8, 45.8, 36.5, 29.7, 27.8 ppm).

**Boc-Phe(4-CN)-OH 18a<sup>74</sup>**

(S)-2-(tert-butoxycarbonylamino)-3-(4-cyanophenyl)propanoic acid



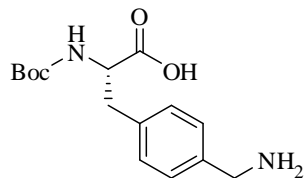
1 g H-Phe(4-CN)-OH (5.26 mmol) was treated with 1.262 g di-*tert*-butyl dicarbonate (5.786 mmol) according to method H.

Yield: 1.566 g (5.4 mmol), white powder.

HPLC: 45.7% B (purity: 95.6%).

**Boc-Phe(4-AMe)-OH **18b****<sup>74</sup>

(S)-3-(4-(aminomethyl)phenyl)-2-(tert-butoxycarbonylamino)propanoic acid



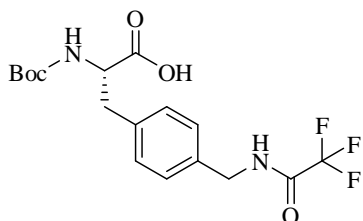
1.4 g Boc-Phe(4-CN)-OH **18a** (4.85 mmol) was treated with ~ 0.15 g Pd/C according to method J. The product was used for the synthesis of intermediate **18c** without further purification.

Yield: 1.15 g (3.9 mmol), yellow oil.

HPLC: 26.9% B (purity: 88.6%).

**Boc-Phe(4-Tfa-AMe)-OH **18c****<sup>74</sup>

(S)-2-(tert-butoxycarbonylamino)-3-(4-((2,2,2-trifluoroacetamido)methyl)phenyl)-propanoic acid



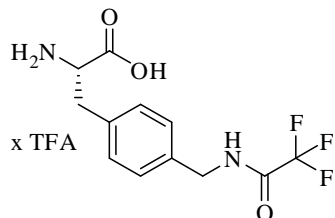
1 g Boc-Phe(4-AMe)-OH **18b** (3.39 mmol) was treated with 478  $\mu$ L trifluoroacetic anhydrid according to method K.

Yield: 1.35 g (3.46 mmol), yellow oil.

HPLC: 48.8% B (purity: 85.3%).

**Phe(4-AMe-Tfa)-OH × TFA **18d****

(S)-2-amino-3-(4-((2,2,2-trifluoroacetamido)methyl)phenyl)propanoic acid × TFA



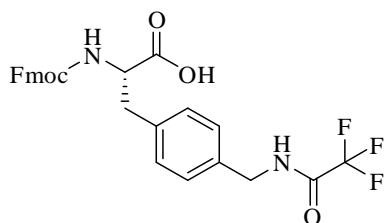
1 g Boc-Phe(4-AMe-Tfa)-OH **18c** ( 2.56 mmol) was treated with ~ 12 mL TFA according to method I. The product was dried *in vacuum*, and used for the synthesis of intermediate **18** without further purification.

Yield: 1.05 g (2.6 mmol as salt), white powder.

HPLC: 22.6% B (purity: 90.2%).

**Fmoc-Phe(4-AMe-Tfa)-OH **18****

(S)-2-(((9H-fluoren-9-yl)methoxy)carbonylamino)-3-(4-((2,2,2-trifluoroacetamido)-methyl)phenyl)propanoic acid



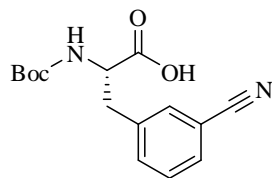
1 g Phe(4-AMe-Tfa)-OH × TFA **18d** (2.47 mmol) was treated with 0.833 g Fmoc-OSu (2.47 mmol, 1 equiv) according to method P.

Yield: 1.1. g (2.14 mmol), white powder.

HPLC: 61.7% B (purity: 84.4%).

**Boc-Phe(3-CN)-OH 19a**<sup>74</sup>

(S)-2-(tert-butoxycarbonylamino)-3-(3-cyanophenyl)propanoic acid



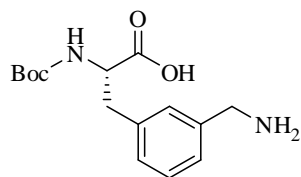
1 g Phe(3-CN)-OH (5.26 mmol) was treated with 1.262 g di-*tert*-butyl dicarbonate (5.786 mmol) according to method H.

Yield: 1.466 g (5.05 mmol), white powder.

HPLC: 45.2% B (purity: 90.1%).

**Boc-Phe(3-AMe)-OH 19b**<sup>74</sup>

(S)-3-(3-(aminomethyl)phenyl)-2-(tert-butoxycarbonylamino)propanoic acid



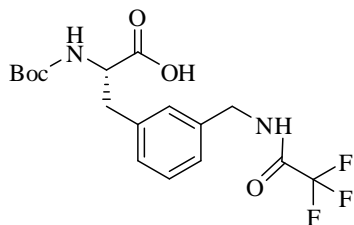
1.2 g Boc-Phe(3-CN)-OH **19a** (4.14 mmol) was treated with ~ 0.15 g Pd/C according to method J. The product was used for the preparation of intermediate **19c** without further purification.

Yield: 0.98 g (3.33 mmol), yellow oil.

HPLC: 26.7% B (purity: 90.4%).

**Boc-Phe(3-AMe-Tfa)-OH **19c****<sup>74</sup>

(S)-2-(tert-butoxycarbonylamino)-3-(3-((2,2,2-trifluoroacetamido)methyl)phenyl)propanoic acid



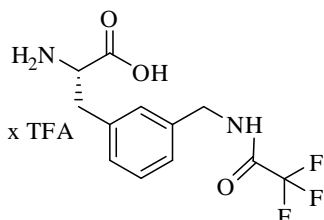
0.95 g Boc-Phe(3-AMe)-OH **19b** (3.23 mmol) was treated with 455  $\mu$ L trifluoroacetic anhydrid (3.23 mmol) according to method K.

Yield: 1.2 g (3.07 mmol), yellow oil.

HPLC: 46.5% B (purity: 77%).

**H-Phe(3-AMe-Tfa)-OH  $\times$  TFA **19d****

(S)-2-amino-3-(3-((2,2,2-trifluoroacetamido)methyl)phenyl)propanoic acid  $\times$  TFA



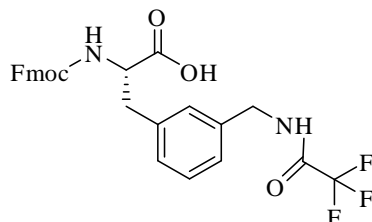
1 g Boc-Phe(3-AMe-Tfa)-OH **19c** (2.56 mmol) was treated with  $\sim$ 12 mL TFA according to method I. The product was precipitated with diethyl ether and separated by centrifugation. Finally, the product was dried *in vacuum*, and used in the synthesis of compound **19** without further purification.

Yield: 0.93g (2.56 mmol as salt), white powder.

HPLC: 23.3% B (purity: 89.4%).

### Fmoc-Phe(3-AMe-Tfa)-OH **19**

(S)-2-(((9H-fluoren-9-yl)methoxy)carbonylamino)-3-(3-((2,2,2-trifluoroacetamido)-methyl)phenyl)propanoic acid



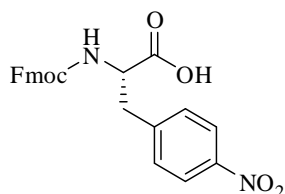
1 g Phe(3-AMe-Tfa)-OH × TFA **19d** (2.22 mmol) was treated with 0.833 g Fmoc-OSu (2.22 mmol) according to method P.

Yield: 1.05. g (2.05 mmol), white powder.

HPLC: 60.2% B (purity: 88.4%).

### Fmoc-Phe(4-NO<sub>2</sub>)-OH **20**

(S)-2-(((9H-fluoren-9-yl)methoxy)carbonylamino)-3-(4-nitrophenyl)propanoic acid

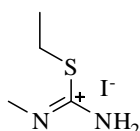


1 g Phe(4-NO<sub>2</sub>)-OH (4.75 mmol) was treated with 1.60 g Fmoc-OSu (4.75 mmol) according to method P.

Yield: 1.3 g, (3.01 mmol), white powder.

HPLC: 63.3% B (purity: 91.9%).

### 2-Ethyl-1-methyl-isothiourea hydroiodide<sup>88</sup> **21**



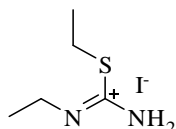
2.166 g 1-methylthiourea (24 mmol) was dissolved in 5 mL absolute ethanol, treated with 1.93 mL iodoethan (24 mmol) and stirred at 60°C for 4 h. The reaction mixture

was concentrated *in vacuum*. The product was obtained as mobile yellowish oil and was used later without further purification.

Yield: 5.6 g (22.9mmol), yellowish oil, MS calcd: 118.06, found: 119.06 (M+H)<sup>+</sup>.

TLC:  $R_f = 0.46$

### 2-Ethyl-1-ethyl-isothiourea hydroiodide<sup>88</sup> **22**



2.5 g 1-ethylthiourea (24 mmol) were converted into 2-ethyl-1-ethyl-isothiourea hydroiodide in analogy to the synthesis of derivative **21**. The intermediate **22** was obtained as mobile yellowish oil and was further used without purification.

Yield: 6.1 g (23.5mmol), yellowish oil, MS calcd: 132.07, found: 133.05 (M+H)<sup>+</sup>.

TLC:  $R_f = 0.47$

### 5.3.3 Synthesis of inhibitors 23-39 containing different P1 residues

#### Inhibitors 23-32, 38 and 39

0.1 g trityl chloride resin (loading 1.5 mmol/g) was treated with the unprotected diamines or with Fmoc-(aminomethyl)cyclohexanamine **17** according to method B. After resin loading (method A), standard Fmoc-protocol as described in method C was used for the subsequent solid phase peptide synthesis to assemble the amino acids and the terminal phenylacetyl-residue. After the final coupling step, the peptides with the general formula Phac-Lys(Cbz)-Lys(Cbz)-X (X: different P1 diamines) were cleaved from the resin using a mixture of 95 % TFA, 2.5 % H<sub>2</sub>O and 2.5 % TIS (method E) to obtain the intermediates **23a**, **25a**, **27a** **29a**, **31a** and **38a**.

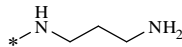
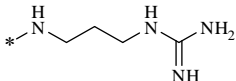
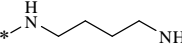
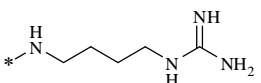
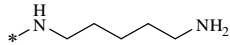
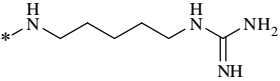
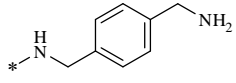
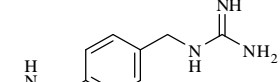
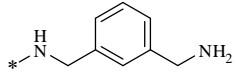
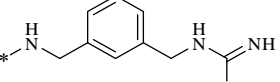
The half amount of these amine intermediates were converted into their corresponding guanidine analogues according to method M, which provided the intermediates **24a**, **26a**, **28a**, **30a** and **39a**.

The Cbz protecting group of these intermediates were cleaved using HBr/acetic acid as described in method G to provide the corresponding inhibitors. All inhibitors were

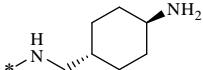
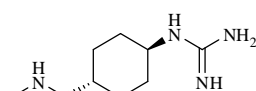
## Experimental part

precipitated by diethyl ether, filtered, washed with diethyl ether, and finally purified by preparative HPLC, and lyophilized from water or 80% *tert*-butanol (Scheme3.1). The analytical data of the inhibitors **23-32**, **38** and **39** and their related intermediates **23a-32a**, **38a** and **39a** are summarized in Table 5.3.

**Table 5.3:** Analytical characterization of the WNV protease inhibitors with the general formula Phac-Lys-Lys-P1. The numbers of their corresponding side-chain protected intermediates Phac-Lys(Cbz)-Lys(Cbz)-P1 are labeled with index **a**.

No.	P1	HPLC (% B)	Purity (%)	MS (calcd/found) (M+H) <sup>+</sup>
<b>23</b> (MI-0631)		16.8	99.0	448.3/449.4
<b>23a</b>		47.5	59.2	n.b.
<b>24</b> (MI-0638)		18.5	91.5	490.3/491.0
<b>24a</b>		48.8	-	n.b.
<b>25</b> (MI-0629)		17.3	99.0	462.3/463.5
<b>25a</b>		49.8	96.8	n.b.
<b>26</b> (MI-0637)		19.4	97.0	504.4/505.2
<b>26a</b>		51.1	-	n.b.
<b>27</b> (MI-0632)		18.4	99.0	476.3/477.4
<b>27a</b>		50.1	45.3	n.b.
<b>28</b> (MI-0635)		20.7	99.0	518.4/519.3
<b>28a</b>		51.3	-	n.b.
<b>29</b> (MI-0639)		20.0	99.0	510.3/511.4
<b>29a</b>		49.0	56.2	n.b.
<b>30</b> (MI-0642)		21.4	96.5	552.4/553.6
<b>30a</b>		50.4	-	n.b.
<b>31</b> (MI-0633)		20.8	99.0	510.3/511.4
<b>31a</b>		49.8	52.2	n.b.
<b>32</b> (MI-0636)		22.8	92.5	552.4/553.4
<b>32a</b>		50.9	-	n.b.

## Experimental part

<b>38</b> (MI-0645)		18.5	99.0	502.4/503.2
<b>38a</b>		51.5	39.0	n.b.
<b>39</b> (MI-0646)		21.5	99.0	544.3/545.3
<b>39a</b>		52.9	-	n.b.

The crude guanylated intermediates labeled with index **a** were directly used for final deprotection, therefore, no purity is given for these analogues.

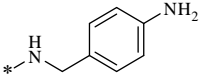
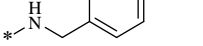
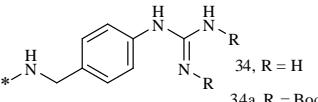
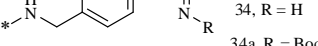
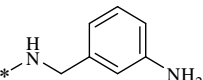
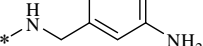
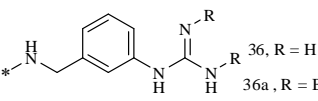
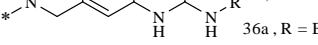
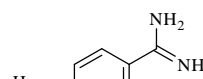
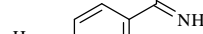
### Inhibitors 33-37

The intermediate Phac-Lys(Cbz)-Lys(Cbz)-OH was obtained using 0.1 g 2-chlorotriyl chloride resin (1.57 mmol/g) for each inhibitor, which was loaded with Fmoc-Lys(Cbz)-OH according to method a. After washing, Fmoc-Lys(Cbz)-OH and the phenylacetyl-residue were coupled as described in method c. The peptide was cleaved from resin as mentioned in method E. The solvent was removed *in vacuum* providing the oily Phac-Lys(Cbz)-Lys(Cbz)-OH (HPLC: 56.5% B, purity: 86.6%).

This intermediate was further coupled with 4-(aminomethyl)aniline, 3-(aminomethyl)aniline or 4-aminobenzimidamide according to method F to provide the Cbz protected intermediates **33a**, **35a** and **37a**. The half amount of analogues **33a** and **35a** and the complete intermediate **37a** were deprotected as described in method G to obtain the corresponding inhibitors **33**, **35**, and **37**. The half amount of the Cbz-protected intermediates **33a** and **35a** were treated with *N,N'*-di-Boc-1*H*-pyrazole-1-carboxamidine according to method N to obtain the derivatives **34a** and **36a**, followed by deprotection using HBr/acetic acid (method G) to reveal the inhibitors **34** and **36**. The inhibitors were precipitated by diethyl ether, filtered, washed with diethyl ether, and finally purified by preparative HPLC, and lyophilized from water (Scheme 3.2). The analytical data of the inhibitors **33-37** and their related intermediates **33a-37a** are given in the Table 5.4.

## Experimental part

**Table 5.4:** Analytical characterization of WNV protease inhibitors and their corresponding intermediates with the general formula Phac-Lys-Lys-P1 and Phac-Lys(Cbz)-Lys(Cbz)-P1, which are labeled with the index a.

No.	P1	HPLC (% B)	Purity (%)	MS (calcd/found) (M+H) <sup>+</sup>
<b>33</b> (MI-0640)		17.4	99.0	496.3/497.3
<b>33a</b>		48.2	-	n.d.
<b>34</b> (MI-0643)		20.6	94.6	538.3/539.6
<b>34a</b>		70.4	-	n.d.
<b>35</b> (MI-0641)		18.9	98.2	496.3/497.3
<b>35a</b>		49.1	-	n.d.
<b>36</b> (MI-0644)		20.4	99.0	538.3/539.6
<b>36a</b>		71.3	-	n.d.
<b>37</b> (MI-0324)		20.7	99.0	523.3/262.7 <sup>[a]</sup>
<b>37a</b>		49.9	-	n.d.

<sup>[a]</sup>(M+2H)<sup>2+</sup>/2

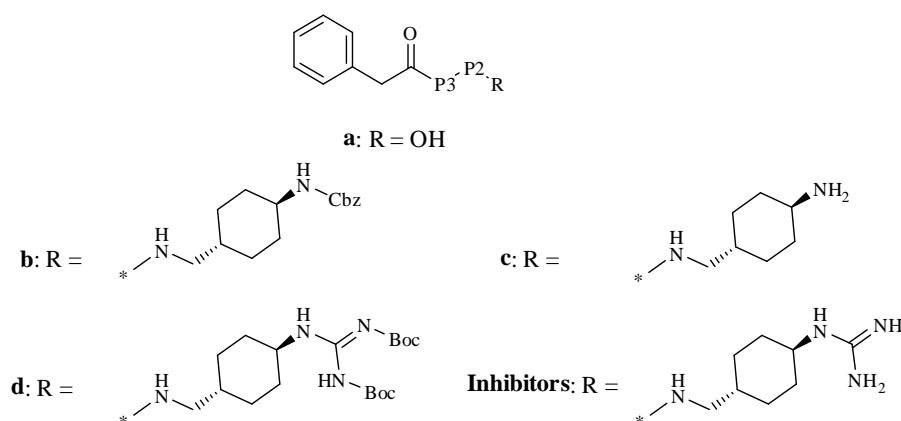
### 5.3.4 Synthesis of inhibitors 40-45 containing Phe(3/4-AMe)

0.1 g 2-chlorotrityl chloride resin (1.57 mmol/g) was loaded with the corresponding protected amino acids Fmoc-Lys(Boc)-OH, Fmoc-Phe(4-AMe-Tfa)-OH or Fmoc-Phe(3-AMe-Tfa)-OH according to method A. After washing and Fmoc removal the following residues were coupled by standard SPPS as described in method C. The peptides were cleaved from resin using mild acidic conditions according to method D to obtain the side chain protected Phac-P3-P2-OH intermediates labeled with index **a**. These derivatives were coupled with (1r,4r)-benzyl 4-(aminomethyl)cyclohexanecarboxylate in solution according to method F to provide intermediates with the general formula Phac-P3-P2-AMCA-Cbz labeled with index **b**. The Cbz protecting group was cleaved as described in method J to give the intermediates of the general formula Phac-P3-P2-AMCA labeled with index **c**. Afterwards, the amino group at P1 residue was converted into a free guanidine or Boc-protected guanidine according to the methods N or O, respectively, providing the intermediates labeled with index **d**. The side chain Tfa

## Experimental part

protecting group was cleaved under basic conditions as described in method L. If necessary, this was followed by an acidic cleavage of the Boc protection using method I (see Scheme 3.3). The analytical data of the final inhibitors **40-45** and their related intermediates are shown in the Table 5.5.

**Table 5.5:** Analytical characterization of WNV protease inhibitors **40-45** and their intermediates with the general formula



No.	P3	P2	HPLC (% B)	Purity (%)	MS (calcd/found) (M+H) <sup>+</sup>
<b>40</b> (MI-0648)	Phe(4-AMe)	Lys	22.14	99.0	592.4/593.2
<b>40a</b>	Phe(4-AMe-Tfa)	Lys(Boc)	56.1	47.1	n.d.
<b>40b</b>	Phe(4-AMe-Tfa)	Lys(Boc)	67.1	-	n.d.
<b>40c</b>	Phe(4-AMe-Tfa)	Lys(Boc)	47.1	-	n.d.
<b>40d</b>	Phe(4-AMe-Tfa)	Lys(Boc)	49.6	-	n.d.
<b>41</b> (MI-0649)	Lys	Phe(4-AMe)	21.5	99.0	592.4/593.1
<b>41a</b>	Lys(Boc)	Phe(4-AMe-Tfa)	56.0	79.8	n.d.
<b>41b</b>	Lys(Boc)	Phe(4-AMe-Tfa)	67.5	-	n.d.
<b>41c</b>	Lys(Boc)	Phe(4-AMe-Tfa)	47.6	-	n.d.
<b>41d</b>	Lys(Boc)	Phe(4-AMe-Tfa)	49.8	-	n.d.
<b>42</b> (MI-0647)	Phe(4-AMe)	Phe(4-AMe)	25.11	97.2	640.4/641.2
<b>42a</b>	Phe(4-AMe-Tfa)	Phe(4-AMe-Tfa)	55.7	24.4	n.d.
<b>42b</b>	Phe(4-AMe-Tfa)	Phe(4-AMe-Tfa)	66.2	-	n.d.
<b>42c</b>	Phe(4-AMe-Tfa)	Phe(4-AMe-Tfa)	47.1	-	n.d.
<b>42d</b>	Phe(4-AMe-Tfa)	Phe(4-AMe-Tfa)	49.1	-	n.d.

## Experimental part

<b>43</b> (MI-0656)	Phe(3-AMe)	Lys	24.3	99.0	592.4/297.4 <sup>[a]</sup>
<b>43a</b>	Phe(3-AMe-Tfa)	Lys(Boc)	56.3	54.2	n.d
<b>43b</b>	Phe(3-AMe-Tfa)	Lys(Boc)	67.4	-	n.d
<b>43c</b>	Phe(3-AMe-Tfa)	Lys(Boc)	47.9	-	n.d
<b>43d</b>	Phe(3-AMe-Tfa)	Lys(Boc)	48.5	-	n.d
<b>44</b> (MI-0653)	Lys	Phe(3-AMe)	24.9	99.0	592.4/593.3
<b>44a</b>	Lys(Boc)	Phe(3-AMe-Tfa)	57.1	88.2	n.d
<b>44b</b>	Lys(Boc)	Phe(3-AMe-Tfa)	67.4	-	n.d
<b>44c</b>	Lys(Boc)	Phe(3-AMe-Tfa)	48.1	-	n.d
<b>44d</b>	Lys(Boc)	Phe(3-AMe-Tfa)	50.2	-	n.d
<b>45</b> (MI-0655)	Phe(3-AMe)	Phe(3-AMe)	26.7	99.0	640.4/641.4
<b>45a</b>	Phe(3-AMe-Tfa)	Phe(3-AMe-Tfa)	57.1	49.2	n.d
<b>45b</b>	Phe(3-AMe-Tfa)	Phe(3-AMe-Tfa)	67.2	-	n.d
<b>45c</b>	Phe(3-AMe-Tfa)	Phe(3-AMe-Tfa)	47.8	-	n.d
<b>45d</b> <sup>[b]</sup>	Phe(3-AMe-Tfa)	Phe(3-AMe-Tfa)	65.8	-	n.d

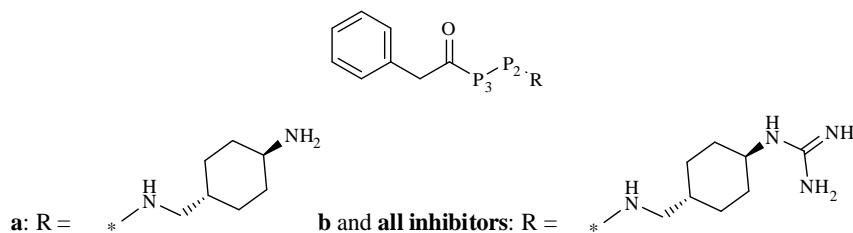
<sup>[a]</sup>(M+2H)<sup>2+</sup>/2, [b]only in case of intermediate 45d the P1 guanidine is di-Boc protected.

### 5.3.5 Synthesis of inhibitors 46-51 containing Phe(3/4-GMe)

To obtain inhibitors containing an additional guanidine group in the side chain at their Phe residues, the Tfa protection from intermediates **40c-45c** was removed under basic conditions using 1 N NaOH according to method L. This provided intermediates **46a-51a**, which were treated with a guanylation reagent according to methods N or O to give inhibitors **48** and **51** and the intermediates **46b**, **47b**, **49b** and **50b**. These intermediates labeled with index **b** were further treated with 90% TFA according to method I to obtain the inhibitors **46**, **47**, **49** and **50** (see Scheme 3.3). The analytical data of these compounds and their related intermediates are shown in Table 5.6.

## Experimental part

**Table 5.6:** Analytical characterization of WNV protease inhibitors **46-51** and their intermediates with the general formula



No.	P3	P2	HPLC (% B)	Purity (%)	MS (calcd/found) (M+H) <sup>+</sup>
<b>46</b> (MI-0651)	Phe(4-GMe)	Lys	22.9	94.5	634.4/635.2
<b>46a</b>	Phe(4-AMe)	Lys(Boc)	29.4	-	n.d
<b>46b</b>	Phe(4-GMe)	Lys(Boc)	36.3	-	n.d
<b>47</b> (MI-0650)	Lys	Phe(4-GMe)	23.4	99	634.4/635.1
<b>47a</b>	Lys(Boc)	Phe(4-AMe)	38.1	-	n.d
<b>47b</b>	Lys(Boc)	Phe(4-GMe)	39.8	-	n.d
<b>48</b> (MI-0652)	Phe(4-GMe)	Phe(4-GMe)	27.9	99	724.4/725.3
<b>48a</b>	Phe(4-AMe)	Phe(4-AMe)	23.1	-	n.d
<b>49</b> (MI-0657)	Phe(3-GMe)	Lys	20.7	99	634.4/635.2
<b>49a</b>	Phe(3-AMe)	Lys(Boc)	54.7	-	n.d
<b>49b</b> <sup>[b]</sup>	Phe(3-GMe(Boc) <sub>2</sub> )	Lys(Boc)	39.4	-	n.d
<b>50</b> (MI-0654)	Lys	Phe(3-GMe)	25.4	99	634.4/635.3
<b>50a</b>	Lys(Boc)	Phe(3-AMe)	34.4	-	n.d
<b>50b</b> <sup>[a]</sup>	Lys(Boc)	Phe(3-GMe(Boc) <sub>2</sub> )	65.6	-	n.d
<b>51</b> (MI-0658)	Phe(3-GMe)	Phe(3-GMe)	29.5	99	724.4/725.3
<b>51a</b>	Phe(3-AMe)	Phe(3-AMe)	24.1	-	n.d

<sup>[a]</sup>This intermediates have the general formula Phac-P3-P1-GCMA(Boc)<sub>2</sub>, <sup>[b]</sup>only in case of intermediate 49d the P1 guanidine is di-Boc protected.

### 5.3.6 Synthesis of the inhibitors 52-53 containing Phe(4-Gua)

0.1 g 2-chlorotrityl chloride resin (1.57 mmol/g) was loaded with Fmoc-Phe(4-NO<sub>2</sub>)-OH or Fmoc-Lys(Boc)-OH according to method A. The additional residues were coupled by standard Fmoc-SPPS as described in method C. The side chain protected intermediates Phac-Lys(Boc)-Phe(4-NO<sub>2</sub>)-OH (**52a**) and Phac-Phe(4-NO<sub>2</sub>)-Lys(Boc)-

## Experimental part

OH (**53a**) were obtained after mild acidic cleavage from the resin according to method D. The intermediates were coupled to (1*r*,4*r*)-benzyl 4-(aminomethyl)cyclohexane-carboxylate in solution as described in method F to provide compounds **52b** and **53b**. The concomitant reduction of the nitro group and Cbz-deprotection by hydrogenation (method J) provided the Phe(4-NH<sub>2</sub>)-containing intermediates **52c** and **53c**. Both amino groups of these intermediates were converted into the di-Boc-protected guanidines **52d** and **53d** using method N, followed by final removal of the Boc-protection by method I (see Scheme 3.4). The analytical data of inhibitors **52-53** and their related intermediates are shown in Table 5.7.

**Table 5.7:** Analytical characterization of WNV protease inhibitors **52-53** and their corresponding precursors with index **a**, **b**, **c** and **d** possessing the general formula.

**a: R = OH**

**b: R =**

**c: R =**

**d: R =**

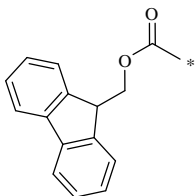
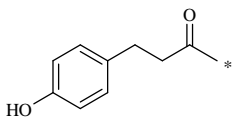
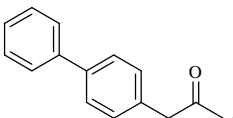
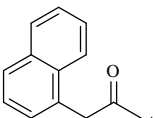
**Inhibitors: R =**

No.	P3	P2	HPLC (% B)	Purity (%)	MS (calcd/found) (M+2H) <sup>2+</sup> /2
<b>52</b> (MI-0659)	Lys	Phe(4-Gua)	26.2	98.0	620.4/311.3
<b>52a</b>	Lys(Boc)	Phe(4-NO <sub>2</sub> )	56.1	96.8	n.d
<b>52b</b>	Lys(Boc)	Phe(4-NO <sub>2</sub> )	67.4	-	n.d
<b>52c</b>	Lys(Boc)	Phe(4-NH <sub>2</sub> )	35.6	-	n.d
<b>52d</b>	Lys(Boc)	Phe(4-Gua(Boc) <sub>2</sub> )	72.7	-	n.d
<b>53</b> (MI-0660)	Phe(4-Gua)	Lys	25.8	99.0	620.4/311.5
<b>53a</b>	Phe(4-NO <sub>2</sub> )	Lys(Boc)	55.8	93.9	n.d
<b>53b</b>	Phe(4-NO <sub>2</sub> )	Lys(Boc)	67.3	-	n.d
<b>53c</b>	Phe(4-NH <sub>2</sub> )	Lys(Boc)	34.4	-	n.d
<b>53d</b>	Phe(4-Gua(Boc) <sub>2</sub> )	Lys(Boc)	72.2	-	n.d

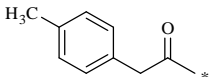
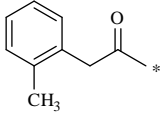
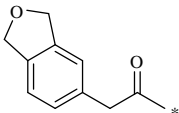
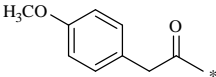
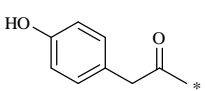
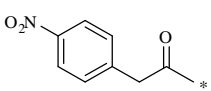
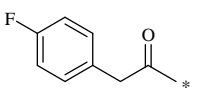
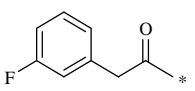
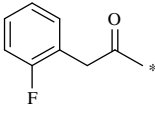
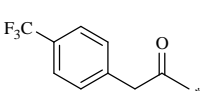
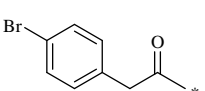
### 5.3.7 Synthesis of inhibitors 54-75 modified in P4 position

0.1 g trityl chloride resin (1.5 mmol/g) was loaded with butan-1,4-diamin according to method B. The P2-P4 segment was coupled by standard Fmoc-SPPS using Fmoc-Lys(Cbz)-OH and different P4 residues (see Table 5.8) according to the method C. The derivatives **54a-75a** with the general formula P4-Lys(Cbz)-Lys(Cbz)-4-aminobutylamide were cleaved from resin as described in method E. The free amino group at their C-terminus was converted into a guanidine as described in method M, which provided the agmatine intermediates **54b-75b**. Finally, the Cbz protecting groups of both lysine side chains were cleaved using 2 mL HBr/acetic acid (method G). The inhibitors **54-75** were purified by preparative HPLC, and lyophilized from water or 80% *tert*-butanol. The analytical data of the inhibitors and their related intermediates are shown in the Table 5.8.

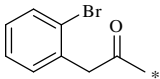
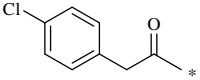
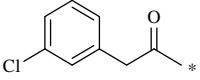
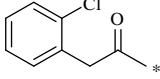
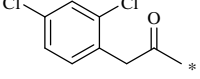
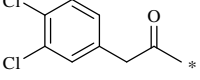
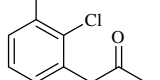
**Table 5.8:** Analytical characterization of inhibitors **54-75** with the general formula P4-Lys-Lys-agmatine and their corresponding Cbz-protected intermediates labeled with index **a** or **b** with the general formulas P4-Lys(Cbz)-Lys(Cbz)-4-aminobutylamide and P4-Lys(Cbz)-Lys(Cbz)-agmatine, respectively.

No.	P4	HPLC (% B)	Purity (%)	MS (calcd/found) (M+H) <sup>+</sup>
<b>54</b> (MI-0662)		32.2	99.0	608.4/609.3
<b>54a</b>		58.5	98.3	n.d.
<b>54b</b>		60.1	-	n.d.
<b>55</b> (MI-0666)		17.7	97.7	534.4/535.5
<b>55a</b>		47.1	70.0	n.d.
<b>55b</b>		47.8	-	n.d.
<b>56</b> (MI-0661)		30.2	97.0	480.4/481.2
<b>56a</b>		55.9	94.8	n.d.
<b>56b</b>		57.2	-	n.d.
<b>57</b> (MI-0668)		25.5	99.0	554.4/555.4
<b>57a</b>		53.0	95.6	n.d.
<b>57b</b>		54.3	-	n.d.

## Experimental part

<b>58</b> (MI-0665)		21.4	99.0	518.4/519.4
<b>58a</b>		51.6	97.0	n.d.
<b>58b</b>		52.8	-	n.d.
<b>59</b> (MI0664)		21.5	99.0	518.4/519.4
<b>59a</b>		51.4	94.8	n.d.
<b>59b</b>		52.5	-	n.d.
<b>60</b> (MI-0676)		20.3	97.7	548.3/549.4
<b>60a</b>		48.5	96.3	n.d.
<b>60b</b>		50.0	-	n.d.
<b>61</b> (MI-0674)		20.6	96.0	534.4/535.4
<b>61a</b>		48.9	93.6	n.d.
<b>61b</b>		50.2	-	n.d.
<b>62</b> (MI-0667)		15.9	95.4	520.3/521.1
<b>62a</b>		46.3	74.8	n.d.
<b>62b</b>		47	-	n.d.
<b>63</b> (MI-0669)		21.5	99.0	549.3/550.4
<b>63a</b>		50.3	83.6	n.d.
<b>63b</b>		51.5	-	n.d.
<b>64</b> (MI-0673)		20.8	99.0	522.3/523.4
<b>64a</b>		50.5	79.2	n.d.
<b>64b</b>		51.4	-	n.d.
<b>65</b> (MI-0677)		20.8	99.0	522.3/262.24 <sup>[a]</sup>
<b>65a</b>		49.6	92.6	n.d.
<b>65b</b>		51.5	-	n.d.
<b>66</b> (MI-0681)		19.8	97.0	522.3/262.25 <sup>[a]</sup>
<b>66a</b>		49.5	57.5	n.d.
<b>66b</b>		50.9	-	n.d.
<b>67</b> (MI-0675)		26.6	98.0	572.3/287.27 <sup>[a]</sup>
<b>67a</b>		53.2	89.2	n.d.
<b>67b</b>		54.7	-	n.d.
<b>68</b> (MI-0670)		24.5	99.0	582.3/583.3
<b>68a</b>		52.8	89.8	n.d.
<b>68b</b>		53.8	-	n.d.

## Experimental part

<b>69</b> (MI-0671)		22.5	99.0	582.3/583.4
<b>69a</b>		51.7	80.5	n.d.
<b>69b</b>		53.6	-	n.d.
<b>70</b> (MI-0672)		23.9	99.0	538.3/539.3
<b>70a</b>		52.6	79.3	n.d.
<b>70b</b>		53.3	-	n.d.
<b>71</b> (MI-0682)		23.3	98.2	538.3/270.3 <sup>[a]</sup>
<b>71a</b>		51.7	64.4	n.d.
<b>71b</b>		52.9	-	n.d.
<b>72</b> (MI-0678)		21.7	99.0	538.3/270.23 <sup>[a]</sup>
<b>72a</b>		50.3	88.5	n.d.
<b>72b</b>		51.9	-	n.d.
<b>73</b> (MI-0680)		25.8	99.0	572.3/287.3 <sup>[a]</sup>
<b>73a</b>		53.7	92.2	n.d.
<b>73b</b>		54.8	-	n.d.
<b>74</b> (MI-0663)		27.0	99.0	572.3/573.3
<b>74a</b>		53.9	92.0	n.d.
<b>74b</b>		56.0	-	n.d.
<b>75</b> (MI-0679)		25.1	99.0	572.3/287.3 <sup>[a]</sup>
<b>75a</b>		52.6	90.7	n.d.
<b>75b</b>		54.0	-	n.d.

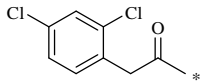
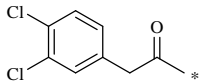
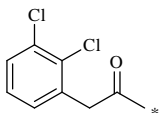
<sup>[a]</sup>(M+2H)<sup>2+</sup>/2

### 5.3.8 Synthesis of inhibitors 76-78 containing best P1 and P4 residues

The inhibitors 76-78 were synthesized in analogy to inhibitors 54-75, whereby the resin was initially loaded with Fmoc-AMCA × TFA (**17**). The intermediates **a** with the formula P4-Lys(Cbz)-Lys(Cbz)-AMCA were treated with the guanylation reagent *N,N'*-di-Boc-1*H*-pyrazole-1-carboxamide according to method N to give the derivatives marked with index **b** with the formula P4-Lys(Cbz)-Lys(Cbz)-GCMA(Boc)<sub>2</sub>, which were finally deprotected using HBr/acetic acid (method G). The inhibitors were purified by preparative HPLC, and lyophilized from water or 80% *tert*-butanol. The analytical data of the inhibitors and their related intermediates are shown in Table 5.9.

## Experimental part

**Table 5.9:** Analytical characterization of WNV protease inhibitors **76-78** with the general formula P4-Lys-Lys-GCMA and the corresponding intermediates a and b. with the general formulas P4-Lys(Cbz)-Lys(Cbz)-AMCA and P4-Lys(Cbz)-Lys(Cbz)-GCMA, respectively.

No.	P4	HPLC (% B)	Purity (%)	MS (calcd/found) (M+H) <sup>+</sup>
<b>76</b> (MI-0680)		27.1	99	612.3/613.4
<b>76a</b>		53.5	78.9	n.d.
<b>76b</b>		71.2	-	n.d.
<b>77</b> (MI-0663)		28.3	99	612.3/613.4
<b>77a</b>		54.1	70	n.d.
<b>77b</b>		71.1	-	n.d.
<b>78</b> (MI-0679)		26.4	99	612.3/613.4
<b>78a</b>		53	78.7	n.d.
<b>78b</b>		70.5	-	n.d.

Additional analytical data were obtained for compound **78**: <sup>1</sup>H NMR ([D<sub>6</sub>]DMSO, 500 MHz):  $\delta$  = 8.33 (d,  $J$ =7.7 Hz, 1H), 7.90 (d,  $J$ =8.0 Hz, 1H), 7.86 (t,  $J$ =5.9 Hz, 1H), 7.78 (br s, 5 H), 7.61-7.66 (m, 1 H), 7.51-7.55 (m, 1 H), 7.28-7.36 (m, 2 H), 4.22-4.28 (m, 1 H), 4.16-4.22 (m, 1 H), 3.68-3.78 (m, 2H), 2.89-2.97 (m, 1H), 2.82-2.89 (m, 1 H), 2.70-2.79 (m, 4 H), 1.82-1.90 (m, 2 H), 1.59-1.73 (m, 4 H), 1.46-1.59 (m, 6 H), 1.21-1.41 (m, 6H), 1.08-1.18 (m, 2H), 0.87-0.98 ppm(m, 2H); <sup>13</sup>C NMR ([D<sub>6</sub>]DMSO, 126 MHz):  $\delta$  = 171.3, 171.2, 168.8, 155.8, 137.0, 131.7, 131.5, 130.5, 128.8, 127.8, 52.6, 52.3, 49.8, 44.3, 40.5, 38.7, 38.7, 36.2, 31.7, 31.5, 31.2, 28.6, 26.6, 26.5, 22.3, 22.2 ppm; HRMS (ESI<sup>+</sup>):  $m/z$  (%): 613.3143 [M+H]<sup>+</sup>.

### Synthesis of P2 and P3 modified agmatine derivatives 79-88

The inhibitors **81-88** were synthesized in analogy to the agmatine derivative **26** using various P2 and P3 amino acids (Fmoc-Lys(Boc), Fmoc-Arg(Pbf)-OH, Fmoc-hPhe-OH, Fmoc-Ser(Bzl)-OH or Fmoc-D/L-hAla(2-Pyr)-OH) and 3,4-dichloro-phenylacetic acid as P4 group. The intermediates **81a-88a** were obtained after mild acidic cleavage from resin according to method D, followed by conversion of their C-terminal amine into guanidine to give derivatives **81b-88b** (method M). Final side chain deprotection using method I provided inhibitor **81-88**.

## Experimental part

The inhibitor **79** was prepared from the loaded trityl chloride resin with butan-1,4-diamin, which was coupled with Fmoc-Dab(Boc)-OH, Fmoc-Lys(Cbz)-OH and 3,4-dichloro-phenylacetyl residue as described previously for the analogue **81**. The cleavage of the peptide from resin was performed using method E to give intermediate **79a** with the formula 3,4-dichloro-phenylacetyl-Lys(Cbz)-Dab-4-aminobutylamide. The P1 4-aminobutylamide and the Dab side chain were concomitant converted into agmatine and norArg residues, respectively (method M). The Cbz side chain protection of intermediate 3,4-dichloro-phenylacetyl-Lys(Cbz)-norArg-agmatine (**79b**) was removed using method G to provide inhibitor **79** (see Scheme 3.5).

Inhibitor **80** was synthesized in analogy to **79**, whereby P2 and P3 were reversed to give 3,4-dichloro-phenylacetyl-norArg-Lys-agmatine. The final products were purified by preparative RP-HPLC, and lyophilized from water or 80% *tert*-butanol. The analytical data of the inhibitors **79-88** and their related intermediates are shown in the Table 5.10.

**Table 5.10:** Analytical characterization of WNV protease inhibitors **79-88** with the general formula 3,4-dichloro-phenylacetyl-P3-P2-agmatine and the corresponding intermediates a and b.

No.	P3	P2	P1	HPLC (% B)	Purity (%)	MS (calcd/found) (M+H) <sup>+</sup>
<b>79</b> (MI-0686)	Lys	norArg	Agm	28.3	99	586.3/294.2 <sup>[a]</sup>
<b>79a</b>	Lys(Cbz)	Dab	Dib	41.2	68.2	n.d.
<b>79b</b>	Lys(Cbz)	norArg	Agm	43	-	n.d.
<b>80</b> (MI-0687)	norArg	Lys	Agm	28.2	99	586.3/587.2
<b>80a</b>	Dab	Lys(Cbz)	Dib	40.3	68	n.d.
<b>80b</b>	norArg	Lys(Cbz)	Agm	42.5	-	n.d.
<b>81</b> (MI-0693)	Lys	Arg	Agm	28.2	99	600.3/601.3
<b>81a</b>	Lys(Cbz)	Arg	Dib	42.1	-	n.d.
<b>81b</b>	Lys(Cbz)	Arg	Agm	43.3	-	n.d.
<b>82</b> (MI-0694)	Arg	Arg	Agm	29.3	98	628.3/629.3
<b>82a</b>	Arg	Arg	Dib	28.5	69.7	n.d.
<b>83</b> (MI-0691)	Lys	hPhe	Agm	40.3	97.5	605.3/606.3
<b>83a</b>	Lys(Boc)	hPhe	Dib	52.1	91.9	n.d.
<b>83b</b>	Lys(Boc)	hPhe	Agm	53.7	-	n.d.

## Experimental part

<b>84</b> (MI-0692)	hPhe	Lys	Agm	40.8	97.2	605.3/606.3
<b>84a</b>	hPhe	Lys(Boc)	Dib	52.6	91.9	n.d.
<b>84b</b>	hPhe	Lys(Boc)	Agm	54.2	-	n.d.
<b>85</b> (MI-0697)	Lys	Ser(Bzl)	Agm	39.4	99	621.3/622.3
<b>85a</b>	Lys(Boc)	Ser(Bzl)	Dib	51.7	83.7	n.d.
<b>85b</b>	Lys(Boc)	Ser(Bzl)	Agm	53.1	-	n.d.
<b>86</b> (MI-0698)	Ser(Bzl)	Lys	Agm	40.1	99	621.3/622.2
<b>86a</b>	Ser(Bzl)	Lys(Boc)	Dib	52.5	92.3	n.d.
<b>86b</b>	Ser(Bzl)	Lys(Boc)	Agm	53.9	-	n.d.
<b>87</b> (MI-0699)	Lys	D/L-hAla(2-Pyr)	Agm	28.5- 29.1	49.7-48.1	606.3/607.3
<b>87a</b>	Lys(Boc)	D/L-hAla(2-Pyr)	Dib	40.3	92.8	n.d.
<b>87b</b>	Lys(Boc)	D/L-hAla(2-Pyr)	Agm	41.4-41.8	-	n.d.
<b>88</b> (MI-0731)	D/L-hAla(2-Pyr)	Lys	Agm	29.5	99	606.3/607.3
<b>88a</b>	D/L-hAla(2-Pyr)	Lys(Boc)	Dib	40.1	94.2	n.d.
<b>88b</b>	D/L-hAla(2-Pyr)	Lys(Boc)	Agm	41.7	-	n.d.

<sup>[a]</sup>(M+2H)<sup>2+</sup>/2, only in this Table the abbreviations Agm and Dib stand for agmatine and butane-1,4-diamine, respectively. Fmoc-D/L-hAla(2-Pyr)-OH was prepared from racemic H-D/L-hAla(2-Pyr)-OH available from previous studies<sup>104</sup>

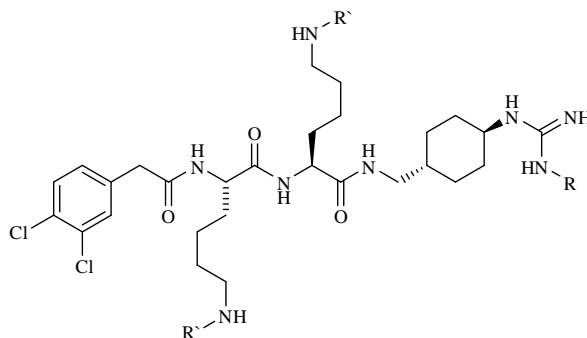
### 5.3.9 Synthesis of inhibitors **89** and **90** with alkylated **P1** guanidines

0.1 g of trityl chloride resin (1.55 mmol/g) was loaded with 1 equiv Fmoc-AMCA × TFA (**17**) as described in method B, followed by twice coupling of Fmoc-Lys(Boc)-OH and of 3,4-dichlorophenyl acetic acid using a standard Fmoc-SPPS protocol according to method C. The intermediate **89a** (3,4-dichlorophenylacetyl-Lys(Boc)-Lys(Boc)-AMCA) was obtained as a yellowish oil after mild cleavage from the resin according to method D. (HPLC:53.2% B (purity: 90.1%)). Its C-terminal amino group was guanylated using 2-ethyl-1-methylisothiuronium iodide (**21**) as described in method O to give the methylguanidine derivative **89b** as yellowish oil. The intermediate **90b** was synthesized in analogy to derivative **89b**, whereby the amino group at the C-terminus was converted into an ethylguanidine by treatment with 2-ethyl-1-ethylisothiuronium iodide (**22**) according to method O.

## Experimental part

Finally, the Boc protecting groups of compounds **89b** and **90b** were removed using TFA (method I) (see Scheme 3.6). The analytical data of the inhibitors **89** and **90** and their related intermediates **89b** and **90b** are shown in Table 5.11.

**Table 5.11:** Analytical characterization of inhibitors **89** and **90** with the general formula 3,4-dichlorophenylacetyl-Lys-Lys-P1 and the corresponding intermediates **89b** and **90b**.



No.	R	R'	HPLC (% B)	Purity (%)	MS (calcd/found) (M+2H) <sup>2+</sup> /2
<b>89</b> (MI-0734)	Methyl	H	30.8	99	626.32/314.3
<b>89b</b>		Boc	55.9	-	n.d.
<b>90</b> (MI-0733)	Ethyl	H	31.9	99	640.34/321.01
<b>90b</b>		Boc	57.3	-	n.d.

### 5.3.10 Synthesis of linearpeptides 91-105

All peptides were synthesized by SPPS on Fmoc-Rink-Amide resin (0.45 mmol/g) using a standard Fmoc protocol according to method C. The peptides were cleaved from the resin as described in method E and were finally precipitated in diethyl ether. After centrifugation, the precipitate was washed twice with diethyl ether, and after repeated centrifugation finally dried *in vacuum*. The peptides were purified by preparative HPLC, and lyophilized from water or 80% *tert*-butanol. The analytical data of inhibitors **91-105** are summarized in Table 5.12. The purity of all peptides was  $\geq 95\%$ .

## Experimental part

**Table 5.12:** Analytical characterization of peptide amides **90** - **105** with the general formulas P4-Lys-Lys-P1-R

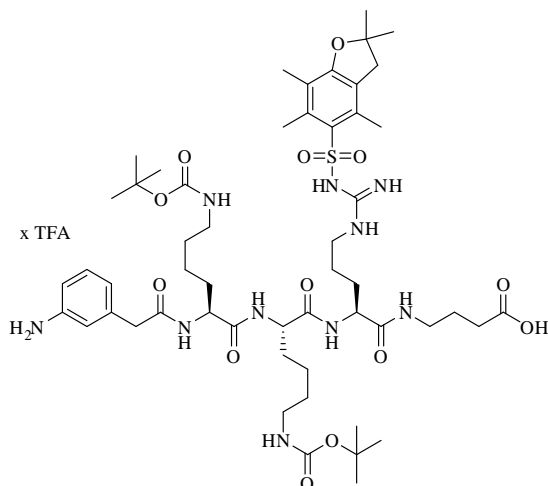
No.	P4	P1	R	HPLC (% B)	MS (calcd/found) (M+H) <sup>+</sup>
<b>91</b> (MI-0751)	Phac	Arg	Gly-Gly-NH <sub>2</sub>	17.4	661.4/662.26
<b>92</b> (MI-0737)	Phac	Arg	Gly-NH <sub>2</sub>	17.9	604.4/605.4
<b>93</b> (MI-0740)	Phac	Arg	Ala-NH <sub>2</sub>	18	618.39/619.27
<b>94</b> (MI-0741)	Phac	Arg	Val-NH <sub>2</sub>	20.5	646.42/647.34
<b>95</b> (MI-0739)	Phac	Arg	Tle-NH <sub>2</sub> *	22.2	660.44/661.35
<b>96</b> (MI-0738)	Phac	Arg	Pro-NH <sub>2</sub>	19.6	644.4/645.36
<b>97</b> (MI-0752)	Phac	Arg	DAla-NH <sub>2</sub>	18.06	618.39/619.52
<b>98</b> (MI-0753)	Phac	Arg	Sar-NH <sub>2</sub> *	18.3	618.39/619.37
<b>99</b> (MI-0754)	Phac	Arg	Gaba-NH <sub>2</sub> *	18.1	632.41/633.29
<b>100</b> (MI-0755)	Phac	Arg	Aca-NH <sub>2</sub> *	19.9	660.44/661.37
<b>101</b> (MI-0756)	Phac	Arg	NH <sub>2</sub>	17.7	547.35/548.3
<b>102</b> (MI-0742)	3,4-dichloro-Phac	Arg	Gly-NH <sub>2</sub>	25.4	672.3/673.22
<b>103</b> (MI-0757)	3,4-dichloro-Phac	Arg	NH <sub>2</sub>	25.8	615.28/616.13
<b>104</b> (MI-0763)	Phac	hArg	NH <sub>2</sub>	18.3	561.37/562.25
<b>105</b> (MI-0762)	3,4-dichloro-Phac	hArg	NH <sub>2</sub>	28.2	629.29/630.12

\*Tle = *tert*-leucine, Sar = sarcosine (2-(Methylamino)acetic acid), Gaba =  $\gamma$ -aminobutyric acid, Aca =  $\epsilon$ -Aminocaproic acid

### 5.3.11 Synthesis of cyclic peptides 106-111

**Inhibitor 106 and related intermediates** (Identical strategy shown in Scheme 3.7)

#### **3-NH<sub>2</sub>-Phac-Lys(Boc)-Lys(Boc)-Arg(Pbf)-Gaba-OH × TFA 106a**

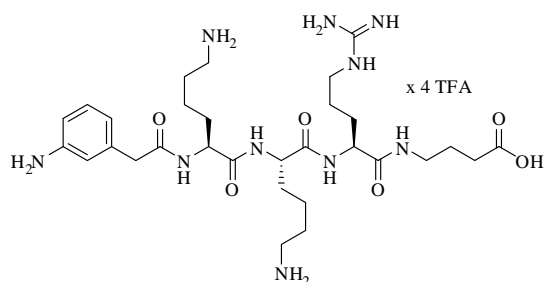


0.1 g of 2-Cl-tritylchlorid resin (1.55 mmol/g) was loaded with Fmoc-Gaba-OH according to method A. The Fmoc group was cleaved using 20 % piperidine in DMF, followed by multiple washing with DMF. The following residues Fmoc-Arg(Pbf)-OH, Fmoc-Lys(Boc)-OH and Fmoc-3-amino-Phac-OH (PolyPeptide) were coupled by standard Fmoc-SPPS as described in method C. The peptide was cleaved from resin according to method E generating the side-chain protected intermediate **106a**. This derivative was used for the synthesis of compounds **106b** and **106c** without further purification.

Yield: 119 mg (0.097 mmol), yellowish oil.

HPLC: 51.7 % B (purity: 94.3%).

**3-NH<sub>2</sub>-Phac-Lys-Lys-Arg-Gaba-OH × 4 TFA 106b**

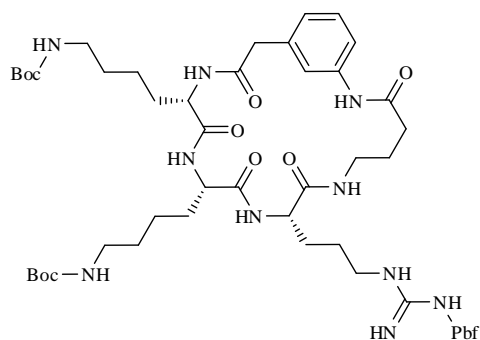


Compound **106a** was deprotected by treating with TFA as described in method I. The peptide was precipitated by diethyl ether. After centrifugation, the precipitate was washed with diethyl ether, and dried *in vacuo*. Intermediate **106b** was purified by preparative HPLC, and lyophilized from water.

Yield: 18.mg (0.016 mmol), white lyophilized powder.

HPLC: 13.3 % B (purity: 99 %).

**3-NH-Phac-Lys(Boc)-Lys(Boc)-Arg(Pbf)-Gaba- 106c**

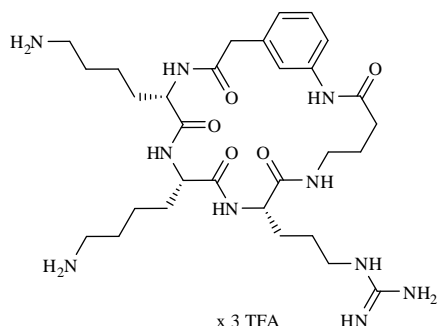


72.8 mg of the linear intermediate **106a** (0.06 mmol) was dissolved in ~ 70 mL DMF and treated with 3 equiv Bop and initially with 3 equiv of DIPEA as described in method Q. After completion of the reaction, the DMF was removed *in vacuo* and the remaining oil was used without further purification for the synthesis of inhibitor **106**.

Yield: 60.mg (0.055 mmol), yellowish oil.

HPLC: 62.4 % B (purity:62.4%).

**3-NH-Phac-Lys-Lys-Arg-Gaba] x 3 TFA 106**



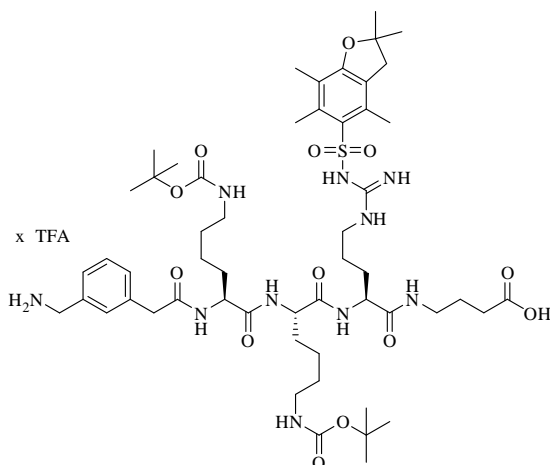
30 mg of the crude intermediate **106c** was treated with TFA as described in method I. The peptide was finally precipitated by diethyl ether. After centrifugation, the precipitate was washed with diethyl ether, and dried *in vacuum*. The inhibitor was purified by preparative HPLC and lyophilized from water.

Yield: 21.4 mg (0.022 mmol), white lyophilized powder.

HPLC: 18 % B (purity: 93.1%).

**Inhibitor 107 and related intermediates**, see Scheme 3.7.

**3-NH<sub>2</sub>-CH<sub>2</sub>-Phac-Lys(Boc)-Lys(Boc)-Arg(Pbf)-Gaba x TFA 107a**

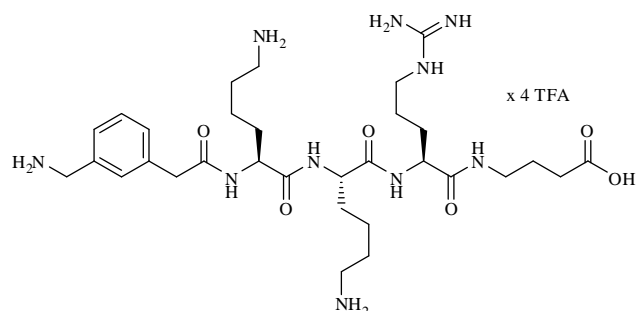


This intermediate was prepared in analogy to compound **106a**, whereby Fmoc-3-NH-CH<sub>2</sub>-Phac-OH (PolyPeptide) was used for the coupling of the terminal P4 residue.

Yield: 123 mg (0.1 mmol), yellowish oil.

HPLC: 51.6 % B (purity: 83.1 %).

**3-NH<sub>2</sub>-CH<sub>2</sub>-Phac-Lys-Lys-Arg-Gaba × 4 TFA 107b**

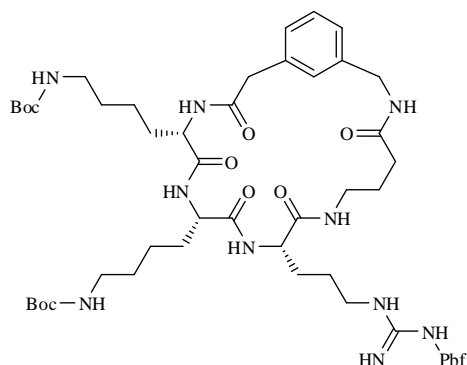


Approximately one third of the intermediate **107a** was deprotected in analogy to the synthesis of compound **106b**.

Yield: 20.4.mg (0.018 mmol), white powder.

HPLC: 14.2 % B (purity: 99%)

**3-NH-CH<sub>2</sub>-Phac-Lys(Boc)-Lys(Boc)-Arg(Pbf)-Gaba 107c**

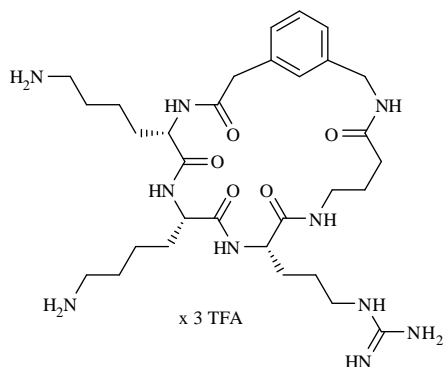


Intermediate **107c** was prepared in analogy to compound **106c** from approximately two third of intermediate **107a**. The oily residue remaining after evaporation, was used for final deprotection described in the next step.

Yield: 64 mg (0.058 mmol), yellowish oil.

HPLC: 61.9 % B (purity: 88.9 %).

**3-NH-CH<sub>2</sub>-Phac-Lys-Lys-Arg-Gaba] x 3 TFA 107**



50 mg of the crude intermediate **107c** (0.045 mmol) was treated with TFA as described in method I. The peptide was finally precipitated by diethyl ether. After centrifugation, the precipitate was washed with diethyl ether, and dried *in vacuo*. The inhibitor was purified by preparative HPLC, and lyophilized from water.

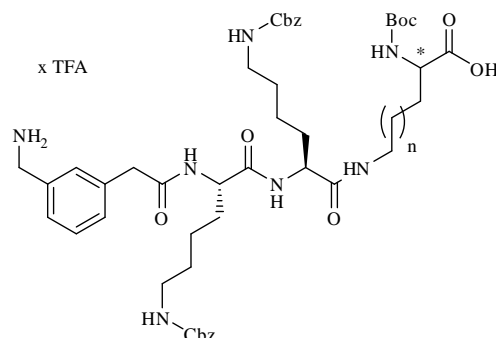
Yield: 26 mg (0.026 mmol), white lyophilized powder.

HPLC: 18.1 % B (purity: 96.2 %).

**Synthesis of cyclic peptides 108-111 and related intermediates (Scheme 3.8)**

**Intermediates 108a-111a**

0.1 g of 2-Cl-tritylchlorid resin (1.55 mmol/g) was loaded with Boc-Lys(Fmoc)-OH, Boc-D-Lys(Fmoc)-OH, Boc-Orn(Fmoc)-OH or Boc-D-Orn(Fmoc)-OH according to the method A. The Fmoc group of the lysine or ornithine side chain was cleaved using 20% piperidine in DMF as described in method C. After washing, the following residues (2 x Fmoc-Lys(Cbz)-OH and Fmoc-3-NH<sub>2</sub>-CH<sub>2</sub>-Phac-OH) were sequentially coupled to the free side chain amino group of the  $\alpha$ -Boc-protected lysine or ornithine residues (Scheme 3.10) on the resin using a standard SPPS Fmoc-protocol as described in method C. After removal of the terminal Fmoc-group the side chain Cbz- and Boc-protected peptide was cleaved from resin under mild acidic conditions according to method D. After evaporation of the solvent the intermediates **108a-111a** were used for the synthesis of intermediates **108b-111b** without further purification. The analytical data of the derivatives **108a-111a** are shown in the Table 5.13.

**Table 5.13:** Analytical characterization of intermediates **108a - 111a** having the general formula.

No.	n	*	HPLC (% B)	Purity (%)
<b>108a</b>	2	L	49.9	76
<b>109a</b>	2	D	49.9	79
<b>110a</b>	1	L	49.3	67
<b>111a</b>	1	D	49.2	82.9

### The cyclic intermediates **108b, c, d-111 b, c, d** and the corresponding inhibitors **108-111**

The intermediates **108a-111a** were dissolved in DMF (~100 mL/0.1mmol), and treated with 3 equiv Bop and initially with 3 equiv DIPEA according to method Q. After completion of the reaction, the DMF was removed *in vacuum* to obtain the cyclic peptides **108b-111b** still containing the Cbz and Boc protection as yellowish oil.

The Boc group of these derivatives **108b-111b** was cleaved by TFA as described in method I. The TFA was removed *in vacuum* to obtain the Cbz protected intermediates **108c-111c**.

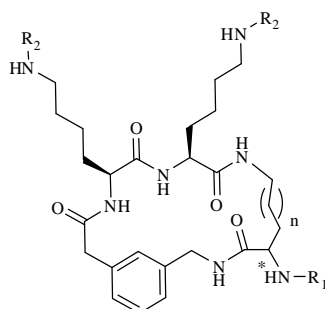
Compounds **108c-111c** were dissolved with 1mL DMF and treated with 2 equiv of the guanylation reagent *N,N'*-di-Boc-1*H*pyrazole-1-carboxamide and 3 equiv DIPEA as described in method N to give the Boc protected guanidine intermediates **108d-111d**.

Final removal of the Cbz- and Boc-protection was achieved by treatment with ~ 2 ml 32% HBr/acetic acid according to method G, which provided the crude inhibitors **108-111**. The solvent was partially removed *in vacuum* and the products were precipitated by diethyl ether. After centrifugation, the precipitate was washed with diethyl ether, and

dried *in vacuuum*. The inhibitors were purified by preparative HPLC, and lyophilized from water. The analytical data of the cyclic peptides **108-111** and their related intermediates are summarized in Table 5.14.

## Experimental part

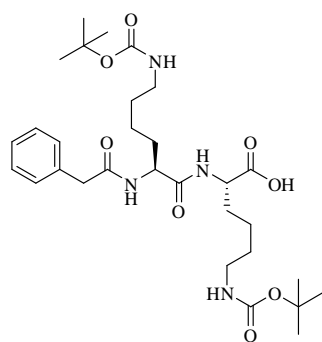
**Table 5.14:** Analytical characterization of inhibitors **108-111** and their related intermediates with index b, c, and d, having the general formula.



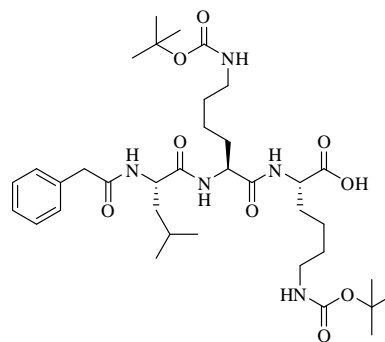
No.	n	R <sub>1</sub>	R <sub>2</sub>	*	HPLC (% B)	Purity (%)	MS (calcd/found) (M+H) <sup>+</sup>
<b>108</b> (MI-0758)	2		H	L	17.5	96.0	573.38/574.3
<b>108b</b>	2	Boc	Cbz	L	60.9	-	n.d.
<b>108c</b>	2	H	Cbz	L	46.7	-	n.d.
<b>108d</b>	2		Cbz	L	67.2	-	n.d.
<b>109</b> (MI-0759)	2		H	D	17.6	87.0	573.38/574.3
<b>109b</b>	2	Boc	Cbz	D	60.6	-	n.d.
<b>109c</b>	2	H	Cbz	D	46.9	-	n.d.
<b>109d</b>	2		Cbz	D	66.5	-	n.d.
<b>110</b> (MI-0760)	1		H	L	17.0	95.5	559.36/560.3
<b>110b</b>	1	Boc	Cbz	L	59.7	-	n.d.
<b>110c</b>	1	H	Cbz	L	46.8	-	n.d.
<b>110d</b>	1		Cbz	L	66.5	-	n.d.
<b>111</b> (MI-0761)	1		H	D	17.1	86.3	559.36/560.3
<b>111b</b>	1	Boc	Cbz	D	59.5	-	n.d.
<b>111c</b>	1	H	Cbz	D	47.0	-	n.d.
<b>111d</b>	1		Cbz	D	17.1	-	n.d.

### 5.3.12 Synthesis of substrates 112-114 and related intermediates

Intermediates 112a and 114a



**112a**



**114a**

0.1 g of 2-Cl-tritylchlorid resin (1.55 mmol/g) was loaded with Fmoc-Lys(Boc)-OH according to method A. Afterwards, the following Fmoc amino acids and phenylacetyl residues were coupled by standard Fmoc SPPS according to method C. The peptides were cleaved from resin under mild acidic conditions as described in method D to give derivatives Phac-Lys(Boc)-Lys(Boc)-OH (**112a**) and Phac-Leu-Lys(Boc)-Lys(Boc)-OH (**114a**), respectively. Compound **112a** was coupled with H-Arg-pNA  $\times$  2 HCl (Orpegen, Heidelberg) or H-Arg-AMC  $\times$  2 HCl (Pentapharm, Basel, Switzerland) according to method F to provide intermediates **112b** and **113b**, respectively. The compound **114a** was also coupled with H-Arg-AMC  $\times$  2 HCl as described in method F to give the intermediate **114b** with the general formula and Phac-Leu-Lys(Boc)-Lys(Boc)-Arg-AMC. All the derivatives **112b-114b** were Boc-deprotected using 90% TFA according to method I to give the compounds **112-114**. The substrates were finally precipitated in diethyl ether. After centrifugation, the precipitate was washed with diethyl ether, and dried *in vacuo*. The products were purified by preparative HPLC, and lyophilized from water. The analytical data of the derivatives **112a, b, 113b and 114a, b** and the corresponding substrates **112-114** are shown in the Table 5.15.

**Table 5.15:** Analytical characterization of the substrates **112-114** and their related intermediates.

No.	sequence	HPLC (% B)	Purity (%)	MS (calcd/found) (M+H) <sup>+</sup>
<b>112</b> (MI-0744)	Phac-Lys-Lys-Arg-pNA × 3TFA	27.1	98	668.4/669.3
<b>112a</b>	Phac-Lys(Boc)-Lys(Boc)-OH	55.3	83	n.d.
<b>112b</b>	Phac-Lys(Boc)-Lys(Boc)-Arg-pNA × HCl	54.7	-	n.d.
<b>113</b> (MI-0749)	Phac-Lys-Lys-Arg-AMC × 3TFA	27	98.5	705.4/706.4
<b>113b</b>	Phac-Lys(Boc)-Lys(Boc)-Arg-AMC × HCl	52.5	-	n.d.
<b>114</b> (MI-0624)	Phac-Leu-Lys-Lys-Arg-AMC × 3TFA	33.5	99	640.4/641.2
<b>114a</b>	Phac-Leu-Lys(Boc)-Lys(Boc)-OH	60.9	91.8	n.d.
<b>114b</b>	Phac-Leu-Lys(Boc)-Lys(Boc)-Arg-AMC × HCl	57.3	-	n.d.

#### 5.4 Stability tests of peptides 91-105

1 mM stock solutions of the peptides, substrates and their possible cleavage products Phac-Lys-Lys-Arg-OH, *p*-nitroaniline, and 7-amino-4-methylcoumarin were prepared in WNV protease assay buffer (see paragraph 5.2.1). 175  $\mu$ L of these 1 mM solutions were mixed with 25  $\mu$ L WNV protease stock (~ 160 nM) providing a total volume of 200  $\mu$ L. The resulting mixtures contained 0.875 mM of the peptides or derivatives and 20 nM of the WNV protease. After 1 h, 4 h and 8 h of incubation with the enzyme, 50  $\mu$ L of each incubation mixture was withdrawn and further diluted with 700  $\mu$ L of a solution prepared from ACN/H<sub>2</sub>O/TFA (49.5/49.5/1, v/v/v) to stop the enzymatic reaction. Finally, 150  $\mu$ L of this mixture, containing 58.3  $\mu$ M of the peptides or derivatives were injected to HPLC.

To get reference HPLC-chromatograms of all compounds under identical concentrations without any influence of the WNV protease, 25  $\mu$ L of buffer was added instead of the enzyme to the 175  $\mu$ L of the 1 mM stock solutions of the peptides in the initial step. The following steps were performed as described above.

## **5.5 Crystal structure determination**

The crystallization of the WNV NS2B-NS3 protease in complex with inhibitor **77** (MI-0683), the data collection, structure determination and refinement was performed by Caroline Haase in the group of Prof. Dr. Rolf Hilgenfeld (Institute of Biochemistry, Ratzeburger Allee 160, Lübeck). These results were recently published.<sup>90</sup>

## References

1. Smithburn, K. C. H., T. P.; Burke, A. W.; Paul, J. H. A neurotropic virus isolated from the blood of a native of Uganda. *American journal of tropical medicine* 1940, 20, 471-2.
2. Campbell, G. L.; Ceianu, C. S.; Savage, H. M. Epidemic West Nile encephalitis in Romania: waiting for history to repeat itself. *Annals of the New York Academy of Sciences* 2001, 951, 94-101.
3. Hubalek, Z.; Halouzka, J. West Nile fever--a reemerging mosquito-borne viral disease in Europe. *Emerging infectious diseases* 1999, 5, 643-50.
4. Dauphin, G.; Zientara, S.; Zeller, H.; Murgue, B. West Nile: worldwide current situation in animals and humans. *Comparative immunology, microbiology and infectious diseases* 2004, 27, 343-55.
5. <http://www.cdc.gov/westnile/statsMaps/finalMapsData/index.html>.
6. Drebot, M. A.; Lindsay, R.; Barker, I. K.; Buck, P. A.; Fearon, M.; Hunter, F.; Sockett, P.; Artsob, H. West Nile virus surveillance and diagnostics: A Canadian perspective. *The Canadian journal of infectious diseases = Journal canadien des maladies infectieuses* 2003, 14, 105-14.
7. Girard, Y. A.; Popov, V.; Wen, J.; Han, V.; Higgs, S. Ultrastructural study of West Nile virus pathogenesis in *Culex pipiens quinquefasciatus* (Diptera: Culicidae). *Journal of medical entomology* 2005, 42, 429-44.
8. Eidson, M. "Neon needles" in a haystack: the advantages of passive surveillance for West Nile virus. *Annals of the New York Academy of Sciences* 2001, 951, 38-53.
9. Komar, N.; Langevin, S.; Hinten, S.; Nemeth, N.; Edwards, E.; Hettler, D.; Davis, B.; Bowen, R.; Bunning, M. Experimental infection of North American birds with the New York 1999 strain of West Nile virus. *Emerg Infect Dis* 2003, 9, 311-22.
10. Komar, O.; Robbins, M. B.; Klenk, K.; Blitvich, B. J.; Marlenee, N. L.; Burkhalter, K. L.; Gubler, D. J.; Gonzalez, G.; Pena, C. J.; Peterson, A. T.; Komar, N.

## References

---

West Nile virus transmission in resident birds, Dominican Republic. *Emerging infectious diseases* 2003, 9, 1299-302.

11. Komar, N. West Nile virus: epidemiology and ecology in North America. *Advances in virus research* 2003, 61, 185-234.

12. Hayes, E. B.; O'Leary, D. R. West Nile virus infection: a pediatric perspective. *Pediatrics* 2004, 113, 1375-81.

13. Chambers, T. J.; Diamond, M. S. Pathogenesis of flavivirus encephalitis. *Advances in virus research* 2003, 60, 273-342.

14. Johnston, B. L.; Conly, J. M. West Nile virus - where did it come from and where might it go? *The Canadian journal of infectious diseases = Journal canadien des maladies infectieuses* 2000, 11, 175-8.

15. Samuel, M. A.; Whitby, K.; Keller, B. C.; Marri, A.; Barchet, W.; Williams, B. R.; Silverman, R. H.; Gale, M., Jr.; Diamond, M. S. PKR and RNase L contribute to protection against lethal West Nile Virus infection by controlling early viral spread in the periphery and replication in neurons. *Journal of virology* 2006, 80, 7009-19.

16. Samuel, M. A.; Diamond, M. S. Pathogenesis of West Nile Virus infection: a balance between virulence, innate and adaptive immunity, and viral evasion. *J Virol* 2006, 80, 9349-60.

17. Guarner, J.; Shieh, W. J.; Hunter, S.; Paddock, C. D.; Morken, T.; Campbell, G. L.; Marfin, A. A.; Zaki, S. R. Clinicopathologic study and laboratory diagnosis of 23 cases with West Nile virus encephalomyelitis. *Human pathology* 2004, 35, 983-90.

18. Wang, T.; Town, T.; Alexopoulou, L.; Anderson, J. F.; Fikrig, E.; Flavell, R. A. Toll-like receptor 3 mediates West Nile virus entry into the brain causing lethal encephalitis. *Nature medicine* 2004, 10, 1366-73.

19. Daffis, S.; Samuel, M. A.; Suthar, M. S.; Gale, M., Jr.; Diamond, M. S. Toll-like receptor 3 has a protective role against West Nile virus infection. *Journal of virology* 2008, 82, 10349-58.

20. Nash, D.; Mostashari, F.; Fine, A.; Miller, J.; O'Leary, D.; Murray, K.; Huang, A.; Rosenberg, A.; Greenberg, A.; Sherman, M.; Wong, S.; Layton, M.; West Nile

## References

---

Outbreak Response Working, G. The outbreak of West Nile virus infection in the New York City area in 1999. *The New England journal of medicine* 2001, 344, 1807-14.

21. Davis, L. E.; DeBiasi, R.; Goade, D. E.; Haaland, K. Y.; Harrington, J. A.; Harnar, J. B.; Pergam, S. A.; King, M. K.; DeMasters, B. K.; Tyler, K. L. West Nile virus neuroinvasive disease. *Annals of neurology* 2006, 60, 286-300.

22. King, N. J.; Getts, D. R.; Getts, M. T.; Rana, S.; Shrestha, B.; Kesson, A. M. Immunopathology of flavivirus infections. *Immunol Cell Biol* 2007, 85, 33-42.

23. Chambers, T. J.; Hahn, C. S.; Galler, R.; Rice, C. M. Flavivirus genome organization, expression, and replication. *Annual review of microbiology* 1990, 44, 649-88.

24. Lindenbach, B. D., H. Thiel, and C. M. Rice. Flaviviridae: The viruses and their replication. In *Fields Virology*, 5 ed, D. M. Knipe, and P. M. Howley, eds.

Lippincott William and Wilkins, Philadelphia

2007.

25. Gubler, D. J., G. Kuno, and L. Markoff. Flaviviruses. In *Fields Virology*, 5 ed. D. M. Knipe, and P. M. Howley, eds. Lippincott William and Wilkins, Philadelphia.

1153-1252. 2007.

26. Lanciotti, R. S.; Roehrig, J. T.; Deubel, V.; Smith, J.; Parker, M.; Steele, K.; Crise, B.; Volpe, K. E.; Crabtree, M. B.; Scherret, J. H.; Hall, R. A.; MacKenzie, J. S.; Cropp, C. B.; Panigrahy, B.; Ostlund, E.; Schmitt, B.; Malkinson, M.; Banet, C.; Weissman, J.; Komar, N.; Savage, H. M.; Stone, W.; McNamara, T.; Gubler, D. J. Origin of the West Nile virus responsible for an outbreak of encephalitis in the northeastern United States. *Science (New York, N.Y.)* 1999, 286, 2333-7.

27. Brinton, M. A. The molecular biology of West Nile Virus: a new invader of the western hemisphere. *Annual review of microbiology* 2002, 56, 371-402.

28. Zhang, Y.; Corver, J.; Chipman, P. R.; Zhang, W.; Pletnev, S. V.; Sedlak, D.; Baker, T. S.; Strauss, J. H.; Kuhn, R. J.; Rossmann, M. G. Structures of immature flavivirus particles. *EMBO J* 2003, 22, 2604-13.

## References

---

29. Zhang, W.; Chipman, P. R.; Corver, J.; Johnson, P. R.; Zhang, Y.; Mukhopadhyay, S.; Baker, T. S.; Strauss, J. H.; Rossmann, M. G.; Kuhn, R. J. Visualization of membrane protein domains by cryo-electron microscopy of dengue virus. *Nature structural biology* 2003, 10, 907-12.
30. Yu, I. M.; Zhang, W.; Holdaway, H. A.; Li, L.; Kostyuchenko, V. A.; Chipman, P. R.; Kuhn, R. J.; Rossmann, M. G.; Chen, J. Structure of the immature dengue virus at low pH primes proteolytic maturation. *Science (New York, N.Y.)* 2008, 319, 1834-7.
31. Heinz, F. X.; Stiasny, K. Flaviviruses and their antigenic structure. *Journal of clinical virology : the official publication of the Pan American Society for Clinical Virology* 2012, 55, 289-95.
32. Davis, C. W.; Nguyen, H. Y.; Hanna, S. L.; Sanchez, M. D.; Doms, R. W.; Pierson, T. C. West Nile virus discriminates between DC-SIGN and DC-SIGNR for cellular attachment and infection. *Journal of virology* 2006, 80, 1290-301.
33. Lee, J. W.; Chu, J. J.; Ng, M. L. Quantifying the specific binding between West Nile virus envelope domain III protein and the cellular receptor alphaVbeta3 integrin. *The Journal of biological chemistry* 2006, 281, 1352-60.
34. Chu, J. J.; Ng, M. L. Interaction of West Nile virus with alpha v beta 3 integrin mediates virus entry into cells. *The Journal of biological chemistry* 2004, 279, 54533-41.
35. Chu, P. W.; Westaway, E. G. Replication strategy of Kunjin virus: evidence for recycling role of replicative form RNA as template in semiconservative and asymmetric replication. *Virology* 1985, 140, 68-79.
36. Suthar, M. S.; Diamond, M. S.; Gale, M., Jr. West Nile virus infection and immunity. *Nature reviews. Microbiology* 2013, 11, 115-28.
37. Brinton, M. A.; Fernandez, A. V.; Dispoto, J. H. The 3'-nucleotides of flavivirus genomic RNA form a conserved secondary structure. *Virology* 1986, 153, 113-21.
38. Wengler, G. Terminal sequences of the genome and replicative-form RNA of the flavivirus West Nile virus: absence of poly(A) and possible role in RNA replication. *Virology* 1981, 113, 544-55.

## References

---

39. Castle, E.; Leidner, U.; Nowak, T.; Wengler, G. Primary structure of the West Nile flavivirus genome region coding for all nonstructural proteins. *Virology* 1986, 149, 10-26.
40. Rice, C. M.; Lenches, E. M.; Eddy, S. R.; Shin, S. J.; Sheets, R. L.; Strauss, J. H. Nucleotide sequence of yellow fever virus: implications for flavivirus gene expression and evolution. *Science (New York, N.Y.)* 1985, 229, 726-33.
41. Wengler, G.; Czaya, G.; Farber, P. M.; Hegemann, J. H. In vitro synthesis of West Nile virus proteins indicates that the amino-terminal segment of the NS3 protein contains the active centre of the protease which cleaves the viral polyprotein after multiple basic amino acids. *The Journal of general virology* 1991, 72 ( Pt 4), 851-8.
42. Bazan, J. F.; Fletterick, R. J. Detection of a trypsin-like serine protease domain in flaviviruses and pestiviruses. *Virology* 1989, 171, 637-9.
43. Gorbalenya, A. E.; Donchenko, A. P.; Koonin, E. V.; Blinov, V. M. N-terminal domains of putative helicases of flavi- and pestiviruses may be serine proteases. *Nucleic acids research* 1989, 17, 3889-97.
44. Lanciotti, R. S.; Ebel, G. D.; Deubel, V.; Kerst, A. J.; Murri, S.; Meyer, R.; Bowen, M.; McKinney, N.; Morrill, W. E.; Crabtree, M. B.; Kramer, L. D.; Roehrig, J. T. Complete genome sequences and phylogenetic analysis of West Nile virus strains isolated from the United States, Europe, and the Middle East. *Virology* 2002, 298, 96-105.
45. Chernov, A. V.; Shiryayev, S. A.; Aleshin, A. E.; Ratnikov, B. I.; Smith, J. W.; Liddington, R. C.; Strongin, A. Y. The two-component NS2B-NS3 proteinase represses DNA unwinding activity of the West Nile virus NS3 helicase. *The Journal of biological chemistry* 2008, 283, 17270-8.
46. Erbel, P.; Schiering, N.; D'Arcy, A.; Renatus, M.; Kroemer, M.; Lim, S. P.; Yin, Z.; Keller, T. H.; Vasudevan, S. G.; Hommel, U. Structural basis for the activation of flaviviral NS3 proteases from dengue and West Nile virus. *Nature structural & molecular biology* 2006, 13, 372-3.

## References

---

47. Clum, S.; Ebner, K. E.; Padmanabhan, R. Cotranslational membrane insertion of the serine proteinase precursor NS2B-NS3(Pro) of dengue virus type 2 is required for efficient in vitro processing and is mediated through the hydrophobic regions of NS2B. *The Journal of biological chemistry* 1997, 272, 30715-23.
48. Brinkworth, R. I.; Fairlie, D. P.; Leung, D.; Young, P. R. Homology model of the dengue 2 virus NS3 protease: putative interactions with both substrate and NS2B cofactor. *The Journal of general virology* 1999, 80 ( Pt 5), 1167-77.
49. Yamshchikov, V. F.; Trent, D. W.; Compans, R. W. Upregulation of signalase processing and induction of prM-E secretion by the flavivirus NS2B-NS3 protease: roles of protease components. *Journal of virology* 1997, 71, 4364-71.
50. Lescar, J.; Luo, D.; Xu, T.; Sampath, A.; Lim, S. P.; Canard, B.; Vasudevan, S. G. Towards the design of antiviral inhibitors against flaviviruses: the case for the multifunctional NS3 protein from Dengue virus as a target. *Antiviral research* 2008, 80, 94-101.
51. Nall, T. A.; Chappell, K. J.; Stoermer, M. J.; Fang, N. X.; Tyndall, J. D.; Young, P. R.; Fairlie, D. P. Enzymatic characterization and homology model of a catalytically active recombinant West Nile virus NS3 protease. *The Journal of biological chemistry* 2004, 279, 48535-42.
52. Shiryayev, S. A.; Aleshin, A. E.; Ratnikov, B. I.; Smith, J. W.; Liddington, R. C.; Strongin, A. Y. Expression and purification of a two-component flaviviral proteinase resistant to autocleavage at the NS2B-NS3 junction region. *Protein expression and purification* 2007, 52, 334-9.
53. Chappell, K. J.; Stoermer, M. J.; Fairlie, D. P.; Young, P. R. Mutagenesis of the West Nile virus NS2B cofactor domain reveals two regions essential for protease activity. *The Journal of general virology* 2008, 89, 1010-4.
54. Koonin, E. V. The phylogeny of RNA-dependent RNA polymerases of positive-strand RNA viruses. *The Journal of general virology* 1991, 72 ( Pt 9), 2197-206.

## References

---

55. Shiryaev, S. A.; Kozlov, I. A.; Ratnikov, B. I.; Smith, J. W.; Lebl, M.; Strongin, A. Y. Cleavage preference distinguishes the two-component NS2B-NS3 serine proteinases of Dengue and West Nile viruses. *Biochem J* 2007, 401, 743-52.
56. Solomon, T.; Ooi, M. H.; Beasley, D. W.; Mallewa, M. West Nile encephalitis. *Bmj* 2003, 326, 865-9.
57. Hayes, E. B.; Sejvar, J. J.; Zaki, S. R.; Lanciotti, R. S.; Bode, A. V.; Campbell, G. L. Virology, pathology, and clinical manifestations of West Nile virus disease. *Emerging infectious diseases* 2005, 11, 1174-9.
58. Arroyo, J.; Miller, C.; Catalan, J.; Myers, G. A.; Ratterree, M. S.; Trent, D. W.; Monath, T. P. ChimeriVax-West Nile virus live-attenuated vaccine: preclinical evaluation of safety, immunogenicity, and efficacy. *Journal of virology* 2004, 78, 12497-507.
59. Geiss, B. J.; Stahla, H.; Hannah, A. M.; Gari, A. M.; Keenan, S. M. Focus on flaviviruses: current and future drug targets. *Future medicinal chemistry* 2009, 1, 327-44.
60. Kramer, L. D.; Styer, L. M.; Ebel, G. D. A global perspective on the epidemiology of West Nile virus. *Annual review of entomology* 2008, 53, 61-81.
61. Kassell, B.; Radicevic, M.; Ansfield, M. J.; Laskowski, M., Sr. The basic trypsin inhibitor of bovine pPancreas. Iv. The linear sequence of the 58 amino acids. *Biochem Biophys Res Commun* 1965, 18, 255-8.
62. Mouton, R.; Finch, D.; Davies, I.; Binks, A.; Zacharowski, K. Effect of aprotinin on renal dysfunction in patients undergoing on-pump and off-pump cardiac surgery: a retrospective observational study. *Lancet* 2008, 371, 475-82.
63. Aleshin, A. E.; Shiryaev, S. A.; Strongin, A. Y.; Liddington, R. C. Structural evidence for regulation and specificity of flaviviral proteases and evolution of the Flaviviridae fold. *Protein science : a publication of the Protein Society* 2007, 16, 795-806.
64. Shiryaev, S. A.; Ratnikov, B. I.; Chekanov, A. V.; Sikora, S.; Rozanov, D. V.; Godzik, A.; Wang, J.; Smith, J. W.; Huang, Z.; Lindberg, I.; Samuel, M. A.; Diamond,

## References

---

- M. S.; Strongin, A. Y. Cleavage targets and the D-arginine-based inhibitors of the West Nile virus NS3 processing proteinase. *Biochem J* 2006, 393, 503-11.
65. Walker, B.; Lynas, J. F. Strategies for the inhibition of serine proteases. *Cellular and molecular life sciences : CMLS* 2001, 58, 596-624.
66. Stoermer, M. J.; Chappell, K. J.; Liebscher, S.; Jensen, C. M.; Gan, C. H.; Gupta, P. K.; Xu, W. J.; Young, P. R.; Fairlie, D. P. Potent cationic inhibitors of West Nile virus NS2B/NS3 protease with serum stability, cell permeability and antiviral activity. *Journal of medicinal chemistry* 2008, 51, 5714-21.
67. Ganesh, V. K.; Muller, N.; Judge, K.; Luan, C. H.; Padmanabhan, R.; Murthy, K. H. Identification and characterization of nonsubstrate based inhibitors of the essential dengue and West Nile virus proteases. *Bioorganic & medicinal chemistry* 2005, 13, 257-64.
68. Mueller, N. H.; Pattabiraman, N.; Ansarah-Sobrinho, C.; Viswanathan, P.; Pierson, T. C.; Padmanabhan, R. Identification and biochemical characterization of small-molecule inhibitors of west nile virus serine protease by a high-throughput screen. *Antimicrobial agents and chemotherapy* 2008, 52, 3385-93.
69. Lim, H. A.; Joy, J.; Hill, J.; San Brian Chia, C. Novel agmatine and agmatine-like peptidomimetic inhibitors of the West Nile virus NS2B/NS3 serine protease. *European journal of medicinal chemistry* 2011, 46, 3130-4.
70. Bajusz, S.; Szell, E.; Barabas, E.; Bagdy, D. Design and synthesis of peptide inhibitors of blood coagulations. *Folia haematologica* 1982, 109, 16-21.
71. Schweinitz, A.; Steinmetzer, T.; Banke, I. J.; Arlt, M. J.; Sturzebecher, A.; Schuster, O.; Geissler, A.; Giersiefen, H.; Zeslawska, E.; Jacob, U.; Kruger, A.; Sturzebecher, J. Design of novel and selective inhibitors of urokinase-type plasminogen activator with improved pharmacokinetic properties for use as antimetastatic agents. *The Journal of biological chemistry* 2004, 279, 33613-22.
72. Steinmetzer, T.; Schweinitz, A.; Sturzebecher, A.; Donnecke, D.; Uhland, K.; Schuster, O.; Steinmetzer, P.; Muller, F.; Friedrich, R.; Than, M. E.; Bode, W.; Sturzebecher, J. Secondary amides of sulfonylated 3-amidinophenylalanine. New potent

- and selective inhibitors of matriptase. *Journal of medicinal chemistry* 2006, 49, 4116-26.
73. Kadono, S.; Sakamoto, A.; Kikuchi, Y.; Oh-eda, M.; Yabuta, N.; Yoshihashi, K.; Kitazawa, T.; Suzuki, T.; Koga, T.; Hattori, K.; Shiraishi, T.; Haramura, M.; Kodama, H.; Ono, Y.; Esaki, T.; Sato, H.; Watanabe, Y.; Itoh, S.; Ohta, M.; Kozono, T. Structure-based design of P3 moieties in the peptide mimetic factor VIIa inhibitor. *Biochemical and biophysical research communications* 2005, 327, 589-96.
74. Saupe, S. M.; Steinmetzer, T. A new strategy for the development of highly potent and selective plasmin inhibitors. *Journal of medicinal chemistry* 2012, 55, 1171-80.
75. Becker, G. L.; Sielaff, F.; Than, M. E.; Lindberg, I.; Routhier, S.; Day, R.; Lu, Y.; Garten, W.; Steinmetzer, T. Potent inhibitors of furin and furin-like proprotein convertases containing decarboxylated P1 arginine mimetics. *J Med Chem* 2010, 53, 1067-75.
76. Sidique, S.; Shiryayev, S. A.; Ratnikov, B. I.; Herath, A.; Su, Y.; Strongin, A. Y.; Cosford, N. D. Structure-activity relationship and improved hydrolytic stability of pyrazole derivatives that are allosteric inhibitors of West Nile Virus NS2B-NS3 proteinase. *Bioorganic & medicinal chemistry letters* 2009, 19, 5773-7.
77. Robin, G.; Chappell, K.; Stoermer, M. J.; Hu, S. H.; Young, P. R.; Fairlie, D. P.; Martin, J. L. Structure of West Nile virus NS3 protease: ligand stabilization of the catalytic conformation. *J Mol Biol* 2009, 385, 1568-77.
78. Sielaff, F.; Than, M. E.; Bevec, D.; Lindberg, I.; Steinmetzer, T. New furin inhibitors based on weakly basic amidinohydrazones. *Bioorg Med Chem Lett* 2011, 21, 836-40.
79. Becker, G. L.; Lu, Y.; Hards, K.; Strehlow, B.; Levesque, C.; Lindberg, I.; Sandvig, K.; Bakowsky, U.; Day, R.; Garten, W.; Steinmetzer, T. Highly potent inhibitors of proprotein convertase furin as potential drugs for treatment of infectious diseases. *J Biol Chem* 2012, 287, 21992-2003.
80. Tucker, T. J.; Lumma, W. C.; Mulichak, A. M.; Chen, Z.; Naylor-Olsen, A. M.; Lewis, S. D.; Lucas, R.; Freidinger, R. M.; Kuo, L. C. Design of highly potent

## References

---

noncovalent thrombin inhibitors that utilize a novel lipophilic binding pocket in the thrombin active site. *J Med Chem* 1997, 40, 830-2.

81. Tucker, T. J.; Lumma, W. C.; Lewis, S. D.; Gardell, S. J.; Lucas, B. J.; Sisko, J. T.; Lynch, J. J.; Lyle, E. A.; Baskin, E. P.; Woltmann, R. F.; Appleby, S. D.; Chen, I. W.; Dancheck, K. B.; Naylor-Olsen, A. M.; Krueger, J. A.; Cooper, C. M.; Vacca, J. P. Synthesis of a series of potent and orally bioavailable thrombin inhibitors that utilize 3,3-disubstituted propionic acid derivatives in the P3 position. *J Med Chem* 1997, 40, 3687-93.

82. Szabo, R.; Bugge, T. H. Type II transmembrane serine proteases in development and disease. *Int J Biochem Cell Biol* 2008, 40, 1297-316.

83. List, K. Matriptase: a culprit in cancer? *Future Oncol* 2009, 5, 97-104.

84. Saupe, S. M.; Leubner, S.; Betz, M.; Klebe, G.; Steinmetzer, T. Development of new cyclic plasmin inhibitors with excellent potency and selectivity. *J Med Chem* 2013, 56, 820-31.

85. Weiss, M. S.; Brandl, M.; Suhnel, J.; Pal, D.; Hilgenfeld, R. More hydrogen bonds for the (structural) biologist. *Trends in biochemical sciences* 2001, 26, 521-3.

86. Brandl, M.; Weiss, M. S.; Jabs, A.; Suhnel, J.; Hilgenfeld, R. C-H...pi-interactions in proteins. *J Mol Biol* 2001, 307, 357-77.

87. Lim, H. A.; Ang, M. J.; Joy, J.; Poulsen, A.; Wu, W.; Ching, S. C.; Hill, J.; Chia, C. S. Novel agmatine dipeptide inhibitors against the West Nile virus NS2B/NS3 protease: a P3 and N-cap optimization study. *European journal of medicinal chemistry* 2013, 62, 199-205.

88. Guiheneuf, S.; Paquin, L.; Carreaux, F.; Durieu, E.; Meijer, L.; Bazureau, J. P. An efficient approach to dispacamide A and its derivatives. *Org Biomol Chem* 2012, 10, 978-87.

89. Davies, J. S. The cyclization of peptides and depsipeptides. *Journal of peptide science : an official publication of the European Peptide Society* 2003, 9, 471-501.

90. Hammamy, M. Z.; Haase, C.; Hammami, M.; Hilgenfeld, R.; Steinmetzer, T. Development and characterization of new peptidomimetic inhibitors of the West Nile virus NS2B-NS3 protease. *ChemMedChem* 2013, 8, 231-41.
91. Maraganore, J. M.; Bourdon, P.; Jablonski, J.; Ramachandran, K. L.; Fenton, J. W., 2nd. Design and characterization of hirulogs: a novel class of bivalent peptide inhibitors of thrombin. *Biochemistry* 1990, 29, 7095-101.
92. Rahfeld, J.; Schierhorn, M.; Hartrodt, B.; Neubert, K.; Heins, J. Are diprotin A (Ile-Pro-Ile) and diprotin B (Val-Pro-Leu) inhibitors or substrates of dipeptidyl peptidase IV? *Biochim Biophys Acta* 1991, 1076, 314-6.
93. Dixon, M. The determination of enzyme inhibitor constants. *Biochem J* 1953, 55, 170-1.
94. Stürzebecher, J.; Prasa, D.; Hauptmann, J.; Vieweg, H.; Wikstrom, P. Synthesis and structure-activity relationships of potent thrombin inhibitors: piperazides of 3-amidinophenylalanine. *J Med Chem* 1997, 40, 3091-9.
95. Steinmetzer, T.; Schweinitz, A.; Stürzebecher, A.; Dönnecke, D.; Uhland, K.; Schuster, O.; Steinmetzer, P.; Müller, F.; Friedrich, R.; Than, M. E.; Bode, W.; Stürzebecher, J. Secondary amides of sulfonylated 3-amidinophenylalanine. New potent and selective inhibitors of matriptase. *J Med Chem* 2006, 49, 4116-26.
96. Walsmann, P. [On the purification of thrombin preparations]. *Pharmazie* 1968, 23, 401-2.
97. Goodman, M., Felix, A., Moroder, L, Toniolo, C. (Eds.) *Methods of Organic Chemistry, (Houben-Weyl). In Additional and Supplementary Volumes to the 4<sup>th</sup> Edition, Synthesis of Peptides and Peptidomimetics*, Workbench Edition ed.; Georg Thieme Verlag Stuttgart New York, 2004; Vol. Vol. E 22a-e.
98. Bodanszky, M.; Bodanszky, A. *The practice of peptide synthesis*. 2nd, rev. ed.; Springer-Verlag: Berlin ; New York, 1994; p xviii, 217 p.
99. Frerot, E.; Coste, J.; Pantaloni, A.; Dufour, M. N.; Jouin, P. PyBop and PyBroP: Two reagents for the difficult coupling of the  $\alpha,\alpha$ -dialkyl amino acid. *Aib. Tetrahedron* 1991, 47, 259-270.

## References

---

100. Bodanszky, M.; Bodanszky, A. *The practice of peptide synthesis*. Springer-Verlag: Berlin ; New York, 1984; p xvii, 284 p.
101. Sheehan, J. C.; Preston, J.; Cruickshank, P. A. A Rapid Synthesis of Oligopeptide Derivatives without Isolation of Intermediates. *J Am Chem Soc* 1965, 87, 2492-3.
102. Bernatowicz, M. S.; Wu, Y.; Matsueda, G. R. 1H-Pyrazole-1-carboxamide hydrochloride an attractive reagent for guanylation of amines and its application to peptide synthesis. *Journal of Organic Chemistry* 1992, 57, 2497-502.
103. Yong, Y. F.; Kowalski, J. A.; Lipton, M. A. Yaw Fui Yong, Jennifer A. Kowalski, and Mark A. Lipton. *Journal of Organic Chemistry* 1999, 62, 1540-1542.
104. Stürzebecher, A.; Dönnecke, D.; Schweinitz, A.; Schuster, O.; Steinmetzer, P.; Stürzebecher, U.; Kotthaus, J.; Clement, B.; Stürzebecher, J.; Steinmetzer, T. Highly potent and selective substrate analogue factor Xa inhibitors containing D-homophenylalanine analogues as P3 residue: part 2. *ChemMedChem* 2007, 2, 1043-53.

---

## Publications

Hammany, M. Z.; Haase, C.; Hammami, M.; Hilgenfeld, R.; Steinmetzer, T. Development and Characterization of New Peptidomimetic Inhibitors of the West Nile Virus NS2B-NS3 Protease. *ChemMedChem* **2013**, 8, 231-41.

Hardes, K.; Becker, G. L.; Hammany, M. Z.; Steinmetzer, T. Design, synthesis, and characterization of chromogenic substrates of coagulation factor XIIIa. *Analytical biochemistry* **2012**, 428, 73-80.

Hardes, K.\*; Hammany, M. Z.\*; Steinmetzer, T. Synthesis, and characterization of nove fluorogenic substrates chromogenic substrates of coagulation factor XIIIa. *Analytical biochemistry* **2013**, 442, 223-30.

## Patent applications

Steinmetzer T., Becker G.L., Hardes K., Hammany M. Z.; Verfahren zur Bestimmung der Aktivität der Transglutaminase Faktor XIIIa. Patent No. WO/2011/089257.

## Posters

*New peptidomimetic inhibitors of the West Nile virus NS2B-NS3 protease*

M. Z. Hammany, C. Haase, R. Hilgenfeld, T. Steinmetzer.

22nd International Symosium on Medical Chemistry, Berlin,2.-6.09.2012

*Inhibition of the West Nile virus NS2B-NS3 protease by new agmatine-like peptidomimetic inhibitors*

M. Z. Hammany, C. Haase, M. Hammami, R. Hilgenfeld, T. Steinmetzer. 23rd Annual Meeting of the Society for Virology, Kiel, 6.-9.3.2013.

\* These two authors contributed equally to this work

## **Acknowledgment**

I would like to give my sincere appreciation to my supervisor Prof. Dr. Torsten Steinmetzer for his generous support during the entire time of my project, numerous scientific discussions, direct guidance, and permanent encouragement. Because of his safeguard, I did not lose my confidence toward my Ph.D. degree even at hardest time. I would like to thank him for his time spent with me and his efforts in all revisions of the manuscript.

My sincere appreciation and gratefulness go to Mr. Yousef Jameel our spiritual father for his kindness, generosity, and his financial support of my project and study period in Germany.

I would like to thank Prof. Dr. Rolf Hilgenfeld and Ms. Caroline Haase for the great cooperation regarding the crystal structure determination of the WNV protease in complex with one of my inhibitors.

My kind regards and thanks go to Prof. Dr. Wibke Diederich for her willingness to be my second reviewer.

I would like to give special thanks to all my committee members; Prof. Dr. Carsten Culmsee and Prof. Dr. Udo Bakowsky for their scientific guidance, encouragement and support.

I thank all my fellow labmates, the former and current members, I have met in our Steinmetzer's group; Kornelia Harges, Daniela Meyer, Heike Lang-Henkel, Wegderes Endreas, Dr. Frank Sielaff, Sebastian Saupe, Dr. Maya Hammami, and Alexander Maiwald, for the stimulating discussions, their friendship and family atmosphere. Many thanks for all the fun we have had in the last four years inside and outside work time. Special thanks go to my colleagues Dr. Dina Robaa, Kornelia, and Alexander for revision of the manuscript.

Last but not the least; my sincere thanks and appreciation are to my lovely family; my parents, my sister Dima, my sister Maya and my nephew Salah for all unconditional love, spiritual support, and sacrifices throughout my life.

## **Erklärung**

Ich versichere, daß ich meine Dissertation

**„Development and characterization of new peptidomimetic  
inhibitors of the West Nile virus NS2B-NS3 protease“**

selbständig ohne unerlaubte Hilfe angefertigt und mich dabei keiner anderen als der von mir ausdrücklich bezeichneten Quellen bedient habe.

Die Dissertation wurde in der jetzigen oder einer ähnlichen Form noch bei keiner anderen Hochschule eingereicht und hat noch keinen sonstigen Prüfungszwecken gedient.

Marburg, den.18.Februar 2014

M. Zouhir Hammamy

## Curriculum Vitae

### PERSONAL DATA

Name M. Zouhir Hammamy  
Birth date / place: 16. March 1985 in Aleppo, Syria  
Nationality: Syrian  
Marital status: Single

### HIGHER EDUCATION

---

Since 05/2009 Doctorate in the group of Prof. Dr. T. Steinmetzer,  
Institute of Pharmaceutical Chemistry, Philipps University  
Marburg  
05/2008–04/2009 Diploma in Pharmacy, Institute of Pharmaceutical Chemistry,  
Friedrich-Schiller University Jena, group of Prof. Dr. J.  
Lehmann  
09/2001–09/2006 Bachelor of Pharmacy and Pharmaceutical Chemistry,  
Faculty of Pharmacy, Aleppo University

### SCHOOL EDUCATION

---

09/1995–06/2001 Secondary and elementary Alkendy school, Aleppo/Syria  
09/1990–06/1995 Elementary Alneshe-Aljadeed school, Aleppo/Syria

18.02.2014, Marburg

M. Zouhir Hammamy